

A POTENTIAL EXTENSION OF THE BARNETT SHALE OIL PLAY: A  
SUBSURFACE PLAY ANALYSIS OF THE MISSISSIPPIAN (OSAGEAN-  
MERAMECIAN) STRATA IN SHACKELFORD COUNTY, TEXAS

BY

JONATHON GLOVER WEISS, JR.

Bachelor of Science, 2015  
Baylor University  
Waco, Texas

Submitted to the Graduate Faculty of  
The College of Science and Engineering  
Texas Christian University  
In partial fulfillment of the requirements for the degree

MASTER OF SCIENCE IN GEOLOGY


May 2017

A POTENTIAL EXTENSION OF THE BARNETT SHALE OIL PLAY: A  
SUBSURFACE PLAY ANALYSIS OF THE MISSISSIPPIAN (OSAGEAN-  
MERAMECIAN) STRATA IN SHACKELFORD COUNTY, TEXAS

By

Jonathon Glover Weiss, Jr.

Thesis Approved:



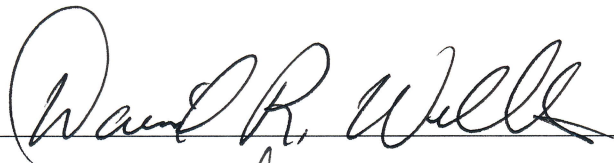
---

Dr. Xiangyang Xie (Major Advisor)



---

Dr. Richard Denne



---

David Wells



---

For the College of Science and Engineering

Copyright by  
Jonathon Glover Weiss, Jr.  
2017

## **Acknowledgements**

I would like to extend thanks to all of those involved with this project on and off campus during my time at TCU. Also, thanks to all of those that I have interacted with and learned from during various jobs in the oil and gas industry. I could not have accomplished this without my prior experiences and guidance received down the line.

Firstly, I would like to thank the following for the industry related support of this project: Jeff Jones and Buford Salters from Van Operating for the initial idea to work on this project within the AOI and for providing the project file in Petra along with the well logs in the area; Jeff Cole from Midville Energy for sharing his ideas and experiences on this play along with providing access to the Green 812 well data, core, and reservoir analysis; Rick Gonzalez from EOG for the access to the W.B. #3 Ranch core.

Secondly, I would like to thank my graduate advisor, Dr. Xiangyang Xie for support and advice during the completion of this project. I would like to also thank my committee members: David Wells for many years of mentoring and for serving on my committee; Dr. Richard Denne for the advice and critique of the text; Milt Enderlin for helping determine methods to obtain the correct data.

Finally, I would like to acknowledge the love and support of my friends and family: My girlfriend, Carly Bylund for constant support and encouragement during these 2 years; my father, Jonathon Weiss, Sr. for life-long guidance and for helping me problem solve throughout this entire process. I could not have made it to where I am today without his constant mentoring and support. All of my family was extremely supportive of my work and helped push me in the direction of accomplishing my goals.

# Table of Contents

ACKNOWLEDGEMENTS .....	ii
LIST OF FIGURES .....	v
LIST OF TABLES .....	vi
1 INTRODUCTION .....	1
1.1 Significance and Rationale for this Study .....	4
1.2 Previous Studies .....	6
2 GEOLOGIC BACKGROUND .....	7
2.1 Bend Arch-Fort Worth Basin Area Geology .....	7
2.2 Regional Stratigraphy .....	8
3.3 Shackelford County Stratigraphy .....	9
3 METHODS .....	10
4 RESULTS .....	14
4.1 Core Analysis .....	14
4.1.1 Midville Green 812 .....	15
4.1.2 EOG W.B. Ranch #3 .....	15
4.2 Lithofacies Analysis .....	16
4.2.1 Facies A.....	16
4.2.2 Facies B.....	16
4.2.3 Facies C.....	17
4.2.4 Facies D.....	17
4.2.5 Facies E.....	17
4.2.6 Facies F.....	17
4.2.7 Facies G.....	18
4.2.8 Facies H.....	18
4.2.9 Facies Summary .....	18
4.3 Bambino Testing .....	19
4.4 Thin Section Analysis.....	21
4.5 SEM and Elemental Analysis .....	23
4.6 Mapping.....	25
4.6.1 Structural .....	25
4.6.2 Isopach .....	26

4.6.3 Porosity .....	27
4.7 Mapping Interpretations .....	28
4.7.1 Structural .....	28
4.7.2 Isopach .....	29
4.7.3 Porosity .....	31
4.8 Depositional Model .....	32
4.8.1 Barnett Shale .....	32
4.8.2 Chester Limestone .....	33
4.8.3 “Mississippian Shale” .....	36
4.8.4 Chappel Limestone .....	37
4.8.5 Depositional Summary .....	37
5 PLAY COMPONENTS .....	38
5.1 Source .....	39
5.2 Reservoir .....	40
5.3 Trapping Mechanism .....	41
5.4 Fracture Barrier .....	42
5.5 Play Definition .....	44
6 DRY HOLE ANALYSIS OF THE NEWCOMB 1H WELL .....	45
6.1 Structural Data .....	46
6.2 Isopach Data .....	47
6.3 Porosity Data .....	47
6.4 Interpretation .....	47
7 SWEET SPOT IDENTIFICATION .....	50
8 CONCLUSIONS .....	53
9 FUTURE WORK .....	54
REFERENCES .....	56
APPENDIX .....	63
VITA	
ABSTRACT	

## List of Figures

1. Fort Worth Basin outline with Shackelford County highlighted .....	64
2. The productivity regions of the Barnett Shale .....	65
3. A stratigraphic column of the geology in Shackelford County and the type log for the AOI from the Lonestar McFarlane 1 well.....	66
4. A map of the AOI with the locations of the type log and the Newcomb 1H well.....	67
5. The extent of the Viola Limestone.....	68
6. The Equotip Bambino micro-rebound hammer .....	69
7. The location of the AOI within Shackelford County.....	70
8. Core description from the Midville Green 812 well.....	71
9. Core Description from the EOG W.B. Ranch #3 well.....	72
10. Facies summary from the core descriptions of the play	
a. Facies A of the Barnett Shale.....	73
b. Facies B of the Barnett Shale.....	74
c. Facies C of the Chester Limestone .....	75
d. Facies D of the Chester Limestone .....	76
e. Facies E of the Chester Limestone.....	77
f. Facies F of the Chester Limestone.....	78
g. Facies G of the “Mississippian Shale” .....	79
h. Facies H of the Chappel Limestone .....	80
11. Bambino data: Depth vs UCS of the W.B. Ranch #3 core .....	81
12. Cross-section A-A’: Sonic response of each of the play components .....	82
13. Thin sections of facies E showing the silt-sized quartz grains .....	83
14. Thin sections of facies E showing siliceous sponge spicules .....	84
15. Thin sections of facies F showing the limestone and chert nodule.....	85
16. Pore space development within a chert nodule in facies F .....	86
17. EDS Elemental analysis of facies E and F .....	87
18. Chart of Facies E and F %Si vs %Al .....	88
19. BSE SEM image of the pore space of a chert nodule in faces F .....	89
20. BSE SEM image of the pore space of the siltstone in facies E.....	90
21. Ellenburger structural map.....	91
22. Chappel Limestone structural map .....	92
23. Chappel Limestone reef identification map.....	93
24. “Mississippian Shale” thickness map .....	94
25. Chester Limestone thickness map.....	95
26. Barnett Shale thickness map .....	96
27. “Mississippian Shale” thickness flanking off of the Chappel reefs.....	97
28. Chester Limestone average porosity map.....	98
29. RHOB difference between “Mississippian Shale” and the Chester Limestone.....	99
30. Depositional diagram of the play components.....	100
31. GR vs RHOB of the Lonestar McFarlane 1 well.....	101
32. Cross-section B-B’: Facies change of the Chester Limestone.....	102
33. Cross-section C-C’: Interpreted OWC in the Chester Limestone.....	103
34. Sweet spot map of the play components.....	104
35. “Mississippian Shale” sweet spot map of the play components .....	105

## List of Core Photos and Tables

1. CORE PHOTOS .....	106
2. Core photos from the Midville Green 812 well .....	107
3. Core photos from the EOG W.B. Ranch #3 well.....	113
4. TABLES .....	117
5. Facies Summary.....	118
6. Bambino data from the W.B. Ranch #3 well .....	118
7. Elemental data from facies E and F in the Green 812 well .....	121

## 1 Introduction

The Bend Arch-Fort Worth Basin area has had historic conventional petroleum production since the early 1900s (Fig. 1) (Pollastro et al., 2007). The Bend Arch is located on the western boundary of the Fort Worth Basin and may represent the forebulge of the basin that formed from flexure caused by loading of the lithosphere during basin development (Pollastro et al., 2002; Ewing and Christensen, 2016). Due to the recent onset of resource plays and associated unconventional completion technologies, this basin has become the location of one of the most prolific source rock unconventional plays in the Barnett Shale and one of the largest shale gas-producing fields in Texas (the Newark, East field) (Montgomery et al., 2005; Pollastro et al., 2007). The current Barnett Shale play productivity is divided into a continuous gas accumulation, continuous gas and oil accumulation, and a continuous oil accumulation by the USGS (Fig. 2), which is based on thermal maturity (Marra et al., 2015). The extent and presence of fracture barriers in the overlying Forestburg Limestone and the underlying Viola Limestone create sweet spot areas in the continuous gas accumulation (Montgomery et al., 2005; Jarvie et al., 2007; Pollastro et al., 2007). The Newark, East field is located in the Barnett Shale continuous gas accumulation (Pollastro et al., 2002; Pollastro et al., 2007; Zhao et al., 2007; Marra et al., 2015). This field (located near Wise County, Texas) is seen as an industry sweet spot area that has the potential to produce nearly 3.0 tcf (trillion cubic feet) of gas from the Barnett Shale play (Pollastro et al., 2007). The field is located in the foredeep region of the Fort Worth Basin; an area where the Barnett Shale thermal maturity ranges from 1.2-2.1%  $R_o$  (vitrinite reflectance) and is prone to producing gas (Pollastro et al., 2002; Montgomery et al., 2005; Jarvie et al., 2007; Pollastro et al., 2007;

Marra et al., 2015). The Barnett Shale within the Fort Worth Basin may contain: 30.0-53.0 tcf of recoverable gas in the continuous gas accumulation, 172 million barrels of shale oil and 176 million barrels of natural gas liquids in the gas and oil continuous accumulation, and a currently undetermined volume of oil in the continuous oil accumulation (Pollastro et al., 2002; Montgomery et al., 2005; Pollastro et al., 2007; Marra et al., 2015).

Drilling for the Barnett Shale in gas prone areas, like the Newark field, has drastically slowed due to the economics associated with low commodity prices for dry gas and wells with EURs (estimated ultimate recovery) ranging from 2.5-3.5 bcf (billion cubic feet) (Jarvie et al., 2007). For Barnett Shale wells to become more economic, future completions will need to be focused in oil prone areas of the play. Due to flexure of the Bend Arch, the Barnett Shale is considerably shallower in this region, ranging from 4,000-6,000 ft total depth (Ewing and Christensen, 2016). On the Bend Arch, the Barnett Shale's thermal maturity is situated within the oil-window (0.60-0.99%  $R_o$ ), which allows this play to be considered a continuous oil accumulation (Pollastro et al., 2002; Pollastro et al., 2004; Jarvie et al., 2007; Marra et al., 2015). The Bend Arch area is located west of the Viola Limestone pinch out (Fig. 3), which is thought to be a fracture barrier that protects wells from unwanted water production from the underlying Ellenburger Group (Jarvie et al., 2007; Pollastro et al., 2007). The Barnett Shale is considerably thinner (50-80 ft thick) in the Bend Arch area compared to the deposits found within the Fort Worth Basin, therefore it contains reduced sourcing potential (Henry, 1982; Pollastro et al., 2002). There are shallow marine shelf deposits that contain conventional play potential on the Bend Arch that do not occur in the rest of the basin (Washburn, 1978; Henry,

1982; Pollastro et al., 2007). The Chappel Limestone and the Chester Limestone are both platform carbonate deposits that are in direct contact with the basal portion of the Barnett Shale in this area and both have been targets for conventional production in the area (Washburn, 1978; Henry, 1982; Parker, 1989). Locally on the arch, this Chester-Barnett play unconformably overlies the Ordovician-aged Ellenburger Group, a dolomitized shelf carbonate (Washburn, 1978; Amthor and Friedman, 1991; Pollastro et al., 2007). The Ellenburger Group has been labeled a “geohazard” due to the potential of producing large volumes of water from the high porosity formed from dolomitization and karsting during subaerial exposure (Amthor and Friedman, 1991; Pollastro et al., 2007 and Jarvie et al., 2007). Currently, there is not thought to be a widespread fracture barrier (similar to the Viola Limestone) between the Chester-Barnett play and the Ellenburger in this area, possibly due to erosion associated with the Bend Arch flexure (Henry, 1982).

The AOI (area of interest) of this project is approximately 64 mi<sup>2</sup> and is located in southern Shackelford Co., TX, which is west of the Bend Arch (highlighted in Fig. 1). The area is determined to be in the oil window of the Barnett Shale from source rock analysis previously conducted and its proximity to a historically oil-rich Mississippian reef play that is sourced by the Barnett Shale (Washburn, 1978; Parker, 1989; Pollastro et al., 2002; Jarvie et al., 2007; Marra et al., 2015). This smaller area was chosen to start the research for this project because it contained a high density of wells, which is needed to capture intricate subsurface relationships of multiple play units. The results of this project could potentially extend the play potential of the Barnett Shale into an area that is in the oil window rather than dry gas (Montgomery et al., 2005; Jarvie et al., 2007; Marra et al.,

2015). This extension has not currently been successful due to the lack of fracture barriers that protect wells from Ellenburger water production (Montgomery et al., 2005).

The purpose of this project was directed towards: (1) determining if Barnett Shale play potential existed within the AOI, (2) identifying a repeatable underlying fracture barrier for this play, and (3) determine a sweet spot area within the AOI that can be utilized for larger-scale exploration purposes in the region. A geologic play, for this project, will be defined by Doust (2010) as similar geologic targets for hydrocarbon production that share the same source, reservoir, trap and seal conditions. These goals were accomplished through subsurface correlations, utilizing core data for reservoir potential and rock mechanical data, and determining depositional mechanisms of individual play components. A “sweet spot” map was generated that identifies an area within the AOI that contains the most geologic potential for successful horizontal completions in this Barnett Shale oil play.

### *1.1 Significance and Rationale for this Study*

A major reason for interest in this Barnett Shale oil play in Shackelford County is due to the potential of shallow (<6,000 ft measured depth), oil-rich completions from a historically gas-rich Barnett Shale. This Barnett oil play well would be cheaper to drill and produce a higher valued product than the historic Barnett Shale gas wells. Van Operating drilled and completed the Newcomb 1H well in 2013 within the AOI that targeted the Chester-Barnett play (Fig. 5), and produced large volumes of water that deemed it uneconomic. It is interpreted that the well was producing Ellenburger water. Complications associated with horizontal completions in this Chester-Barnett play

include encountering faults or stimulating fractures, which may allow communication with the underlying water-bearing Ellenburger Group (Washburn, 1978; Amthor and Friedman, 1991; Pollastro et al., 2007 and Jarvie et al., 2007).

Local operators in the Bend Arch area informally call both of the platform carbonate units (Chester and Chappel Limestone) the “Mississippian Lime”, which can lead to confusion when attempting to properly identify the components of the play (Flippin, 1982). This “Mississippian Lime” is often described as a shallow water platform carbonate system that contains reef cores and reef flanks (Washburn, 1978; Henry, 1982). This system makes up a conventional play where the target is either a silica-rich cherty facies within the Chester Limestone along flanking beds of the Chappel reefs or oil accumulations trapped structurally within Chappel Limestone reefs that are sourced by the overlying Barnett Shale (Washburn, 1978; Henry, 1982; Knebel, 1982; Parker, 1989). The “Mississippian Lime” play is up to 300 ft thick and has historically been drilled through or produced conventionally by multiple operators in Shackelford Co., TX (Washburn, 1978; Dougherty, 1982). Some operators have recently attempted horizontal completions in the “Mississippian Lime” play since the EURs of previously completed conventional wells in the Chester Limestone are estimated to exceed 100,000 BOE (barrels of oil equivalent) (personal communication with Van Operating). Since the Barnett Shale is within the oil-window, attempting to stimulate both the Chester Limestone and the Barnett Shale may be key to increasing the volumes of hydrocarbons produced. A stratigraphic column of the area and a type log from Lone Star McFarlane 1 well show the stratigraphy of the Chester-Barnett play and break out the play units (Fig. 4).

There is a shale facies situated between the Chester Limestone and the underlying Ellenburger Group identified in this study that will be referred to as the “Mississippian Shale”. Since this “Mississippian Shale” is situated between the Ellenburger Group and Barnett Shale play, it becomes of interest to determine if the shale acts as a fracture barrier in areas of increased thickness of this shaley unit. This unit could act as a fracture barrier due to heterogeneity of rock types and rock strengths in the play when present (Cooke and Underwood, 2001). This potential fracture barrier was identified by observing a regional facies change present within the Chester Limestone. Utilizing a micro-rebound hammer (Equotip Bambino) on available slabbed cores provided evidence for heterogeneity of rock strength and mechanics in the “Mississippian Shale”. The requirements of maintaining this facies as a fracture barrier for this study was based on: (1) maintaining thickness over a continuous area, (2) alternating laminated lithologies that create rock mechanic heterogeneity, and (3) an overall shift in rock strength from the Chester Limestone (used as a proxy for a more ductile rock response in a known clay-rich interval). Similar components of fracture barrier identification were presented in Chalmers (2016) while attempting to identify a fracture barrier that could reduce communication with an underlying, water-rich interval.

### *1.2 Previous Studies*

Numerous papers on the play potential and productivity of the Barnett Shale in the Fort Worth Basin have been published during the timespan of this unconventional play boom (e.g., Pollastro et al., 2002; Montgomery et al., 2005; Pollastro et al., 2007; Jarvie et al., 2007; Zhao et al., 2007; Monroe and Breyer, 2012; Fu et al., 2015; Marra et al., 2015). Industry “sweet spots” have been generated for this play in areas where

fracture barriers are present and protect the play from Ellenburger water production (Pollastro et al., 2007). Work has also been done by Baruch et al. (2012) on identifying clay-rich parasequences within the Barnett Shale near Ellenburger karst features, west of the Viola pinch out. This work was conducted in Parker County, where the Barnett Shale contains potential for mixed oil and gas production (Montgomery et al., 2005).

There has been little published work on the Barnett Shale continuous oil accumulation, west of the Newark, East field; specifically addressing the Chester Limestone near Shackelford County. An exception is the study Washburn (1978) conducted on the diagenesis and porosity development of the Osagean Chappel Limestone reefs in Shackelford County as conventional targets. This study aimed at identifying the facies present within and near the reefs along with diagenetic effects on the porosity. The presence of the Chester Limestone is mentioned as the “Chappel A”. Distinct depositional environments of both components of the “Mississippian Lime” were determined from this study. The Chappel Limestone formed on paleo-highs of the underlying Ellenburger as echinoid-bryozoan dominated reef mounds in a shallow epicontinental sea (Washburn, 1978).

## **2 Geologic Background**

### *2.1 Fort Worth Basin-Bend Arch Geology*

The geologic region of the Bend Arch-Fort Worth Basin contains an elongated trough resulting from the late Paleozoic Ouachita orogeny (Pollastro et al., 2002; Pollastro et al., 2007). The Fort Worth Basin is described as a Paleozoic foreland basin (Zhao et al., 2007). The sedimentary rocks in the Fort Worth Basin are underlain by

Precambrian granite and diorite basement (Pollastro, 2007). The Ouachita thrust forms the eastern boundary of the Fort Worth Basin and the Bend Arch forms the western boundary (Pollastro et al., 2007). During the Cambrian to Mississippian epochs, the basin was associated with a stable cratonic shelf that contained mainly marine carbonate deposits (Turner, 1957; Burgess, 1976). The basin shallows near its western boundary, the Bend Arch (Pollastro et al., 2007). The Bend Arch can be described as a positive subsurface structure that was formed by flexure of the Fort Worth Basin during the Late Mississippian (Pollastro et al., 2007), and it includes fractures and karst collapse features related to the diagenesis of the Ellenburger Group (Pollastro et al., 2007).

The southern midcontinent region of North America occupied a carbonate setting that underwent rapid eustatic cycles of transgression and regression of epeiric, shallow seas, allowing for thin carbonates to be deposited during transgressive events (Manger and Evans, 2012). This setting of warm, shallow seas allowed for the growth of Mississippian-aged reefs towards the southern portion of the North American plate in a shallow shelf setting (Henry, 1982).

## *2.2 Regional Stratigraphy*

Laurussia occupied a position that spanned the equator; the southern portion of the North American continent lay between 20-30° S latitude, which was within the carbonate belt (Manger and Evans, 2012). Sedimentation occurred during the Cambro-Ordovician, followed by erosion during the Late Devonian to Late Mississippian (Henry, 1982). During the Cambrian-Ordovician, shallow epeiric seas advanced from the southeast on to the flank of the Texas craton, which resulted in the deposition of

Ellenburger Group, a regionally spanning carbonate platform found in Texas (Turner, 1957; Washburn, 1978; Kerans, 1988). At the end of the Ellenburger Group deposition, a drop in sea-level occurred, which exposed the rocks and allowed for karsting to occur in the upper carbonate layer (Sloss, 1976; Kerans, 1988). During the Mississippian, the growth of platform carbonates on the North American plate resulted directly from changes in sea-level driven by subsidence caused by the collision of the North and South American plates (Flippin, 1982; Henry 1982; Zhao et al., 2007; Manger and Evans, 2012). The Barnett Shale was deposited on the shallow shelf area as a result of flooding over the exposed North American craton (Henry, 1982; Monroe and Breyer, 2012). The sediment for the deposition of the Barnett Shale appears to be sourced from: erosion of the Texas craton (Henry, 1982) and by westward prograding shale wedges from the Ouachita front (Monroe and Breyer, 2012). The structural trend of the Barnett Shale within the Fort Worth Basin is NW-SE due to its deposition on the shallow shelf adjacent to the Southern Oklahoma aulacogen to the NE (a 3-way rift of continental plate break-up) (Martin, 1982).

### *2.3 Shackelford County Stratigraphy*

Shackelford County, TX is located on the Bend Arch, where platform carbonates from the Chappel Limestone were deposited unconformably over the Ellenburger Group as reefs that grew in the warm, shallow Barnett Sea (Henry, 1982). These Chappel reefs are described as pinnacle reefs that have thicknesses commonly around 150 ft with flanking beds composed of reefal debris that randomly grew in the windward direction (Henry, 1982). It is inferred that the Chester was deposited on the flanks of these Chappel reefs contemporaneously (Henry, 1982).

The deposition of the Barnett Shale occurred during the Mississippian, as the North American plate collided with the South American plate (Flippin, 1982; Henry, 1982; Zhao et al., 2007). In areas where the Chappel Limestone is present, reefs and mounds are deposited on to the Ellenburger Group unconformity that was produced by a major drop in sea level (Pollastro et al., 2007). The Barnett Shale drapes over this unconformity throughout most of the Fort Worth Basin and acts as a seal to the Chappel Limestone (Plummer, 1950; Flippin, 1982; Henry 1982; Pollastro et al., 2007). When the Barnett Shale was deposited over the Chappel reef crests it became significantly thinned compared to the thicknesses in areas absent of reefs (Henry, 1982).

### **3 Methods**

Stratigraphic relationships in this project were determined using wireline log data from over 100 wells provided by Van Operating and two cores provided by EOG Resources and Midville Energy (Fig. 5). The wells chosen for this study are from within a 64 mi<sup>2</sup> AOI chosen by Van Operating and were logged through the entire Mississippian strata. Gamma ray, resistivity, and bulk density logs were all used in the correlations of formation tops. Gamma ray, bulk density, and sonic log images from each well were traced to create digital log curves that were then used to make cross plots that helped set parameters for the identification of each depositional unit. The bulk density values were also utilized in estimating the density porosity of the Chester Limestone reservoir.

The data gathered from each of the wells served as the basis for the following types of subsurface maps that were created using the IHS Petra™ software: isopach (thickness), structure, calculated density porosity, and a “sweet spot”. These maps were

created by a combination of hand contours along with computer-generated contours based on measured and calculated data. The “sweet spot” map considered specific subsurface attributes where the Van Operating Newcomb 1H well was located and up-scaled those values to determine an area that contains the most potential for horizontal completions that may not fracture into the Ellenburger. This method required analyzing each map and capturing the range of data that the Newcomb 1H well exhibits within the prospective zone.

The calculated density porosity map was used to interpret the quality of reservoir zones, but also heterogeneity within a formation between the facies present. This information was used to infer whether or not there will be a change in rock material strength and mechanics that could identify a potential fracture barrier/baffle. The data for creating the density porosity maps were obtained by digitally tracing raster RHOB (density) logs and extracting bulk density values at depth and then applying them to the density porosity equation (1.1):

$$(1.1) PHID = (RHOM - RHOB)/(RHOM - RHOF)$$

*RHOM = Density of the rock type matrix*

*RHOB = Density of the rock grain at depth*

*RHOF = Density of the drilling fluid (1.1 g/cc was used for a salt-based mud)*

$$(1.2) RHOM = (\% mineral_1 \times mineral1 density) + (\% mineral_2 \times mineral2 density)$$

A “RHOM” value of 2.68 g/cc was used to represent the average of sandstone and carbonate matrices (the density of silty limestone or limey sand; 2.65 g/cc for quartz and 2.71 g/cc for carbonate) that would best represent the entire section of the Chester Limestone since it is composed of alternating layers of siltstone with calcareous cement and limestone. This Chester density data was compared to the “Mississippian Shale” and

used to determine if any heterogeneity is present between the two formations. An increase in pore space of the rock affects a rock's strength. Changes in rock mechanics could affect how the stimulated fractures act as they propagate through the matrix during completions.

A micro-rebound hammer (Equotip Bambino) was used on the slabbed core from the EOG W.B. Ranch #3 well (Fig. 6) to collect rock strength data, as described by Daniels et al. (2012). The Bambino collects rock strength data in Leeb's Hardness values (HLD), which can be converted to unconfined compressive stress (UCS) in psi. Multiple published equations were available to convert HLD values to UCS, but the equation from Daniels et al. (2012) was used in this study. The Bambino identifies the relative strength of different lithofacies, which allows for predictions to be made for rocks that are more prone to baffle fractures due to rock strength and mechanical properties. The initial data collected by the Bambino are recorded as HLD, which can then be converted to measure the UCS of the rock material as outlined by Daniels et al. (2012) by the following equation (2):

$$(2) \text{ UCS} = (8 \times 10^{-6})(L^{2.5})(145.03773801)$$

where UCS in psi and L' in HLD

The slabbed core was left in its Styrofoam backing and laid out horizontally on a table where the Bambino was used by placing the hammer perpendicular to the flat surfaces of the core (Zahm and Enderlin, 2010); careful attention was taken not to take measurements near fractures. Data collection was taken in 1 ft increments on the EOG WB Ranch #3 core from the base of the Barnett Shale through the upper 3 ft of the

Chappel Limestone (1402.4-1431.2 m or 4,601.1-4,695.5 ft). Measurements were taken three times from the middle of the slabbed core (where the rock is thickest) and averaged. A total of 270 measurements were recorded. This core is not located within the AOI in Shackelford Co., but is located nearby and was used as an analog. Each well used in the study is shown relative to the AOI (Fig. 7). A core description was also undertaken on this well to match the Bambino data with the appropriate facies. This type of micro-rebound hammer data has also been found to be reliable by McClave (2014) in outlining the relative lithofacies rock strength changes in the Niobrara formation based on comparing Bambino results to electric wire line logs. The use of the Bambino provides data about relative hardness and brittleness of the lithofacies that is relatable to log derived Poisson's ratio, Young's modulus, and bulk modulus (McClave, 2014). Since rock mechanics are important for propagating fractures in low porosity, permeability plays (McClave, 2014), the study described here utilized this data for identification of a potential fracture baffle/barrier.

A second core was also described from the Midville Energy Green 812 1H well (see Fig. 7). This well is located ~10 mi northeast of the AOI, but it was used as an analog data point due to the lack of available cores. This core was described from the Chester Limestone up through the base of the Barnett Shale (1381.8-1392.2 m or 4,533.5-4,567.6 ft). The core description was used to determine facies throughout the lower Barnett Shale and the pay zone of the Chester Limestone. The descriptions of both cores were digitized using the Easy Core™ software to represent the facies observed.

Three samples were collected from the Green 812 core and sent to Precimat Lab for elemental and porosity evaluation. Areas on the samples were picked for creating thin

sections. Three thin sections were then analyzed via a SEM (scanning electron microscope) and an EDS (energy-dispersive x-ray spectroscopy) detector. A BSE (backscatter electron) image was used from the SEM to determine the elemental analysis of each sample. Points within the thin sections were picked randomly to create ROIs (regions of interest) to analyze. Three random points within each ROI were chosen for elemental analysis of each sample. Porosity evaluation was conducted by using a BSE at ~5 $\mu$ m resolution. Each image was binarized to indicate porous areas by detecting void fraction distribution.

Midville Energy provided additional core data from the Green 812 in the form of: core photos, thin sections, and core samples. Nearly 60 additional thin sections were made available by Midville Energy from a previous in-house study. This data helped to better understand the various rock material mechanical properties of the subsurface formations. The material properties allows for interpretations of lithology differences that could lead to the identification of a fracture baffle/barrier.

## **4 Results**

### *4.1 Core Analysis*

The first core described was the Midville Green 812, which was taken in a location absent of Chappel reefs (Fig. 7). This core recovered 70 ft of rock from the base of the Chester Limestone to the top of the Barnett Shale (4500-4570 ft). The second core described was the EOG WB Ranch #3, which was located proximal to the Chappel reefs. This core recovered ~130 ft of rock from the top of the Chappel Limestone to the top of the Barnett Shale (4565-4692 ft)

The Midville Green 812 core was utilized to take samples of a Chester Limestone cherty pay zone. This core helped to understand the depositional mechanisms of the Chester-Barnett play and to help create a model for the Chester Limestone distal from the Chappel reefs. The EOG W.B. Ranch #3 core was described and tested with the Bambino tool. This core description was compared with the Green 812 core description to help understand the relationship between the Chappel reefs and Chester Limestone deposition.

The goal of the two core descriptions was to understand the lithologies and break out the major lithofacies of the Chester Limestone in the subsurface. The main zones of interest in the core study were the “Mississippian Shale” and the Chester Limestone cherty zone. Unfortunately, the Green 812 well did not core through this zone, but the EOG WB Ranch did contain a condensed section of this shaley facies (due to the structure of the Chappel reefs).

#### 4.1.1 Midville Green 812

The Midville Green 812 core was described from the base of the Chester cherty pay zone up to the basal portion of the Barnett Shale (Fig. 8). This core was provided along with a comprehensive of the play in the area near where this well was drilled (~15 mi NE of the AOI). Data from this well was utilized as analog information for the play.

#### 4.1.2 EOG WB Ranch #3

The EOG W.B. Ranch #3 core was described from the top of the Chappel Limestone to the basal portion of the Barnett Shale (Fig. 9). This core was utilized for obtaining information about the rock strength from the Bambino tool. Rock strength data obtained from this core was utilized as analog rock data for the AOI.

## *4.2 Lithofacies Analysis*

After conducting core descriptions of the Green 812 core and the W.B. Ranch #3 core, several facies could be broken out from the Chappel Limestone up to the Barnett Shale. These facies were first identified by hand sample and were then further analyzed by thin section analysis due to the higher level of resolution required to characterize carbonate and fine-grained sedimentary samples. The facies identified were given a label if present in either core.

### 4.2.1 Facies A: Barnett Shale

Facies A is a black laminated siliceous mudrock that contains pyrite and vertical calcite-healed fractures (Fig. 10a). The laminations of the black mudrock are less than 1 inch thick and the vertical fractures observed were about 6 inches long. The fractures present were either partially or completely healed with calcite. Pyrite nodules are present towards the base of this facies.

### 4.2.2 Facies B: Barnett Shale

Facies B is a brown, mudrock that contains pyrite and phosphate nodules. The facies appeared to be clay-rich due to the way in which it was crumbling in the core box (Fig. 10b). It contains rounded, pyrite nodules and phosphate nodules along with a significant mud component. There is no reaction when HCl was applied to this facies. This facies is located at the contact between the Chester Limestone and the Barnett Shale in both cores and is roughly 2" thick.

#### 4.2.3 Facies C: Chester Limestone

Facies C is a light grey pelecypod packstone that is weakly laminated and contains bryozoan remains (Fig. 10c). This facies has both intact and broken pieces of pelecypod shells and intact bryozoan remains. This facies is present in the top of the Chester Limestone near the contact of the Barnett Shale.

#### 4.2.4 Facies D: Chester Limestone

Facies D is a grey mudstone-wackestone that contains echinoderm and pelecypod fossils along with pyrite (Fig. 10d). The fossils present are small, ~.078 in (2 mm), and in some cases shell material has been completely replaced by pyrite. The shells are intact and supported in a fine-grained mud sized matrix.

#### 4.2.5 Facies E: Chester Limestone

Facies E is a dark grey calcareous siltstone that contains cross-beds and amorphous light grey chert nodules, commonly scoured at the base (Fig. 10e). The chert nodules range from white-grey in color and are ~1 in x 2-3 in and the nodules have an amorphous geometry. When HCl is applied to this facies, it readily flows through the matrix and weakly reacts a few seconds after contact. The rock matrix appears to have been reworked by bioturbation; the shape of the chert nodules may represent burrows of organisms moving through the sediment dwelling and feeding.

#### 4.2.6 Facies F: Chester Limestone

Facies F is a grey, ostracodal wackestone - packstone that contains ripples and amorphous light grey chert nodules; there are abrupt contacts associated with this facies (Fig. 10f). Bioturbation is present within this facies that destroyed the original bedding

structures. Facies F contains thin-walled ostracod valves that have silt-sized quartz as the matrix; there are small, scattered crinoid stems that are mixed in with the sediment as well. Facies F is found in conjunction with Facies E and the two comprise the Chester Limestone cherty zone. When HCl is applied to this sample, it has a much faster reaction than exhibited in Facies E; the acid tends to move through the matrix and spread out rather than bead up. Similar to Facies E, the chert nodules are white-grey in color and ~1 in x 2-3 in; the nodules have an amorphous geometry and appear to occur in burrows.

#### 4.2.7 Facies G: “Mississippian Shale”

Facies G is a grey pelecypod packstone-grainstone that contains crinoid fragments, pelecypods, abundant glauconite pellets, and pyrite. It is composed of whole shells and fragments interbedded with thin dark grey rippled mudrock beds (< 2 in thick) (Fig. 10g). This facies underlies the cherty zone (facies E and F) and overlies the Chappel Limestone.

#### 4.2.8 Facies H: Chappel Limestone

This facies is a white, crinoidal packstone-grainstone. The appearance of this facies is crystalline due to calcite overgrowths (Fig. 10h). The crinoids occur mostly as individual pieces and parts of stems. When HCl is applied, it strongly reacts with this facies.

#### 4.2.9 Facies Summary

The facies observed from both of the cores are summarized in a Table 1. The higher porosity zones (identified on wire line logs by a decrease in RHOB values), facies E and F, informally makes up the Chester cherty zone. The cherty facies (facies E and F) is of interest for conventional completions due to its calculated reservoir quality porosity

and permeability values along with its direct contact to the Barnett Shale. This zone exists directly under the Barnett Shale contact, usually in the upper Chester. This study found the zone to be composed of alternating units of the siltstone facies (facies E) and the carbonate wackestone-packstone facies (facies F) containing chert nodules. Under this cherty zone is the equivalent of the “Mississippian Shale” in the AOI (facies G). This zone was composed of pelecypod-rich limestone that contains glauconite interbedded with thin shale laminations. This shaley facies could potentially act as a fracture baffle/barrier towards fractures growing downward during stimulation because of its ductility from the shale laminations and glauconite.

#### *4.3 Bambino Testing*

The Bambino tool was utilized by collecting 3 readings directly in the middle of the slabbed core every 1 ft on the WB Ranch #3 core which were then averaged. The Bambino data was used as an analog for rock strength since no rock data was available for this study in the AOI. The interval tested ranged from the base of the Chappel Limestone up to the base of the Barnett Shale. The goal of this exercise was to investigate the hypothesis that because the “Mississippian Shale” (facies G) contains interbedded layers of limestone and shale that it could have different rock mechanics, based on hardness values and lithology, from the Chester Limestone (facies E and F). A change in rock mechanics would create heterogeneity below the target interval that could cause the “Mississippian Shale” to act as a downward fracture baffle/barrier during stimulation. The data collected from the Bambino tool for each facies was averaged to show the rock strength of each lithofacies.

The strength data collected were initially recorded as Leeb's Hardness values HLD (L') values and were converted using equation (2) to obtain data in UCS (unconfined compressive strength) values so that interpretations about rock strength can be made (Zahm and Enderlin, 2010; Daniels et al., 2012). A graphical representation of depth vs. UCS (Fig. 11) allows for interpretations to be made to determine if there is heterogeneity present between the strength and rock mechanics of the facies. The brittle Chester chert zone displayed an UCS average of 15,834 psi and the clay-rich "Mississippian Shale" displayed an UCS average of 12,555 psi. A difference in UCS values of ~3,300 psi highlights the heterogeneity in strength and rock mechanics that occurs between these facies. The Chester Limestone contains a higher amount of carbonate content, which makes it a more brittle rock. The "Mississippian Shale" contains a higher amount of clay (thin shales and glauconite pellets) and siliciclastic material, which makes it a more ductile rock. This heterogeneity could allow the "Mississippian Shale" to baffle stimulated fractures during completions based on rapid changes in rock strength and rock mechanical properties within the interbedded limestones and shales (Cooke and Underwood, 2001).

These results do not imply that weaker rocks baffle fractures, but suggest that abrupt changes in rock mechanics in layered intervals may have the potential to alter vertical fracture growth (Cooke and Underwood, 2001). Multiple bedding contacts of different lithologies can limit the vertical extent of stimulated fractures by terminating them at more ductile horizons (Cooke and Underwood, 2001). Similarly, flaws in bedding planes (such as the scours noted in facies E or the nodules present in facies E and F) can result in creating step-over fractures that become weakened as they propagate due

to tortuous pathways at the bedding contacts (Cooke and Underwood, 2001). To utilize this interpretation for exploration purposes, areas chosen for the consideration of drilling will need to contain the thickest “Mississippian Shale” to have geologic potential for baffling downward fracture networks from well completions and prevent communication with the underlying Ellenburger.

Comparing the results from the Bambino test to a regional cross-section of wells with available sonic logs (Fig. 12) reveals a similar response in the basal portion of the “Mississippian Shale” with slower interval transit times ( $\sim 70 \mu\text{s}/\text{ft}$ ) compared to the Chester Limestone ( $\sim 50 \mu\text{s}/\text{ft}$ ). This difference in interval transit times is a response from the lithology difference in the Chester Limestone compared to the “Mississippian Shale”. Not only is there a rock strength difference present between these two units, but there is also an apparent difference in mechanical properties that was identified from the facies analysis. The change from brittle material (silica and calcium-rich) to more ductile material (clay-rich) combined with rock strength differences creates apparent heterogeneity between units in this play. Based on these results, the Bambino may have the potential to be used to also predict rock mechanics based on comparing the hardness data if the samples used do not have fractures and are similar sizes.

#### *4.4 Thin Section Analysis*

Samples for thin section and SEM study were collected from facies E and F (in the Chester Limestone) from the Midville Green 812 core. These facies were chosen since they appeared to have the most reservoir potential for this play. Additional thin sections from the Green 812 were also available from a previous in-house study. These

thin sections also focused on the cherty zone of the Chester since that was the completion target.

A sample of facies E, taken from 1,392.39 m (4,568.2 ft) (Fig. 13) contains silt-sized quartz, calcite, and dolomite grains. The make-up of the facies appears to be detrital due to the consistent size and relative well-sorting exhibited. This facies does not contain a large carbonate component, which was first determined from HCl testing and confirmed by thin section analysis. This facies contains allochthonous quartz grains that were potentially sourced from the exposure and erosion of older rock during basin evolution. Siliceous sponge spicules are found within this facies (Fig. 14); these spicules may have been deposited during periods of detrital deposition during relative lowstand settings.

A sample of facies F, taken from 1,390.95 m (4,563.5 ft) (Fig. 15), was found to be composed of mostly carbonate content and contained ostracods, crinoids, and silt-sized quartz grains. The quartz grains act as the matrix to this facies, which may add to the reservoir properties due to the lack of swelling clays present. Facies F contains the highest carbonate material within the Chester Limestone, which may be reflective of stable water depths during highstand settings. The ostracod valves appear to be both intact and broken up. Bioturbation is evident in this facies due to the lack of preserved bedding structures along with the presence of the chert nodules where burrowing was most likely present.

The presence of chert nodules within this facies may be explained by a detrital deposition of facies E. A relative sea-level drop could redistribute the exposed detrital sediment along with the siliceous sponges, which allows the spicules to be precipitated

and transported in a basinward direction. Once these spicules are transported, they may be reprecipitated in the underlying burrows of the carbonate-rich facies to form the chert nodules similar to the diagenetic pore-water silica described by Neuweiler et al. (2014). Accumulations of these chert nodules are targeted as a conventional play near the AOI due to high associated porosity (personal communication with Midville Energy and Van Operating). Further thin section analysis of the chert nodules revealed ostracod valves and calcite present within the nodules. In one thin section, some of the calcite has dissolved, which created pore space (Fig. 16). The presence of dissolved calcite within the chert nodules indicates multiple diagenetic events occurred in the Chester cherty section.

#### *4.5 SEM and Elemental Analysis*

Samples from the Green 812 core were chosen for thin section analysis and sent to Precimat Lab for SEM analysis to determine the mineralogy and the pore geometry of the facies. The Green 812 well had ~12% PHID through the cherty facies (facies E and F) run on a limestone matrix (2.71 g/cc); this well was used as an analog to determine a potential mechanism for porosity within the Chester Limestone. Precimat Lab chose points on each sample for analysis; both porosity evaluation and elemental data came from the same ROI chosen. Elemental values of the ROIs were utilized to make interpretations about the depositional environments.

The results of each ROI (region of interest) were used to create a point graph to show the distribution of major and minor elements in weight percentage from both samples (Fig. 17). The analysis revealed that the limestone facies (facies F) contains an

average of 22.3% silica by weight and the siltstone facies (facies E) contains an average of 16.1% silica by weight. Comparing the weight percentage values of %Si vs. %Al from each ROI in both samples potentially reveals the origin of the silica in each facies (Fig. 18) as described by Rowe et al. (2012). There is linear relationship between Si and Al in detrital sediment due to their presence in clays; interpretations on the source of the silica can be made based on the amount of silica and whether it falls above a “clay line”, which would cause it to be considered “silica-excess” or biogenically sourced (Rowe et al., 2012). The clay line used is from Rowe et al. (2012) and was determined by the co-occurrence of these elements in clays. Facies E shows a near linear correlation between %Si and %Al, which could be attributed to a detrital source (Rowe et al., 2012). Facies F shows less of a linear correlation between %Si and %Al, and appears to contain excess silica for a detrital origin with the %Si plotting above the clay line. This increase in silica content is attributed to a biogenic source of silica in the chert nodules (Rowe et al., 2012). Determination of the mechanism for the source of silica will be useful as supplemental data to reinforce the interpretations of the depositional environments.

SEM results from facies F reveals pore spaces that are up to 1  $\mu\text{m}$  in length associated with dissolution of carbonate material from within a chert nodule (Fig. 19). This dissolution of calcite identified in the thin sections is repeated at a smaller scale, which explains how the chert zone exhibits reservoir quality porosity and permeability in some areas. These chert nodules appear to be related to extensive burrow networks, which may allow for a connected reservoir with this dissolution porosity component. The intergranular voids between the silt-sized quartz, which are up to 1  $\mu\text{m}$  in length, may contribute as matrix porosity to this reservoir facies (Fig. 20).

## 4.6 Mapping

Mapping was done using the IHS software Petra™. Up to 6 unit tops from more than 100 wells within the 64 mi<sup>2</sup> AOI were used as data points and correlated to create these maps (Fig. 4). The maps were first gridded based on formation attributes that were identified through log analysis (gamma ray, resistivity, bulk density, and sonic), and then hand contoured by posting those attributes at the well site on the AOI maps. These two resulting maps (one computer generated, the other hand-contoured) were then meshed together to create a user-defined grid that took into account the depositional model for this play. Their intended use is to help understand and illustrate the depositional controls of the play at a regional level. The location of the Van Operating Newcomb 1H is shown on each of the maps for later use in the dry hole analysis.

### 4.6.1 Structural Mapping

The top of the Ellenburger Group was mapped (Fig. 21) to identify the paleotopography for Chappel reef growth, but this top was determined to not be appropriate since it marks a major unconformity in the area and may have karsts present that do not maintain a relatively flat surface (Pollastro et al., 2007). The Ellenburger has a predictable overall dip of ~1° to the NW with the exception of some local dipping features along the -2,900 ft contour on the east side of the AOI.

The top of the Chappel Limestone was picked and mapped (Fig. 22) to display the changes of the reef growth throughout the AOI. The Chappel Limestone dips to the NW by <1°. Mapping reveals a NE-SW trend of Chappel pinnacle reefs that are generally in

an arcuate shape. The reefs have up to ~200 ft of relief within the AOI. The average area of these pinnacle reefs is approximately 40 acres.

#### 4.6.2 Isopach Mapping

Isopach maps track the extent of deposition and change in thickness of rock units by mapping the tops and bases of these units. This data can help identify favorable areas based on thickness and could potentially aid in identifying stratigraphic trapping by means of the reservoir formation pinching out. These maps tracked the thickness of the Chappel Limestone (Fig. 23), the Chester Limestone (Fig. 24), “Mississippian Shale” (Fig. 25), and the Barnett Shale (Fig. 26).

The first formation thickness mapped was the Chappel Limestone to determine the location of the reef trends due to the reefs effect on the deposition of overlying sediment. To correctly identify the location of the reefs, the contours from the isopach map of the Chappel Limestone were overlaid on the contours Chappel structure map (Fig. 23) to exhibit how thicknesses matched up with structural highs.

The “Mississippian Shale” (Fig. 25) thins over the crests of the Chappel reefs, but the sediment begins to thicken in a NW-SE direction away from the reef trend on either side (up to 60 ft thick in the N and up to 40 ft thick in the S).

The Chester Limestone (Fig. 24) thickens towards the NW of the map, where it is up to 55 ft thick. The unit thins in the SE direction of the map towards the pinnacle reef trend. The Chester Limestone gradationally thins from ~60-20 ft until it abruptly thins at the reefs down to <10'. The Chester appears to preferentially fill the structural low

feature created between the Chappel reef system, which appears as a channel-like thick section occurring between the Chappel reefs.

The Barnett Shale isopach (Fig. 26) shows that there is a trend increasing in thickness towards the SE corner of the AOI. The thickness of the Barnett Shale does not seem to experience any changes over the structurally low features formed in the underlying Chappel Limestone and Ellenburger. The shale does appear to thin over the crests of the underlying Chappel reefs.

The Ellenberger Group thickness was not mapped since few wells drill through the formation due to the threat of water production in structural lows (Jarvie et al., 2007; Pollastro et al., 2007).

#### 4.6.3 Porosity Mapping

Bulk density log data was utilized to calculate density porosity for individual wells (as outlined in the methods section from equation (1.1). The rock matrix density (RHOM) for the equation was 2.68 g/cc. This value was chosen to represent the average matrix density of carbonate (2.71 g/cc) and silica (2.65 g/cc). This average density was used to represent the high silica and carbonate content as the bulk density of the Chester Limestone. Average values were utilized to understand how the whole formation would affect the volume of hydrocarbons being held rather than thin, high porosity streaks secluded within the formation. This map helped to identify the better areas for the Chester Limestone as a secondary reservoir for this play with higher PHID values (Fig. 27). The Chester average porosity map contains isolated, elongated features that have considerably higher porosity compared to the directly adjacent Chester sediment

## 4.7 Mapping Interpretations

### 4.7.1 Structural

The overall dip of  $\sim 1^\circ$  NW indicates the modern-day direction for the strata within in this AOI. Since this is the paleotopographic surface for the overlying units, this data can be useful in identifying structural highs and lows in order to find oil-water contacts in more conventional portions of the play. There is a structural low feature that could represent a karst along the -2,900 ft subsea contour of the Ellenburger structure in the southeast portion of the AOI (Fig. 21). This karst feature is seen within the overlying Chappel Limestone by the canyon feature between reefs that is located near the same area that the Ellenburger karst feature is located (Fig. 22). This canyon could be formed by the geometry of the surrounding reefs or because of the underlying karst and is seen as paleo-accommodation space that can be filled.

This structurally low valley is important to consider when identifying areas of continuous sediment vs. areas that are more sediment-starved, and areas with potentially rapid lithologic changes. As sediment is funneled in the canyon, it can only fill the available accommodation space and build upwards rather than expand horizontally to cover a larger area. The Barnett Shale, the Chester Limestone, and the “Mississippian Shale” all gradationally thin to the SE until they abruptly thin to 50-60% of their post-depositional thickness over the Chappel reef crests.

Paleotopography can be helpful for identifying reef buildups; a datum must be chosen to flatten on in cross section view to show what the original topography resembled. The datum chosen to show the difference in topographic features from cross

sections (Fig. 12 and 32) in this study was the base of the Barnett Shale as a flooding surface over the Chester Limestone. This top was chosen since it is interpreted to be a basinal facies that would have a negligible dip associated with its sediments (Pollastro et al., 2002).

#### 4.7.2 Isopach

The Chappel reefs locations were defined as buildups that were greater than 50 ft in thickness (Fig. 23). Each of the other play components thicknesses were also mapped out. The trend of the Chappel reefs strikes NE-SW within the AOI. Reefs within the AOI are up to 200 ft thick. These reefs have narrow cores that gradually widen out towards the base; the area between the reef flanks is initially what causes the formation of a valley area in the AOI. The overlying Barnett Shale thickens towards the SE after passing the line of pinnacle reefs (Fig. 26). The shale is 30-50 ft thick on top of the reef crests. The Barnett is ~25 ft thick in the NW portion of the AOI and thickens to ~90 ft past the reef trend to the SE. Isolated Chappel reefs within thicker trends of the Barnett Shale cause abrupt thinning; in the NW corner section 61 of the AOI, the Barnett Shale thins from ~60 ft off of the flank to ~20 ft towards the crest of a Chappel reef.

The Chester Limestone isopach map has a channel-like feature trending NW-SE through the structurally low Chappel reefs (Fig. 24). Thickness trends suggest that the Chester was sourced from sediment in the NW. Deposition of the Chester Limestone may be related to a shoreward erosional event that transported channelized detrital sediment basinward. This Chester channel may have formed between the Chappel reefs due to the accommodation space present from the underlying Ellenburger karst-collapse feature creating a structurally low inter-reef area. These types of channels between outer ramp

reefs are present in the depositional model interpreted by Wood (2013) for the Marble Falls Limestone. The sediment that comprises the Chester Limestone could be sourced by erosion that occurs from the relative lowering of sea-level exposing older rock, or basin evolution causing a migration of the Bend Arch (Henry, 1982).

The “Mississippian Shale” thins distally from the reef trend, which appears to resemble flanking sediments shed off of the reefs (Fig. 25). This interpretation is confirmed by overlaying the Chappel reef isopach contours over the “Mississippian Shale” isopach map (Fig. 28). The resulting product is a visual of how the shale geometrically composes the flanks of the reefs within the AOI on either side of the Chappel reef trend. The shale is more widespread north of the reef trend; this may be due to adjacent reefs surrounding this area. This interpretation proposes that the “Mississippian Shale” is a part of a separate depositional system from the overlying Chester Limestone and is more likely to be related to the Chappel Limestone’s reef system.

Since the Barnett Shale may have been deposited as westward prograding shale wedges during major flooding based on the regional work of Monroe and Breyer (2012), there is evidence of depositional deepening within the AOI. The Barnett Shale isopach thickens towards the SE of the AOI (Fig. 26), which is interpreted to be the basinward direction. Post-depositional deformation of the Bend Arch has given the AOI its present day dip direction towards the NW (Henry, 1982). The AOI may have also been subjected to forebulge migration that deformed the strata post-depositionally. This interpretation is derived from the directional changes of facies and the structural controls of the AOI, and the present day location of the Bend Arch forebulge (Christensen, 2016). The present day dip direction is to the NW, but the depositional dip appeared to be to the SE direction

based on Barnett Shale thickness trends and changes in Chester Limestone facies. This change in dip direction could be attributed to forebulge migration from basin evolution after the units have been deposited.

#### 4.7.3 Porosity

Based on density-derived porosity, the Chester Limestone porosity appears to be highest in the same location where the Chester Limestone incised channel meets the shore ward side of the Chappel reef trend (Fig. 27). The high porosity section makes a geometric feature that is associated with the Chappel Limestone valley with high values of 16% average porosity. The area of increased Chester Limestone porosity could be controlled by 2 components: (1) Differential compaction: the Chester Limestone has increased porosity when it is located off of the crests of the Chappel reefs; (2) Lithology: porosity is enhanced when the Chester Limestone is associated with thicker cherty facies due to diagenesis of the calcite present in the chert nodules creating voids. These thicker cherty sections appear to be related, as they are located on the shoreward sides of the Chappel reefs. Facies E appears to contain transported sponge spicules along with detrital sediment; the burrows in facies F may be more susceptible to being replaced by chert if they contained spicules. The porosity map of the Chester Limestone was dependent on the wells that contained bulk density logs, and contours were not carried far into areas that contained little to no data.

The RHOB (g/cc) data for the Chester Limestone and the “Mississippian Shale” were compared within the AOI, and heterogeneity between the two facies was identified by a difference in bulk density values (Fig. 29). This difference was greatest in the same area where an enhanced PHID (> .07) for the Chester Limestone was found (Fig. 27).

## *4.8 Depositional Model*

### 4.8.1 Barnett Shale

Facies A: This facies is interpreted to be part of the restricted, sediment-starved deposits described by Henry (1982). This facies was deposited within an oxygen-restricted environment that allowed for the preservation of organic matter and the sulfate-reduction that enabled the formation of pyrite (Raiswell and Berner, 1985). The lack of oxygen is supported by the lack of bioturbation and the presence of well-defined laminations along with a lack of benthic fossil abundance.

Facies B: This facies is interpreted to be a major flooding surface of an overall transgression associated with a rise in Barnett sea-level. The high clay content is sourced by fine detrital material that gets carried out during the sea-level rise. The pyrite nodules were formed from sulfate reduction caused by anoxia from the rapid deepening and oxygen deprivation (Raiswell et al., 1988). This event covers a large area and is regionally traceable in Shackelford County to a change in depositional environment between the Green 812 and W.B. Ranch #3 cores. Facies B may be equivalent to the pyrite and phosphate lithology (B3) on the east side of the Fort Worth Basin described by Monroe and Breyer (2012).

The Barnett Shale is interpreted to be part of a restricted, reducing environment that did not allow for benthic organisms to live and feed. The abundance of pyrite and the laminated, fine grained shale lithology with a lack of benthic fossils allows for this interpretation to be made.

#### 4.8.2 Chester Limestone

Facies C: This facies is interpreted to be part of the early onset of Barnett transgression. The combination of bioclastic detritus and intact fossils suggests that this facies may have been part of a shallower shelf environment that was beginning to be flooded.

Facies D: This facies is interpreted to be part of a shallow platform environment due to the carbonate rock matrix. The water was likely oxygenated and this facies may have been deposited during highstand conditions due to the lack of evidence for high energy present. The pyrite present was likely created by diagenesis from iron present in the system during or shortly after deposition (Raiswell and Berner, 1985).

Facies E: This facies is interpreted to be the part of an oxygen-rich, high energy platform environment that flowed down dip towards the basin and incised channels between outer ramp Chappel reef features. The siliciclastic grains that dominate this facies in combination with the cross-beds and scouring support this interpretation. The source of siliciclastic grains may be part of repeated exposure and erosion associated with forebulge growth and continued basin evolution. The depositional mechanism for this facies could be increased energy in a shallow setting that prograded across the platform. This facies is interpreted to be marine influenced due to the presence of marine fossils. The chert nodules may have formed from silica filled burrows, which explains the rounded, amorphous geometry exhibited. The source of this silica may be from siliceous sponge spicules that lived on the carbonate platform. Post-mortem, the spicules were precipitated into the water as an early diagenetic event and reprecipitated as a dense bottom water flow that traveled down the slope basinward (Neuweiler et al., 2014). The

chert nodules readily allow the HCl to flow through their matrix; this is indicative of their higher porosity and permeability present.

Facies F: This facies is interpreted to be a part of an oxygen-rich, carbonate platform environment. There are similarities between this environment and the environment associated with Facies E. The presence of the ostracod valves is difficult to use as a specific indicator of an environment since they are interpreted to be pelagic and fall out of the shallow water column after death. This facies could be associated with periods of carbonate production between the high energy flows represented by facies E. The source of the chert nodules is most likely the same as for Facies E, precipitated remains of siliceous sponges that lived in a shallower environment.

The Chester Limestone is interpreted to be part of a shallow water, oxygenated environment that underwent cycles of aggradational highstand carbonate growth and detrital lowstand progradation. The lowstand environment may have incised valleys between shallow carbonate reefs that contained a lack of benthic fauna due to higher energy. Core analysis reveals that the Chester Limestone appears to contain less carbonate content than the Chappel Limestone and is composed of a larger percentage of silica. The formation is composed of alternating beds of ostracod and pelecypod skeletal wackestone-packstone (facies F) with amorphous chert nodules and rippled-planar horizontal bedded silt-sized detrital quartz with carbonate cement (facies E) that contains scouring surfaces. Thin section reveals siliceous sponge spicules within facies F of the Chester Limestone, which may explain the silica source for the chert nodules. SEM data reveals that these reservoir facies contain both dissolution and matrix porosity.

This formation has been previously interpreted as the product of bedded reef debris or as a reef flank facies (Washburn, 1978; Henry, 1982; Parker, 1989). Combining core data with the results of the mapping and log analysis, suggests a different interpretation of the Chester Limestone. Rather than being a product of bedded carbonate reef debris, the Chester Limestone appears to be part of a shallow marine platform progradational system that was sourced from northwest of the AOI. The progradation of the Chester Limestone may be related to higher energy, turbidity flows during the eastward progradation of the Chappel shelf deposits across the platform (Ruppel, 1984). This interpretation is reinforced by the linear relationship identified by comparing Si vs. Al (Fig. 18) and the interpretation that the silica is sourced by a detrital mechanism (Rowe et al., 2012). This sediment was deposited as a marine, channelized system that transported sediment basinward across the platform. The system appears to have gone through periods of periodic sea-level changes, indicated by the mixed lithology (facies E and F). The limestone facies (F) may represent periods of stable sea-level where the carbonate factory is active, whereas the siltstone facies (E) may represent periods of sea-level fall where sediment prograded across the platform and shut down the carbonate factory. The Chester Limestone cannot be described as one distinct sea-level due to these cyclical deposits, but based on the abundance of siltstone and the channelized geometry; they appear to be part of an overall sea-level fall. The channelized features of the Chester limestone could be expressions of paleo-structural lows in the Ellenburger or be related to incision during sea-level fall.

A regional cross section of the Chester Limestone (Fig. 32) through the AOI gives additional support to the interpretation that the formation is sourced from the NW as

indicated by the facies change to a muddier response on the gamma ray signature. This facies change to a muddier facies could represent the extent of the point-sourced sediment flow where only the fine-grained sediment is able to travel further out due to a decrease in depositional energy. The Chester Limestone appears to pinch out towards the SW near the Chappel reef trend on the cross section. All of this evidence helps to support the interpretation that the Chester Limestone is deposited by progradational system. The siltstone facies (facies E) may represent periods of lowstand whereas the limestone facies (facies F) may represent a period of highstand during an overall sea-level rise associated with Barnett Shale deposition. The source of the Chester silica is associated with detrital sediment from a period of uplift and exposure of previously deposited sediments that contained biogenic silica in the form of the siliceous sponge spicules.

#### 4.8.3 "Mississippian Shale"

Facies G: This facies is interpreted to be reefal debris shed from the Chappel Limestone. The facies shows evidence of being oxygen-rich based on the abundance of benthic fossils from pelecypods and crinoidal remains, but appears to also contain evidence for a euxinic, reducing environment based on the thin shale layers with pyrite (Raiswell and Berner, 1985). A potential explanation for the presence of the thin shales could be from muddy sediment being shed off due to vertical reef growth during periods of time that may shut down the carbonate factory off of the reefs rather than euxinic water conditions. The presence of organic carbon in the interbedded shale layers could also be the source for the increased amount of pyrite present (Raiswell and Berner, 1985). The presence of the glauconite is seen as reinforcement for deposition on an oxygenated, platform environment from the glauconite-producing environments described by Chafetz

and Reid (2000). This facies is interpreted to be the equivalent of the “Mississippian Shale” previously identified on wire line logs. The increased source of carbonate grains and crinoidal remains indicate a Chappel reef source.

#### 4.8.4 Chappel Limestone

Facies H: This facies is interpreted to be part of an oxygen-rich, outer ramp or mud mound community environment that is situated within the carbonate production window similar to the depositional model defined by Wood (2013) for the Marble Falls Limestone. Crinoids are the major components of this facies. This facies represented a lime mud-rich environment, which is interpreted from the crystalline appearance of the facies with the calcite overgrowths. The Chappel Limestone is represented by pinnacle reefs within the AOI.

#### 4.8.5 Depositional Model Summary

A depositional model was created from interpretations of the facies from core and thin section analysis along with the results of the maps (Fig. 30). This model considers the Bend Arch as a platform setting for carbonate growth. The order of unit deposition was considered to explain how the Mississippian-aged strata interacted through different depositional periods starting with the Chappel Limestone growth unconformably atop the Ellenburger Group. A sea-level vs. time curve is shown for each unit during deposition to reflect the potential eustatic conditions in the area. The basin ward direction was determined through facies relationships within the Chester Limestone and the thickness trend of the Barnett Shale. An assumption of basin subsidence is inferred by the change in rock type and depositional environment.

Two different depositional mechanisms have been determined for the Chester Limestone and the “Mississippian Shale”. The Chester Limestone is interpreted to be associated with a channelized, progradational system that transported detrital sediment basin ward from shallow shelf deposits down to the basin. This system may be sourced by the exposure of older rock proximal to the shoreline (NW to SE) that becomes exposed through basin evolution. The “Mississippian Shale” is interpreted to be part of a reef debris flank facies of the Chappel Limestone. The shale is thickest off the flanks (NW and SE) of the reefs and thins distally.

## **5 Play Components**

The units of this potential Chester-Barnett play are composed of repeatable geologic features that appear to be related to the depositional controls of the Chappel reef trend. Due to these units being repeatable along this regional trend, there appears to be play potential with the Barnett Shale as defined by Doust (2010). This Chester-Barnett play will be structured by each of the following play attributes: source, reservoir, trap/seal, and fracture barrier. Located west of the Viola Limestone pinch out, this play is geologically defined by: the Barnett shale, Chester Limestone, “Mississippian Shale”, and the Chappel Limestone. These units all serve a specific role in this play and will individually contribute to potential production. To have the highest geologic potential for successful unconventional completions, the best area must include all play attributes from each unique role. A cross plot comparing gamma ray log values vs. bulk density log values of the Lonestar McFarlane 1 type log shows wireline log attributes that define each of these play units (Fig. 31).

### *5.1 Source*

The Barnett Shale is typified by a black laminated organic-rich, siliceous shale that represents a restricted, marine suboxic-anoxic platform to basin environment that allowed for preservation of organic material (Pollastro et al., 2002; Jarvie et al., 2007). It is represented by facies A in the W.B Ranch #3 core. The Barnett Shale is identified by its high gamma ray signature (100-300 API) and is associated with low bulk density values (<2.55 g/cc).

The Barnett Shale is seen as source of the hydrocarbons for production. This play is focused on targeting both the hydrocarbons that have migrated into the directly underlying Chester Limestone and the hydrocarbons that are not yet expelled from the shale. As it represents the hydrocarbon source, it is important to be in an area with a sufficient thickness of Barnett Shale present so that the OOIP (original oil in place) values will be increased (Asquith, 2014). To determine areas with the best productivity, the Barnett shale should have the largest H (thickness) and pyrolysis tests should be run from intervals in the Barnett Shale that appear to have the best productivity potential (Asquith, 2014). The areas with higher corresponding S1 values (represents free hydrocarbons in the sample) should be targeted due to the potential of having more hydrocarbons present in the matrix (Asquith, 2014).

Organic matter abundances for this shale range from an average of 4% TOC to a maximum value of 12% TOC (Pollastro et al., 2002). This source shale contains mainly Type II kerogen, based on pyrolysis results yielding >350 mg HC/g TOC that produces high gravity oil (>38°) in Shackelford county (Pollastro et al., 2002; Jarvie et al., 2007).

The potential of this resource in lower maturity areas such as Shackelford County (~.9 Ro), is estimated at nearly 350 barrels of oil per ac/ft in place (Pollastro et al., 2002). Within the AOI, the Barnett Shale is ~60 ft thick and has OOIP (original oil in place) values of ~9MMBO/640 acres. These geochemical attributes explain how the Barnett Shale is the primary source rock on the Bend Arch (Pollastro et al., 2002).

## *5.2 Reservoir*

The Chester Limestone is located directly under the Barnett Shale and above the Chappel Limestone when present (Parker, 1989). This formation has been historically produced conventionally in fields that have targeted the crests of Chappel reefs (Knebel, 1982; Parker, 1989). The thinning towards the reef crests combined with reservoir quality porosity creates a pinch-out reservoir (Parker, 1989).

The Chester Limestone can be treated as the landing target and primary reservoir for unconventional completions. This is due to the difference in both gamma ray and resistivity log signature that could be easily identified during drilling using an MWD tool (measurement while drilling). The Chester Limestone will also add to the OOIP as a reservoir in areas of increased porosity due to exhibiting reservoir attributes within the cherty zone. Porosity comes from the grain-to-grain interaction within the siltstone facies, and the dissolution of calcite that is contained within the chert nodules in the pay zone. The high porosity chert nodules are linked to Chester deposits that are located on the shoreward side of the Chappel reefs since the siliceous sponge spicules are redistributed as part of the detrital sediment found in facies E. Calculated average porosities for this unit range up to 16% porosity and thicknesses can range up to 50 ft thick. The micro-

rebound hammer data revealed that the Chester Limestone has an average UCS 3,000 psi higher than the “Mississippian Shale”. This strength difference might explain why fractures have propagated through the Chester to the Ellenburger if the frac design did not consider this lower UCS boundary issue in areas of thinner “Mississippian Shale”.

### *5.3 Trapping Mechanism*

The Chappel Limestone is composed of gentle-water carbonate shelf deposits that are pinnacle reefs formed from crinoidal and bryozoan wackestone-grainstone (Ruppel, 1989). These reefs are represented by facies H in the W.B. Ranch #3 core. These deposits commonly form reef structures that appear as bioherms and mud mounds in a proximal platform setting (Ruppel, 1989). The Chappel Limestone is composed of numerous pinnacle reefs that resemble mud mounds that trap hydrocarbons and also create a structural component for overlying reservoirs in the area (Washburn, 1978; Ruppel, 1989; Pollastro et al., 2007). The depositional energy of the Mississippian bioherms and pinnacles is inferred to have been relatively low due to the lack of sparry calcite found in drill cuttings (Henry, 1982). The bioherms are also inferred to have grown laterally covering flank deposits and older buildups. Reefs grew to be approximately 100-350 ft thick in the Bend Arch area (Henry, 1982), and the reefs have approximately 200 ft of vertical relief within the AOI. The adjacent and overlying formations to the Chappel Limestone appear to thicken and thin at the expense of the reef’s structure; sediments thin towards the reef crest due to the structural highs formed by the build ups (Henry, 1982; Ruppel, 1989).

The Chappel reef trend is situated up-dip from the Chester Limestone and could act as structural and stratigraphic trapping mechanism for this play. The structural component is from the sloping flanks of the reefs creating structural highs in the overlying units for hydrocarbons to accumulate. The stratigraphic component is how the Chester Limestone appeared to change facies as it encountered the Chappel reef trend during deposition. This facies change will act as a trapping mechanism that will be situated up-dip that allows for hydrocarbons to accumulate. The timing of the trap formation would have been related to deposition, allowing these facies changes to be viable traps. Also, the presence of the “Mississippian Shale” appears to be related to flanking Chappel reefal debris. The deposition of this unit is crucial for potentially containing or slowing the fractures from growing downward into the Ellenburger Group. Another important aspect of this play component to consider is the effect of the reef’s structure on the overlying sediment deposited. Deposition off of the flanks of the reefs would have had a flatter, more predictable dip that allowed for more continuous deposition of the overlying and adjacent sediment. This is important because a more predictable dip will allow for faster drilling times due to fewer directional corrections needed and more efficient stimulations of the play within the pay zone.

#### *5.4 Fracture Barrier*

The “Mississippian Shale” is a facies located in the basal portion of the Chester Limestone. It varies in thickness from 20-50 ft thick and was identified as a separate unit from the Chester Limestone by its elevated gamma ray response and increased RHOB values. Its separate existence was confirmed during the core analysis through the increased clay content and the fossil assemblage. The depositional controls of this unit

are related to flank forming processes sourced by reef debris of the Chappel Limestone. The “Mississippian Shale” separates the Chester Limestone from the Ellenburger Group in some areas on the Bend Arch where it is present.

In the W.B. Ranch #3 core, this unit was represented by facies G. The alternating layers of glauconitic limestone beds interbedded with thin layers of shale create a variety of rock strengths and mechanics that vary vertically through the unit. These laminated brittle and ductile layers could dampen downward stimulated fractures due to the heterogeneity encountered of rapidly changing rock types during completions of the Chester-Barnett play. As a whole, the “Mississippian Shale” is more ductile than the Chester Limestone and fractures that are started in the Chester may terminate at the contact or within the “Mississippian Shale” (Cooke and Underwood, 2001). Due to this potential fracture barrier, the play may be economically dependent on areas within the thickest, most continuous accumulations of this unit.

This play component could add the potential of a fracture barrier or baffle based on the difference of rock mechanics. The interpretation that the “Mississippian Shale” would have different rock mechanics than the Chester Limestone was confirmed by the observed heterogeneity between the two units from analyzing log data (RHOB (g/cc) and interval transit ( $\mu\text{s}/\text{ft}$ ) values), UCS data, and lithology. This difference in rock mechanics was determined by the observed clay content in the “Mississippian Shale” combined with having an average UCS value  $\sim 3,000$  psi lower than the Chester Limestone in the W.B. Ranch #3 core. The lower UCS value was attributed to the “Mississippian Shale” having a more ductile response due to the increased clay content. This unit could act as a fracture barrier in areas where it is thickest and large in areal extent, due to its ductile nature

underlying the brittle Chester Limestone. This brittle-ductile transition will be more persistent in areas that contain high porosity Chester Limestone and the thickest accumulations of the “Mississippian Shale”. Based on mapping results, areas off of the Chappel reefs appear to hold the most potential to contain the thickest deposits of the “Mississippian Shale” due to its relationship to flank forming processes related to reefal debris. Fractures may tend to grow upward due to the difference in overburden and pore pressure (usually decreases upward), but the added barrier that the heterogeneity in this facies exhibits may stop fractures from growing downward and therefore protect the play from producing unwanted water from the Ellenburger Group.

### *5.5 Play Definition*

The Chester-Barnett play has been defined by each individual play component that has a unique role in contributing towards production. The Chester-Barnett horizontal play can be summarized as follows:

- **Source** = Barnett Shale
- **Hydrocarbon Migration** = Direct contact with the Barnett Shale source rock
- **Reservoir** = Chester Limestone and Barnett Shale
- **Trapping Mechanism** = structural and stratigraphic controls of the Chappel reefs on the overlying Chester Limestone
- **Seal** = Barnett Shale
- **Fracture Barrier** = “Mississippian Shale”

Future completions in this play may require: (1) Identifying areas within the Chester Limestone that contain the highest porosity values for lateral landing zones that will also maximize the difference between the rock strength and rock mechanics of the ductile “Mississippian Shale”, (2) Regionally mapping the “Mississippian Shale” along the Chappel reef trend and targeting areas with the thickest, most continuous deposition,

and (3) Possibly changing the lateral target to above the Chester, in the lower Barnett, to utilize the Chester's strength as a fracture barrier. Areas with higher porosity in the Chester Limestone will create heterogeneity when compared to the adjacent non-porous rock. This heterogeneity is extended into rock mechanics by comparing porous, brittle Chester Limestone to ductile "Mississippian Shale". It will be crucial to target this portion of the play in areas that contain heterogeneity in rock strength between the Chester and "Mississippian Shale" if operators want to avoid potential water production from the Ellenburger Group. Based on mapping results, the Chester is related to basinward erosion that prograded across the marine shelf deposits. Exploration for this unit as a landing target and secondary reservoir should be directed in a parallel direction (NE-SW) of the shoreward side of the Chappel reef trend.

## **6 Dry Hole Analysis of the Van Operating Newcomb 1H Well**

The Van Operating Newcomb 1H is a horizontal well drilled in September 2013 that was planned to prove up commercial production from the Chester Limestone in an area of a mappable porosity streak within the cherty facies. The play was located in a structural low that had more predictable dip than neighboring Chester wells drilled off the flanks of the Chappel reefs. It was interpreted that this play would have lower porosity and permeability in the southern portion of the AOI that would inhibit water migration into this zone. The Newcomb 1H initially landed the heel of its 3,000 ft lateral in the Chester Limestone, but drilled out of zone due to issues with the identification of the high porosity zone with the MWD tools. Upon completion, the initial production revealed a high water cut (ratio of barrels of water compared to barrels of oil) and it was interpreted

to be a result of crossing faults or stimulated fractures intersecting a natural fracture network that connected into the Ellenburger Group.

This well is located in the southwest portion of the AOI in section 61 (Fig. 4). This location was used as a control point for each of the maps created in an attempt to understand why the Newcomb 1H was unsuccessful in avoiding water production from the Ellenburger Group. Results from this analysis will be utilized to help identify different areas to provide more geologic potential for a future successful completion in this play.

### *6.1 Structural Data*

The Newcomb 1H well appears to have been drilled and completed within the Chappel reef structural low present in the AOI. This structural feature is interpreted to be a Chappel Limestone canyon created by an underlying karst-collapse that controlled the geometry of the strata that the Newcomb 1H well encountered by acting as a funnel for the overlying sediment. Reef slopes on either side of the canyons are dipping 3-5°, which implies that this canyon only allowed the sediment to fill the accommodation space vertically. Due to this, there is potential for Chappel Limestone to be directly adjacent to the “Mississippian Shale”. This type of funneling does not ensure a widespread “blanket” deposition of the “Mississippian Shale”; therefore the fracture barrier may not be present across the entire extent of the stimulated rock volume.

### *6.2 Isopach Data*

The Barnett Shale maintains a thickness of ~65 ft thick in this well. The funneling effect of the Chester Limestone and “Mississippian Shale” appears to fill up the available

accommodation space and does not appear to translate to the overlying Barnett Shale. This would have allowed the Barnett Shale to have been deposited laterally over the feature with only minimal variances in thickness. The thickness of the Chester limestone ranges from 30-35 ft, but due to its channelized nature it is only laterally extensive for ~1 mi either side from the well bore. The thickness for the “Mississippian Shale” ranges from 30-35 ft over the length of the well bore, but this thickness is maintained for less than an area of 2 mi<sup>2</sup>. The shale quickly thins to ~20 ft directly east of the well as shown by the isopach map (Fig. 26).

### *6.3 Porosity Data*

The average Chester Limestone PHID for the Newcomb 1H well ranges from 4-6%, which is a lower value than found in the high porosity zone ~2 mi north of the well (Fig. 27). The high porosity section of this facies ranges from 5-15 ft thick and has up to 15% porosity, while the remainder of the unit has values closer to 2-3% porosity. The lower average porosity is due to the reservoir being comprised of a proportionally thin, high porosity limestone/siltstone chert target, which is ~30% of the total thickness, and the remainder being composed of the tighter limestone facies. The compartmentalized reservoir zone does not explain the lack of production in this well. Since the chert facies of the Chester Limestone does contain quality reservoir attributes (from log analysis), it should still produce oil, even with a higher water cut.

### *6.4 Dry Hole Interpretation*

The reservoir properties that exist around the Newcomb 1H are not undesirable for unconventional resource completions. The reservoir attributes of the Chester

Limestone found in the Newcomb 1H well increase up to 35% in areas that have the best rock quality within the AOI. The major issue with the Newcomb 1H well appears to be its structurally low location within the Chappel reef canyon. The funneling effect of this Chappel canyon did not allow for a widespread, continuous deposition of the “Mississippian Shale”. Due to this, stimulated fractures may have traveled laterally through the adjacent brittle Chappel Limestone that lies directly under the Chester Limestone in areas up the slopes of the canyon walls. This communication with the Chappel Limestone may allow for fracture tips to travel into the similarly brittle Ellenburger Group (composed of dolomite).

Another explanation for the excess water production may be that the Newcomb 1H was below a potential OWC (oil-water contact), and therefore located within the water leg of the play. The presence of an oil-water contact can be interpreted from the decrease in  $R_t$  (deep resistivity) response from wells that are located within the Chappel structural low compared to wells that are located structurally higher (Fig. 33). The area located structurally higher from the Chappel valley should contain a lower  $S_w$  (water saturation). The Lone Star McFarlane 1 well is in the structurally lowest location within this canyon feature. The high porosity streak interval in the Lone Star McFarlane 1 PHID is calculated to be 10% and has a  $R_t$  of  $\sim 8 \text{ ohm}\cdot\text{m}$ . The structurally higher Seely McFarlane 1, which has a high porosity streak PHID of 15% and a  $R_t$  of  $\sim 35 \text{ ohm}\cdot\text{m}$  will calculate a lower  $S_w$  value. This drastic decrease of  $R_t$  in the Lone Star McFarlane 1 high porosity interval could be attributed to a higher  $S_w$  within the reservoir interval. This OWC may be a function of the up-dip, plunging high porosity channel allowing water to invade further into the reservoir.

Since the “Mississippian Shale” has different rock strength and mechanics (from differences in RHOB values and Bambino results) from the overlying Chester Limestone, it will be necessary to identify areas that primarily contain thicker layers of this shale between the Chester and the Ellenburger Group. These thicker layers of the shale will increase the underlying ductile rock properties and overall heterogeneity of rock properties for the play. The idea that the heterogeneity within the Chester Limestone (“Mississippian Shale”, scoured contacts, and irregular bedding due to the chert nodules) will create a baffle is a hypothesis, since there is no published data that supports the idea of an extension in the Barnett Shale play near this AOI. The identification of the potential OWC in this play illustrates that unconventional plays can have similar reservoir characteristics of conventional plays. This play still requires identifying appropriate reservoir attributes, which resemble conventional play attributes, in order to produce economic volumes of hydrocarbons along with low volumes of water.

The results of this dry-hole analysis give insight into areas that could contain more geologic potential: (1) the area should contain “blanket” or widespread deposition of all units included in the play, which will require relatively flat underlying formations, (2) due to the high water production in the structural low, there may be structural implications for determining an oil-water contact zone within the Chester Limestone, and (3) the presence of heterogeneity in the reservoir and underlying unit could have an effect on baffling downward propagating fractures.

## 7 Sweet Spot Identification

Multiple attributes should be considered when attempting to identify an area suitable for a successful resource play. To do this, multiple maps must be utilized to high-grade areas that contain all attributes deemed important by a geologist. Overlaying each contour of play components unique role will identify an area of overlap that contains all of the desirable attributes for the “sweet spot”. Since the depositional environments of the Chester Limestone and the “Mississippian Shale” are interpreted to be non-related, a sweet spot map based on these two components should result in identifying an area of overlap that contains enhanced play attributes in the lateral landing zone and fracture barrier. This technique is useful for quickly identifying potential areas rather than utilizing one map at a time. Using the Newcomb 1H well as a control point for this play, a sweet spot area was created by overlaying map contours from that control point (Fig. 34).

The contours used for creating this map:

- Chappel Structure (light blue) = > -2,900 ft SS
- Chester Limestone average PHID (light green) = > .010
- Chester Isopach (blue) = > 35 ft
- “Mississippian Shale” Isopach (grey) = > 30 ft
- Barnett Shale Isopach (black) = > 50 ft

Before overlaying these contours, the goal of the map must be decided upon so that an order of importance of the contours can be determined. This study was focused on identifying areas with a significant fracture barrier present; therefore the fracture barrier contour has the highest priority. The Chappel structure also controls the ability for the “Mississippian Shale” to have been deposited more widespread since it is interpreted to

be sourced by its reef debris. Areas with the thickest deposits of the “Mississippian Shale” will give the play the most potential to be protected from water production from the Ellenburger Group. Also, the Chappel structural contours set up the Chester Limestone in an up-dip stratigraphic trap on the shoreward side of the reefs. Since the Chester Limestone is the reservoir and landing zone, thicker Chester will contain more hydrocarbon capacity and will be easier to maintain horizontal drilling within zone. Areas that contain the highest Chester Limestone average PHID may contain more heterogeneity between the reservoir and fracture barrier. The Barnett Shale thickness allows for a larger rock volume to source and produce hydrocarbons from this play. The order of contour relevance was decided as:

1. Fracture Barrier (“Mississippian Shale” Isopach)
2. Trapping Mechanism (Chappel Structure)
3. Primary Reservoir Porosity (Chester Limestone average PHID)
4. Primary Reservoir (Chester Limestone Isopach)
5. Source (Barnett Shale Isopach)

These contours were overlaid and the polygon was created preferentially (by the order of relevance) tracing overlapping contours. The polygon created overlapped some contours because the attributes underlying it were out ranked by contours with a higher priority.

The area identified from this mapping equaled ~1,200 acres.

The sweet spot map identified ~8% of the AOI as an area that contains geologic potential for unconventional completions without stimulating fractures into the Ellenburger Group. The final mapping product of this study is not grossly impressive, but if the strategy used from this study was applied to a larger, regional area then results could bear more acreage with potential. The usefulness of this type of mapping can be

observed when applied in exploration settings or reevaluating acreage that was deemed uneconomic for conventional production.

A second attempt at a “sweet spot” map was created (Fig. 35) that may be more realistic for exploration in areas with less well control and variety of logs from older completions. The AOI contained a lower frequency of wells towards the west and also many of those wells available did not contain bulk density logs that were required to calculate density porosity. This map considers the importance of the “Mississippian Shale” as the fracture barrier and the effect of the Chappel reefs as a trapping mechanism to accumulate hydrocarbons. The area of overlap was determined by using the Chappel Limestone structure greater than -2,900 ft SS and the “Mississippian Shale” isopach contour of greater than 35 ft. Overlapping these two contours identifies an area that is on the shoreward side and down-dip of the Chappel reef trend, but is a greater area that contains potential for horizontal completion. This area is located adjacent to a structurally higher stratigraphic change as the Chester Limestone thins towards the crest of the Chappel reefs, which could act as a trap and position this area above a potentially plunging oil-water contact that is located within the channel feature. This area is anticipated to have lower permeability due to the lower porosity, which may also aid in keeping water out of the reservoir portion. This second sweet spot area is ~4,200 ac (~26% of the AOI) and more realistically represents a result that could be useful in the future development of this play. Since the depositional mechanisms for this fracture barrier appear to be related with reefal debris and the reservoir is related to basinward prograding sediment, future exploration may need to be directed shoreward from the Chappel reefs.

## 8 Conclusions

This subsurface study started by identifying units of the Chester-Barnett play through log analysis within the AOI in Shackelford County. The Chester Limestone was identified to have potential as both a reservoir and landing zone while the “Mississippian Shale” was identified as a potential fracture barrier due to the heterogeneity caused by its observed ductility. Each of these play units were mapped in the subsurface to understand their depositional mechanisms. Core descriptions of the EOG W.B. Ranch #3 revealed the specific lithologies of each unit: calcite and silica rich in the Chester Limestone and more clay-rich in the “Mississippian Shale”. Then each unit was hardness tested with the Equotip Bambino micro-rebound hammer, which identified the fracture barrier potential of the “Mississippian Shale”. Core samples from the Chester Limestone taken from the Midville Green 812 were turned into thin sections, SEM photos, and BSE elemental data to identify the intervals of increased porosity through the cherty zone of this interval. After all of the data was obtained, a depositional model was determined for each of the units. This model revealed two distinct depositional mechanisms of the Chester Limestone and “Mississippian Shale”. The Chester Limestone was deposited as a channelized, progradational system that moved basinward across the shallow shelf and may have been channelized; the “Mississippian Shale” was deposited as reef debris that was sourced by the muddy sediment and carbonate debris from the Chappel Limestone reefs.

In areas west of the Viola pinchout in the Chappel reef trend, previous operators may have targeted the Barnett Shale in areas of these Chappel reefs due to the potential for natural fractures caused by differential compaction over the reef features. These

completions have not been considered economic due to communication with the Ellenburger, possibly because of a minimal presence of the “Mississippian Shale”. Since the Viola Limestone is not present as a fracture barrier under the play, the future of this oil prone play could depend on targeting areas off of these Chappel reefs where the “Mississippian Shale” is thicker and more widespread. This study has revealed a distinct difference in deposition between the Chester Limestone and the “Mississippian Shale” that creates areas of overlap of thick deposition that provides areas within the AOI with geologic potential for oil-rich unconventional completions.

The quantifiable results obtained from this project were: (1) the identification of Barnett Shale play potential with the Chester Limestone within the continuous oil accumulation, (2) the identification of a potential fracture barrier in the “Mississippian Shale” due to the difference in rock mechanics from the rest of the play components, and (3) an economical method (when compared to using specialized wireline logs) for identifying a potential fracture barrier by use of subsurface mapping, core analysis, and micro-rebound hammer data. These results can be utilized as a model for workflow exploration of this play in this region. Understanding the relationship between the Chappel Limestone reefs and the adjacent and overlying units helps to predict areas that will contain more potential for unconventional completions in areas where the Barnett Shale is oil-rich.

## **9 Future Work**

Due to the local nature of this study within a smaller AOI, the data and results gathered from this study should be applied to a larger regional study along this Chappel

reef trend. Taking these interpretations to non-productive areas of this reef trend may identify additional sweet spots for potential horizontal completions in the Barnett Shale similar to this study. These prospective areas that exist will be located shoreward and proximal to the Chappel reef trend, as these areas will provide operators with better quality reservoir rock in the Chester Limestone and more thickness and lateral extent of the “Mississippian Shale” as a fracture barrier. The identification of similar “Mississippian Shale” petrophysical properties from multiple cores along this Chappel reef trend will be critical in maintaining this unit’s role as a fracture barrier for this Chester-Barnett play regionally.

## REFERENCES

- Amthor, J.E., and Friedman, G.M., 1991, Early-to-late diagenetic dolomitization of platform carbonates; Lower Ordovician Ellenburger Group, Permian Basin, West Texas and southeastern New Mexico: AAPG Bulletin, v. 75, p. 534.
- Asquith, G., August 11, 2014, OOIP Utilizing GEOCHEM [ECS] Data, Triple Combo Data Only, and Pyrolysis S1 Data, Permian Wolfcamp “A” and “B” Shales, *in* Midland, TX, AAPG, p. 1-29.
- Baruch, E.T., Slatt, R.M., and Marfurt, K.J., 2012, Seismic stratigraphic analysis of the Barnett Shale and Ellenburger unconformity southwest of the core area of the Newark East Field, Fort Worth Basin, Texas: AAPG Memoir, v. 97, p. 403-418.
- Burgess, W. J., 1976, Geologic evaluation of mid-continent and Gulf coast areas; plate tectonics view: Gulf Coast Association of Geological Societies Transactions, v. 26, p. 132-143.
- Chafetz, H. S., and Reid, A., 2000, Syndepositional shallow-water precipitation of glauconitic minerals: Sedimentary Geology, v. 136, no. 1–2, p. 29-42.
- Chalmers, G.R., 2016, Souring of kaybob duvernay wells: investigation of frac barrier effectiveness, completions design and pre-duvernay structural features: Abstracts: Annual Meeting - American Association of Petroleum Geologists, v. 2016.

Cooke, M.L., and Underwood, C.A., 2001, Fracture termination and step-over at bedding interfaces due to frictional slip and interface opening: *Journal of Structural Geology*, v. 23, p. 223-238.

Daniels, G., Mcphee, C.A., Sorrentino, Y.C., and McCurdy, P., Non-Destructive Strength Index Testing Applications for Sand Failure Evaluation, *in* SPE Asia Pacific Oil and Gas Conference and Exhibition, , Society of Petroleum Engineers, p. 22-24.

Dougherty, T., 1982, Statistical Trends of Activity in the Bend Arch Area: Dallas Geological Society, *Petroleum Geology of the Fort Worth basin and Bend arch area*, p. 3-7.

Doust, H., 2010, The exploration play; what do we mean by it? *AAPG Bulletin*, v. 94, p. 1657-1672.

Ewing, T.E., and Christensen, H., 2016, Texas through time; Long Star geology, landscapes, and resources: Austin, TX, United States (USA), University of Texas, Bureau of Economic Geology, Austin, TX, p. 431.

Flippin, J.W., 1982, The Stratigraphy, Structure, and Economic Aspects of the Paleozoic Strata in Erath County, North-Central Texas in Martin C. A., ed., *Petroleum Geology of the Fort Worth Basin and Bend Arch Area: Dallas Geological Society*, p. 129-155.

- Fu, Q., Horvath, S.C., Potter, E.C., Roberts, F., Tinker, S.W., Ikonnikova, S., Fisher, W.L., and Yan, J., 2015, Log-derived thickness and porosity of the Barnett Shale, Fort Worth Basin, Texas; implications for assessment of gas shale resources: AAPG Bulletin, v. 99, p. 119-141.
- Henry, J.D., 1982, Stratigraphy of the Barnett shale (Mississippian) and associated reefs in the northern Fort Worth Basin, in Martin C. A., ed., Petroleum Geology of the Fort Worth Basin and Bend Arch Area: Dallas Geological Society, p. 157-178.
- Jarvie, D.M., Hill, R.J., Ruble, T.E., and Pollastro, R.M., 2007, Unconventional shale-gas systems; the Mississippian Barnett Shale of North-Central Texas as one model for thermogenic shale-gas assessment: AAPG Bulletin, v. 91, p. 475-499.
- Kerans, C., 1988, Karst-controlled reservoir heterogeneity in the Ellenburger Group carbonates of west Texas: AAPG Bulletin, v.72, p.1160-1183.
- King, D.T., Jr, 1986, Waulsortian-type buildups and resedimented (carbonate-turbidite) facies, Early Mississippian Burlington Shelf, central Missouri: Journal of Sedimentary Petrology, v. 56, p. 471-479.
- Knebel, R.M., 1982, Mississippian Structural Implications at the Shirk Field Complex Young County, Texas in Martin C. A., ed., Petroleum Geology of the Fort Worth Basin and Bend Arch Area: Dallas Geological Society, p. 369-376.

Manger, W. L., Evans, K. R., 2012, An introduction to the Lower Mississippian (Kinderhookian-Osagean) geology of the tri-state region, southern ozarks, Atlas Resource Partners, L. P. Fieldbook, p. 15-81.

Marra, K.R., Charpentier, R.R., Schenk, C.J., Lewan, M.D., Leathers-Miller, H.M., Klett, T.R., Gaswirth, S.B., Le, P.A., Mercier, T.J., Pitman, J.K., and Tennyson, M.E., 2015, Assessment of undiscovered shale gas and shale oil resources in the Mississippian Barnett Shale, Bend Arch-Fort Worth Basin Province, north-central Texas: Fact Sheet - U.S.Geological Survey, p. 1-2.

McClave, G. A., 2014, Correlation of Rebound-Hammer Rock Strength With Core and Sonic-log Derived Mechanical Rock Properties in Cretaceous Niobrara and Frontier Formation Cores, Piceance Basin, Colorado, *in* Unconventional Resources Technology Conference, Denver, Colorado, 25-27 August 2014: Society of Exploration Geophysicists, American Association of Petroleum Geologists, Society of Petroleum Engineers, p. 847-863.

Monroe, R.M., and Breyer, J.A., 2012, Shale wedges and stratal architecture, Barnett Shale (Mississippian), southern Fort Worth Basin, Texas: AAPG Memoir, v. 97, p. 41-45.

Montgomery, S.L., Jarvie, D.M., Bowker, K.A., and Pollastro, R.M., 2005, Mississippian Barnett Shale, Fort Worth Basin, north-central Texas; gas-shale play with multitrillion cubic foot potential: AAPG Bulletin, v. 89, p. 155-175.

- Neuweiler, F., Larmagnat, S., Molson, J., and Fortin-Morin, F., 2014, Sponge spicules, silicification, and sequence stratigraphy: *Journal of Sedimentary Research*, v. 84, p. 1107-1119.
- Parker, D.C., 1989, The Fort Griffin N.E. (Mississippian) Field, Shackelford County, Texas, *in* Mear, C.E., McNulty, C.L. and McNulty, M.E., eds., *Petroleum Geology of Mississippian Carbonates of North Central Texas: Fort Worth, TX, United States (USA)*, Fort Worth Geol. Surv., Fort Worth, TX, p. 105-108.
- Pollastro, R.M., Hill, R.J., Jarvie, D.M., and Henry, M.E., March 1, 2003, Assessing undiscovered resources of the Barnett-Paleozoic total petroleum system, Bend Arch-Fort Worth Basin province, *in* : Tulsa, OK, United States (USA), American Association of Petroleum Geologists, Tulsa, OK, p. 1-17.
- Pollastro, R.M., Hill, R.J., Jarvie, D.M., and Adams, C., 2004, Geologic and organic geochemical framework of the Barnett-Paleozoic total petroleum system, Bend Arch-Fort Worth Basin, Texas: Annual Meeting Expanded Abstracts - American Association of Petroleum Geologists, v. 13, p. 113.
- Pollastro, R.M., Jarvie, D.M., Hill, R.J., and Adams, C.W., 2007, Geologic framework of the Mississippian Barnett Shale, Barnett-Paleozoic total petroleum system, Bend Arch-Fort Worth Basin, Texas: *AAPG Bulletin*, v. 91, p. 405-436.

Plummer, F.B., 1950, The Carboniferous rocks of the Llano region of Central Texas. Texas Univ., Bur. Econ. Geol. Publ. 4621, p. 473.

Raiswell, R., and Berner, R.A., 1985, Pyrite formation in euxinic and semi-euxinic sediments: American Journal of Science, v. 285, p. 710-724.

Rowe, H., Hughes, N., and Robinson, K., 2012, The quantification and application of handheld energy-dispersive X-ray fluorescence (ED-XRF) in mudrock chemostratigraphy and geochemistry: Chemical Geology, v. 324-325, p. 122-131.

Ruppel, S.C., 1984, The Chappel Formation (Mississippian) of the eastern Palo Duro Basin; development of a carbonate shoal: SEPM Core Workshop, v. 5, p. 58-93.

Ruppel, S.C., 1989, Summary of Mississippian stratigraphy in north and north central Texas: Fort Worth, TX, United States (USA), Fort Worth Geol. Surv., Fort Worth, TX, p. 7.

Sloss, L. L., 1976, Areas and volumes of cratonic sediments, western North America and Eastern Europe: Geology, v. 4, p. 272-276.

Turner, G. I., 1957, Paleozoic stratigraphy of the Fort Worth basin, in W. C. Bell ed., Abilene and Fort Worth Geological Societies Joint Field Trip Guidebook, p. 57-77.

Washburn, J.R.H., 1978, Deposition, Diagenesis and Porosity Relationships of the Mississippian Chappel Limestone, Master of Science Thesis, Texas Tech University, p. 180.

Wood, S.G., 2013, Lithofacies, depositional environments, and sequence stratigraphy of the Pennsylvanian (Morrowan-Atokan) Marble Falls Formation, central Texas, Master of Science Thesis, Texas University, p. 276.

Zahm, C.K., and Enderlin, M., 2010, Characterization of rock strength in Cretaceous strata along the Stuart City Trend, Texas: Transactions - Gulf Coast Association of Geological Societies, v. 60, p. 693-702.

Zhao, H., Givens, N.B., Curtis, B., Hill, R.J., and Jarvie, D.M., 2007, Thermal maturity of the Barnett Shale determined from well-log analysis: AAPG Bulletin, v. 91, p. 535-549.

**APPENDIX**

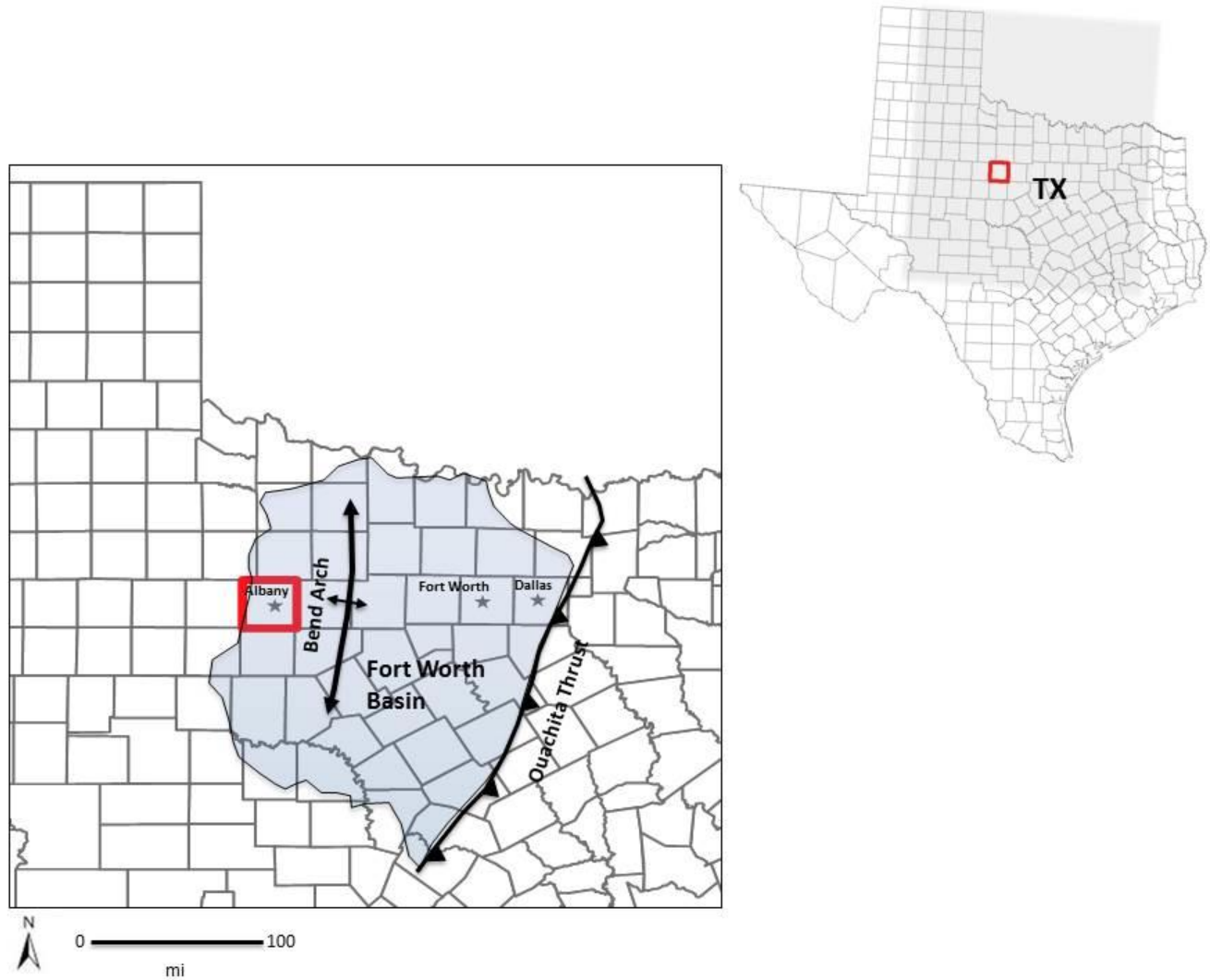


**Fig. 1:** Map of the state of Texas with the Fort Worth Basin shaded in blue and the major geologic components of the Fort Worth Basin labeled. The AOI (area of interest) is located in Shackelford County (outlined in red), west of the Bend Arch.

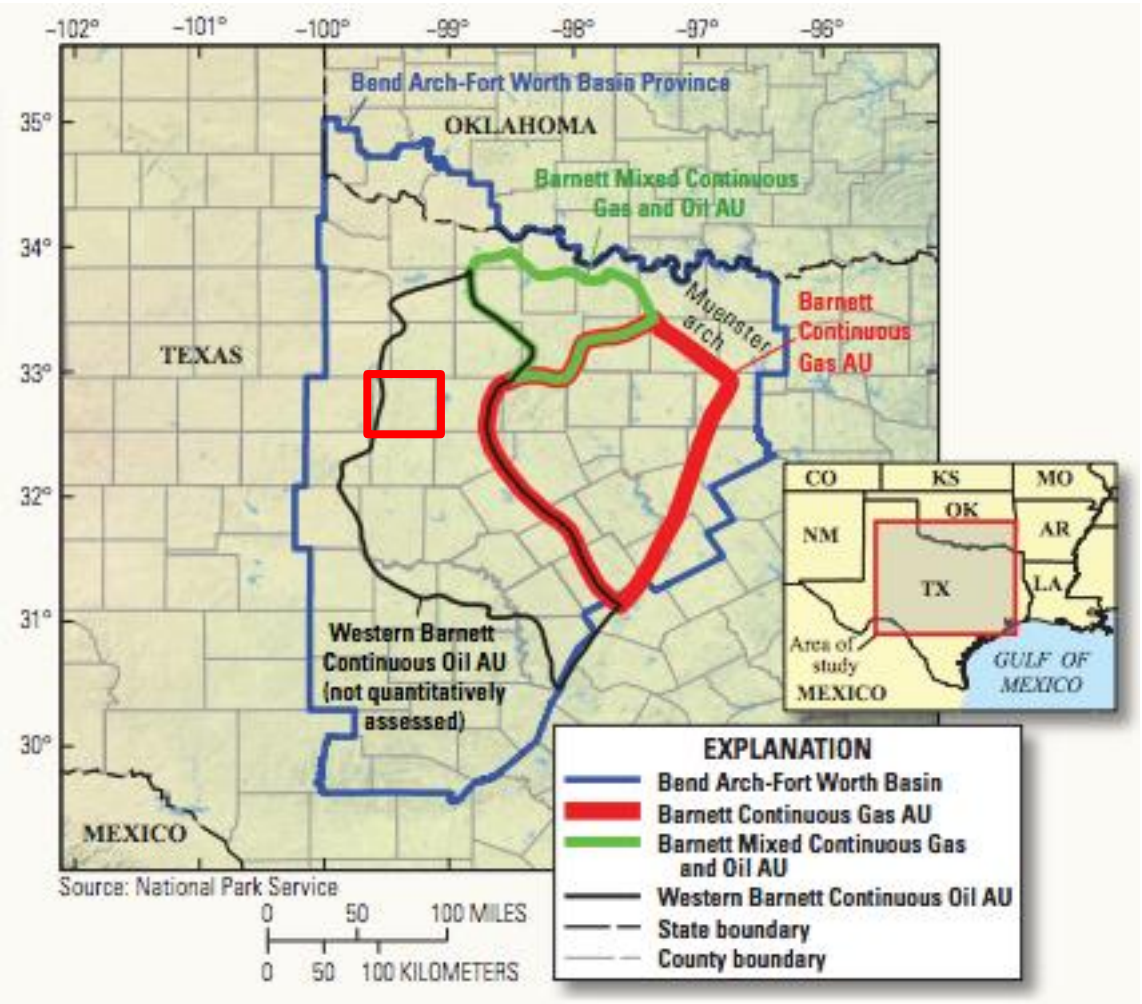


**Fig. 2:** The productivity of the Barnett Shale as defined by the continuous accumulation regions (modified from Marra et al., 2015). Shackelford County is outlined in the red rectangle. The AOI is located in the continuous oil accumulation region.

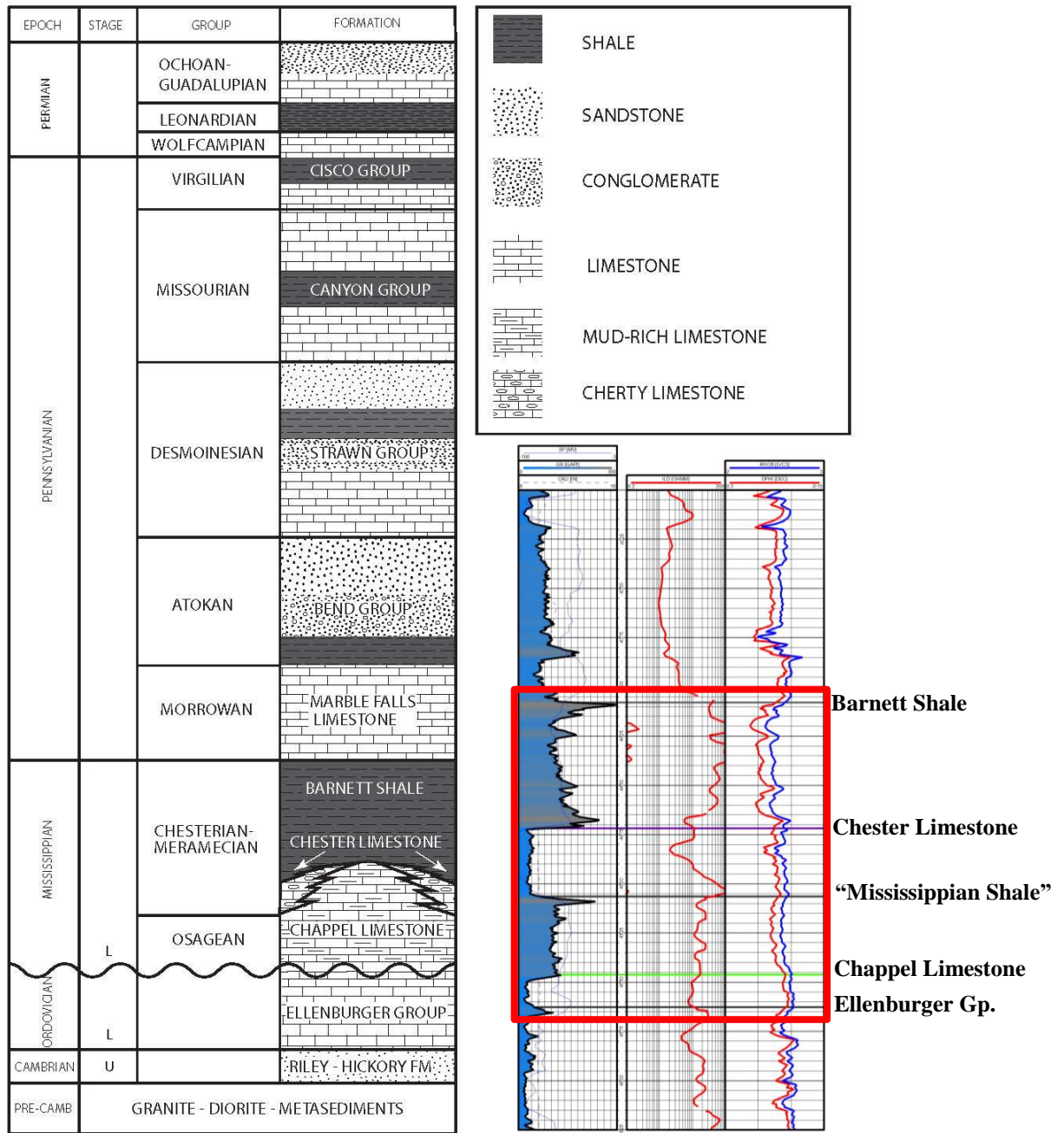


**Fig. 3:** Stratigraphic column showing the general geology of Shackelford County and the relative position of the units associated with the Chester-Barnett Shale play. The type log from the Lonestar McFarlane 1 well is shown next to the stratigraphic column to show the wireline log response of each unit. The Chester-Barnett play units are labeled and outlined in red.

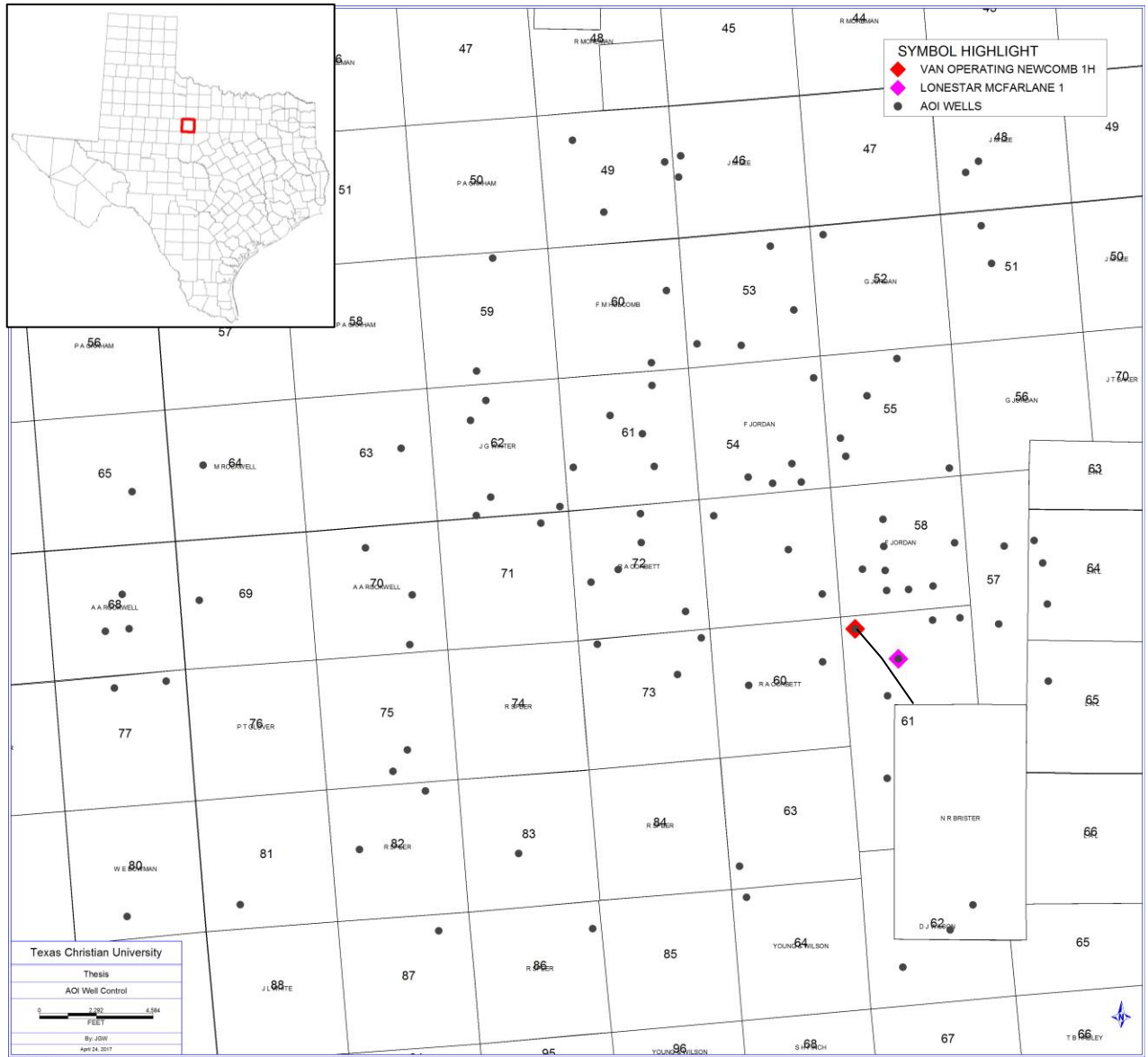


**Fig. 4:** Map of the AOI within southern Shackelford County that shows the location of the type log from the Lonestar McFarlane 1 and the location of the Van Operating Newcomb 1H well. The wells highlighted are the ones that were used as well control to create the subsurface maps.

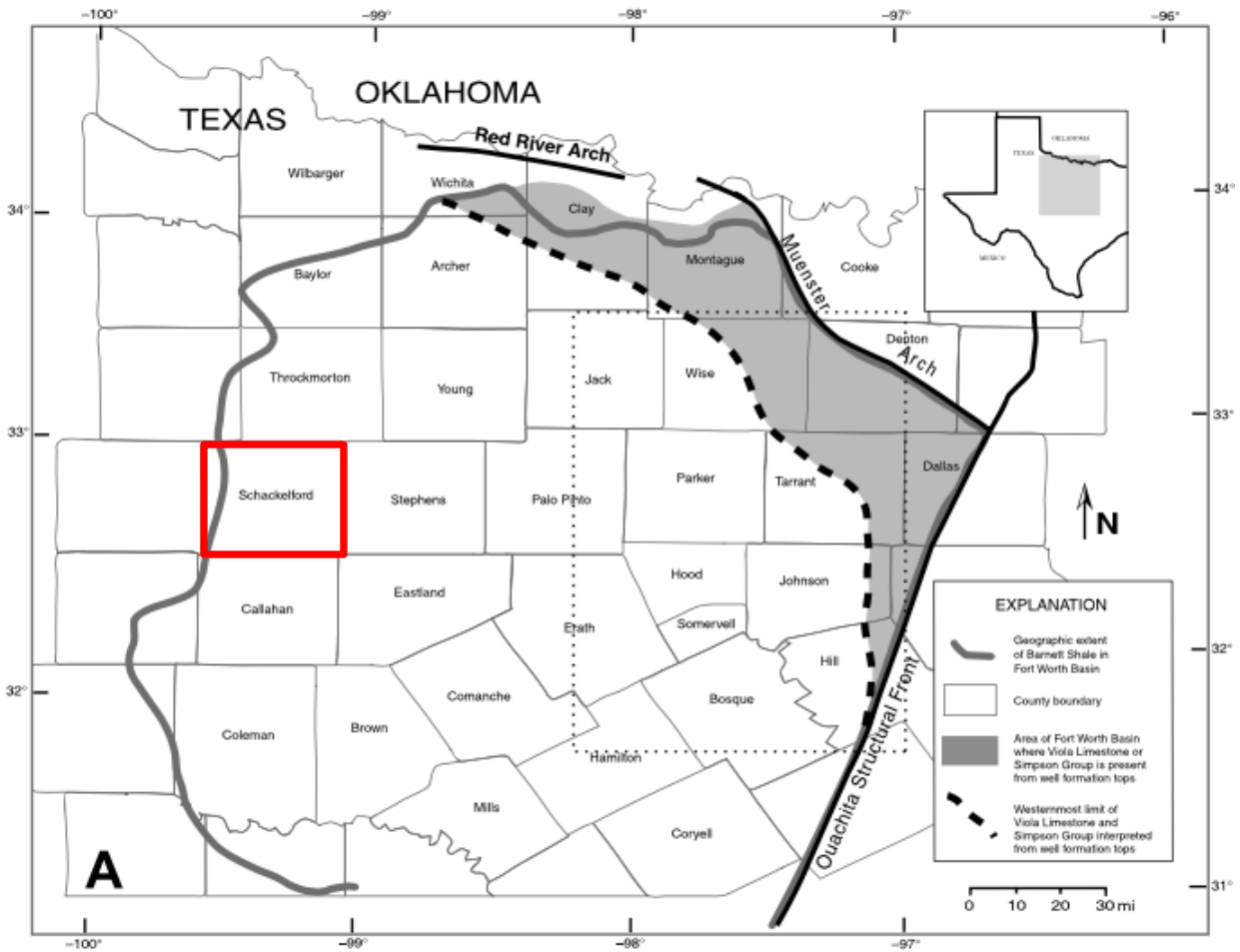


**Fig. 5:** Map showing the extent of the Viola Limestone (dotted line) and the outline of Shackelford County (red) (modified from Pollastro et al., 2007). This unit overlies the Ellenburger when present and functions as a fracture barrier for the play. In areas where the Viola is absent, completed wells have frequently produced large volumes of water.



**Fig. 6:** Photograph of the Equotip Bambino micro-rebound hammer and showing how it was used on the EOG W.B. Ranch #3 core. This tool gathers information about relative rock strength by taking measurements perpendicular to the thickest portion of the slabbed core.

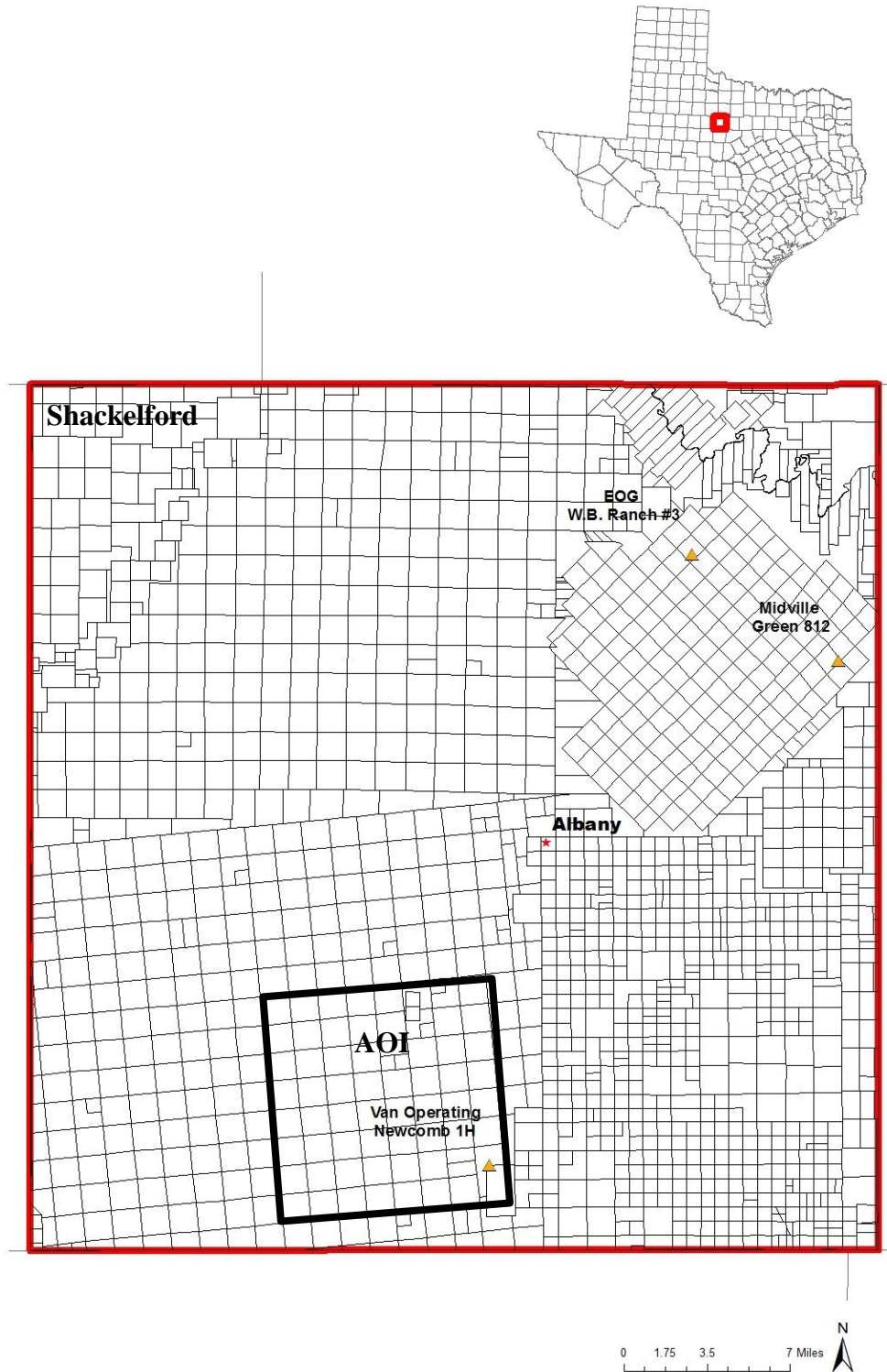
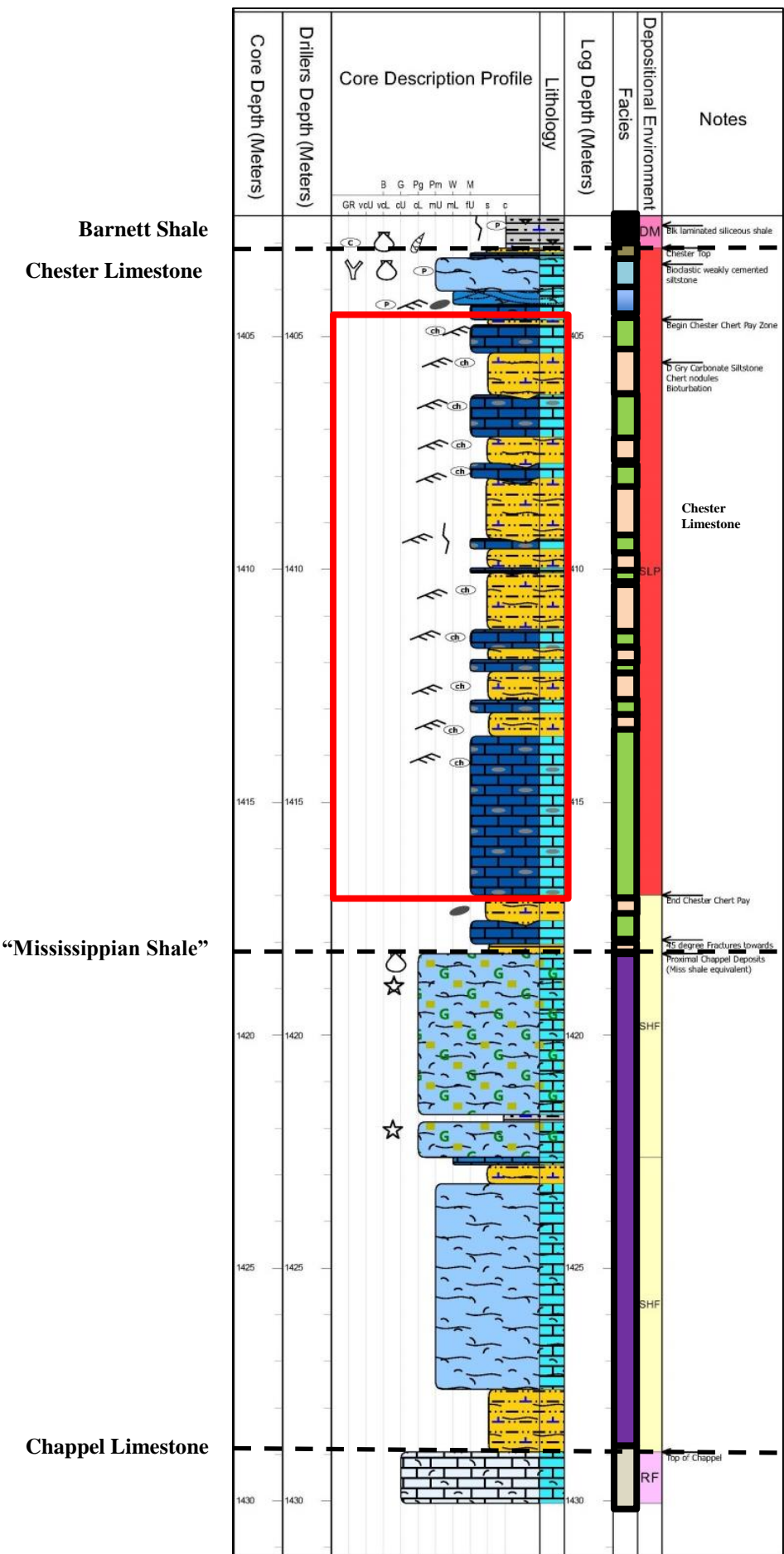


**Fig 7:** Map of Shackelford County shows the sections and townships. The AOI of this study is shown in the black towards the southern portion of the county. The locations of the cores from the EOG Resources and Midville Energy wells are shown relative to the Van Operating well.



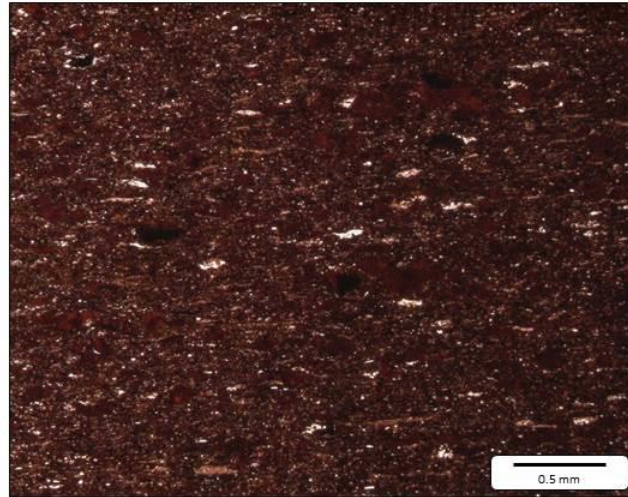


**Facies Legend**

- A
- B
- C
- D
- E
- F
- G
- H

**Fig. 9:** Core description of the W.B. Ranch #3 core from the top of the Chappel Limestone to the base of the Barnett Shale. Grain coarseness is indicated by the width of the coarseness profile. Any fossils are noted to the left of the lithology track. Relative depositional environment is indicated. The Chester cherty zone is outlined in red. The specific facies are noted by colors to the right of the lithology track.

# Facies A



Green 812 4516.3 ft

Barnett Shale: Black laminated siliceous mudrock that contains pyrite and vertical healed fractures

**Fig. 10A:** Photos of core and thin section examples of facies A within the Barnett Shale.

# Facies B

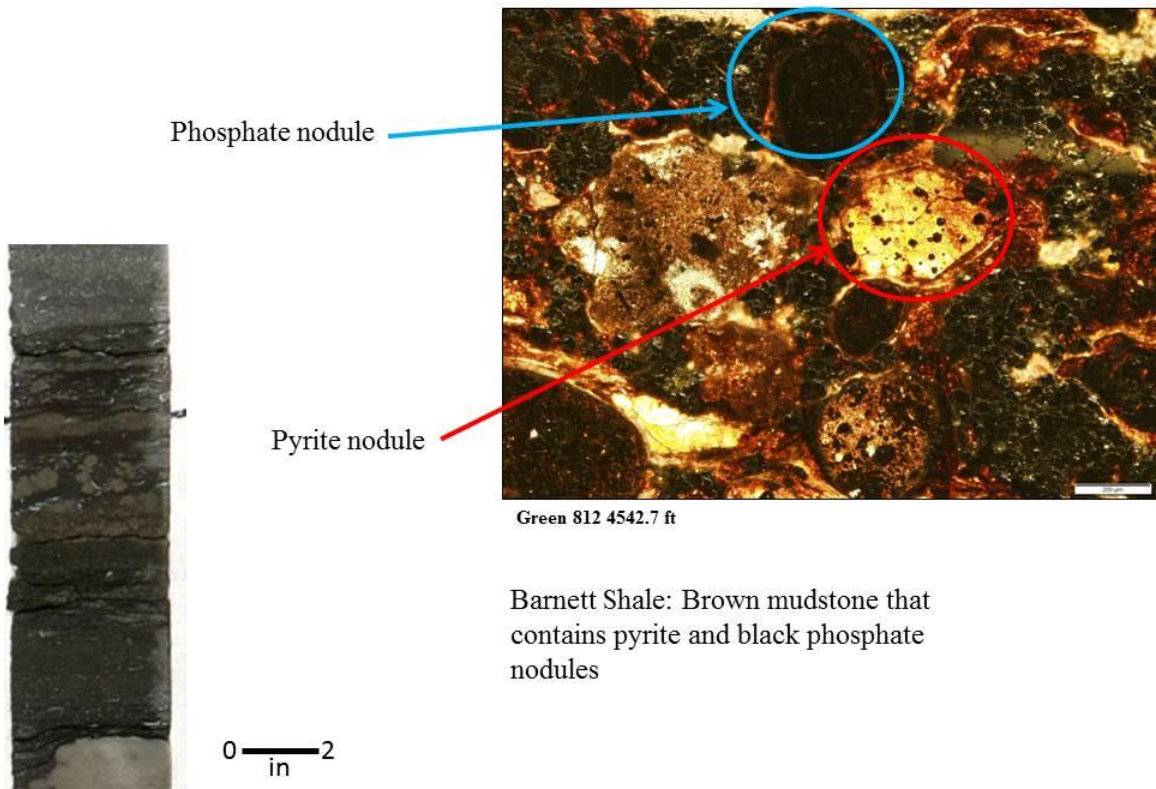
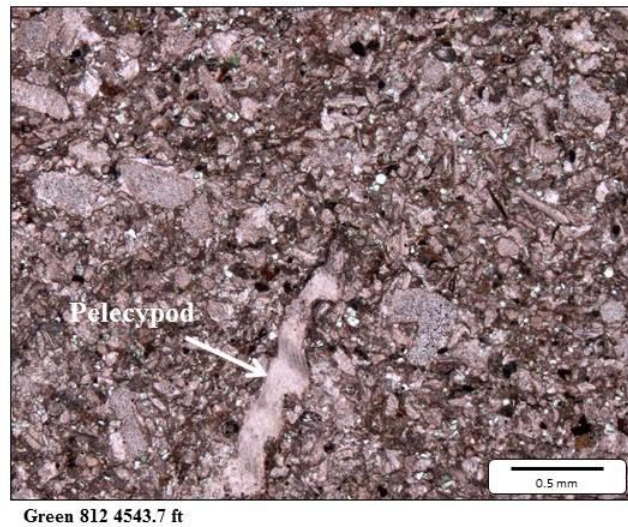
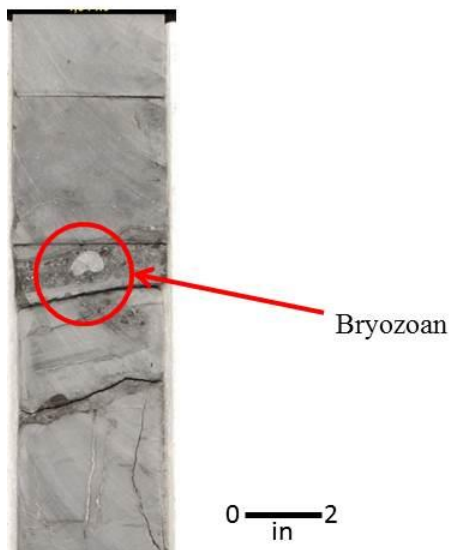


**Fig. 10B:** Photos of core and thin section examples of facies B within the Barnett Shale.

# Facies C



Chester Limestone: Light grey pelecypod packstone that contains bryozoans, weak laminations, and pyrite

**Fig. 10C:** Photos of core and thin section examples of facies C within the Chester Limestone.

# Facies D

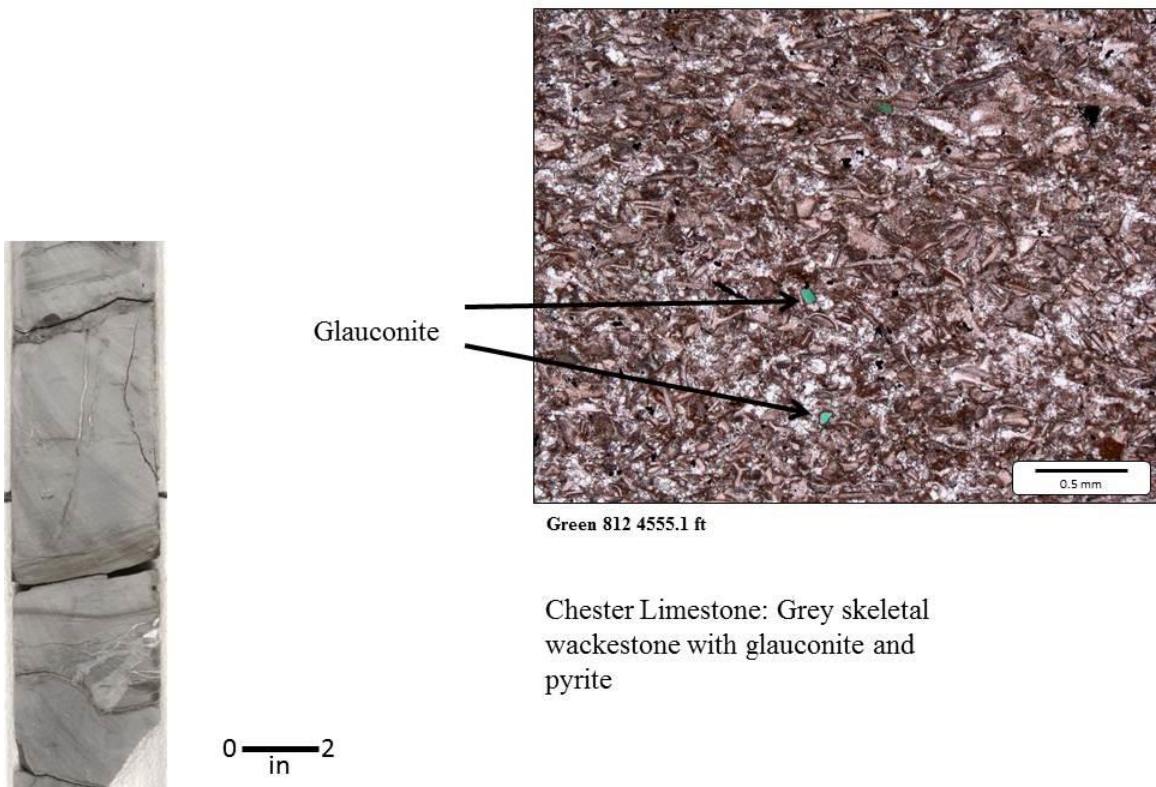
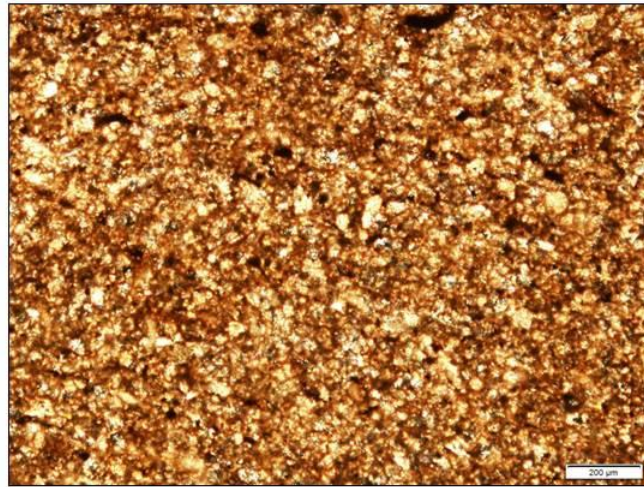
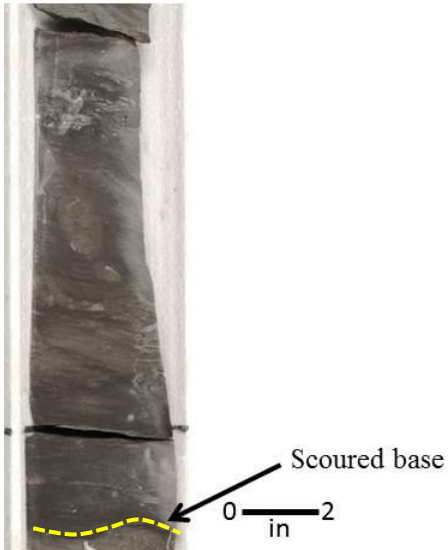


**Fig. 10D:** Photos of core and thin section examples of facies D within the Chester Limestone.

# Facies E

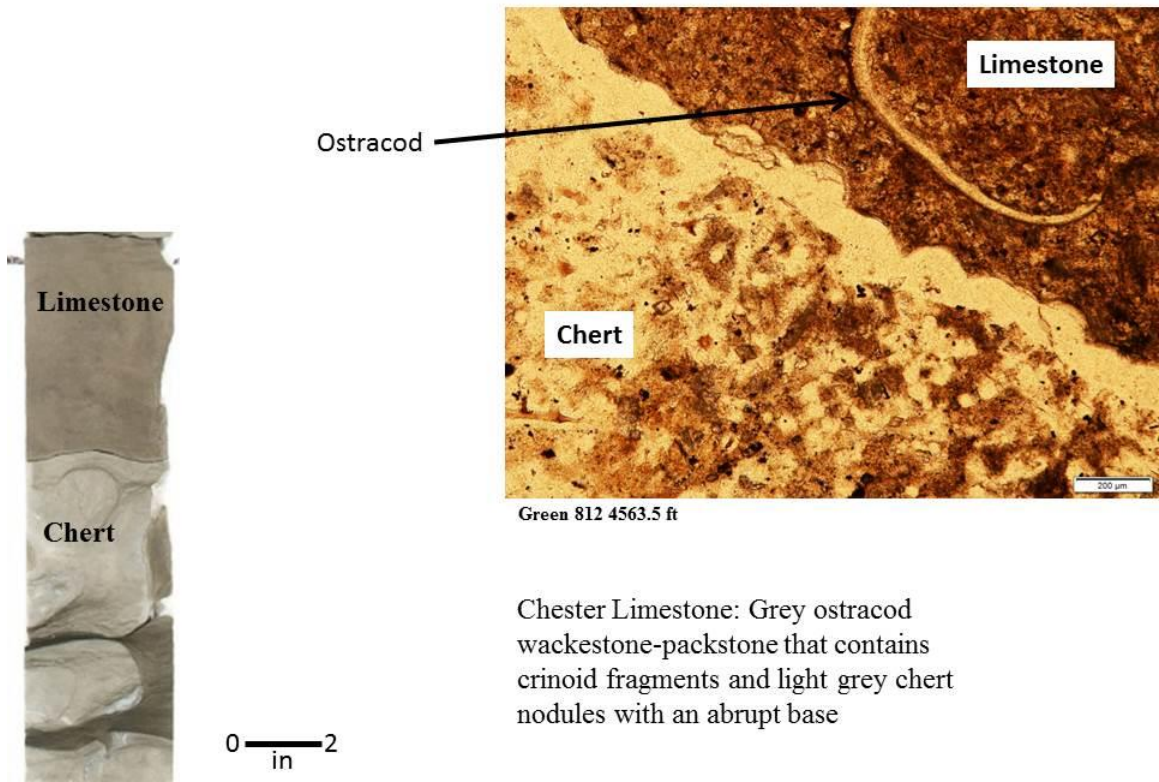


Green 812 4568.2 ft

Chester Limestone: Dark grey calcareous siltstone that contains ripples and light grey chert nodules with a commonly scoured base

**Fig. 10E:** Photos of core and thin section examples of facies E within the Chester Limestone cherty zone.

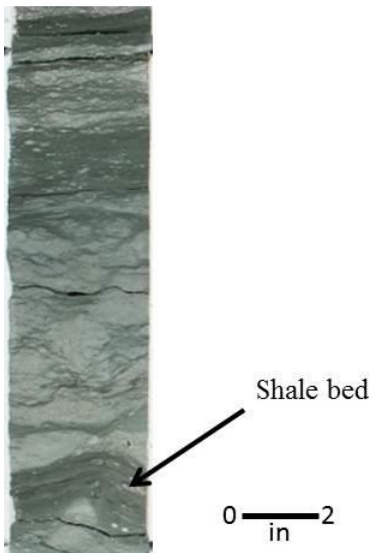
# Facies F



Chester Limestone: Grey ostracod wackestone-packstone that contains crinoid fragments and light grey chert nodules with an abrupt base

**Fig. 10F:** Photos of core and thin section examples of facies F within the Chester Limestone cherty zone.

## Facies G



“Mississippian Shale”: Grey wackestone-packstone that contains crinoid fragments, glauconite, and pyrite interbedded with thin dark grey, rippled mudrock beds

**Fig. 10G:** Photos of core and thin section examples of facies G within the “Mississippian Shale”.

# Facies H

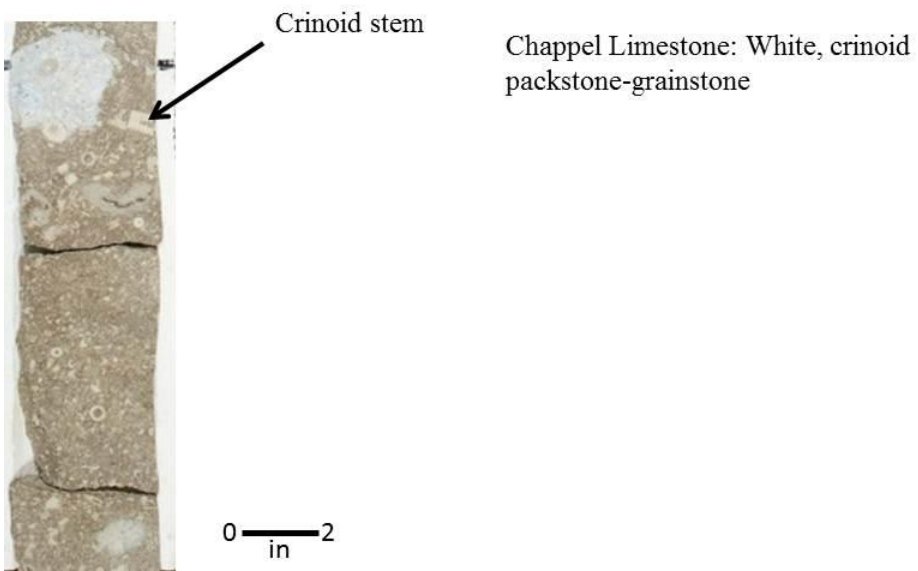


**Fig. 10H:** Photos of core and thin section examples of facies H within the Chappel Limestone.

### Depth vs UCS from EOG W.B. Ranch #3 Core

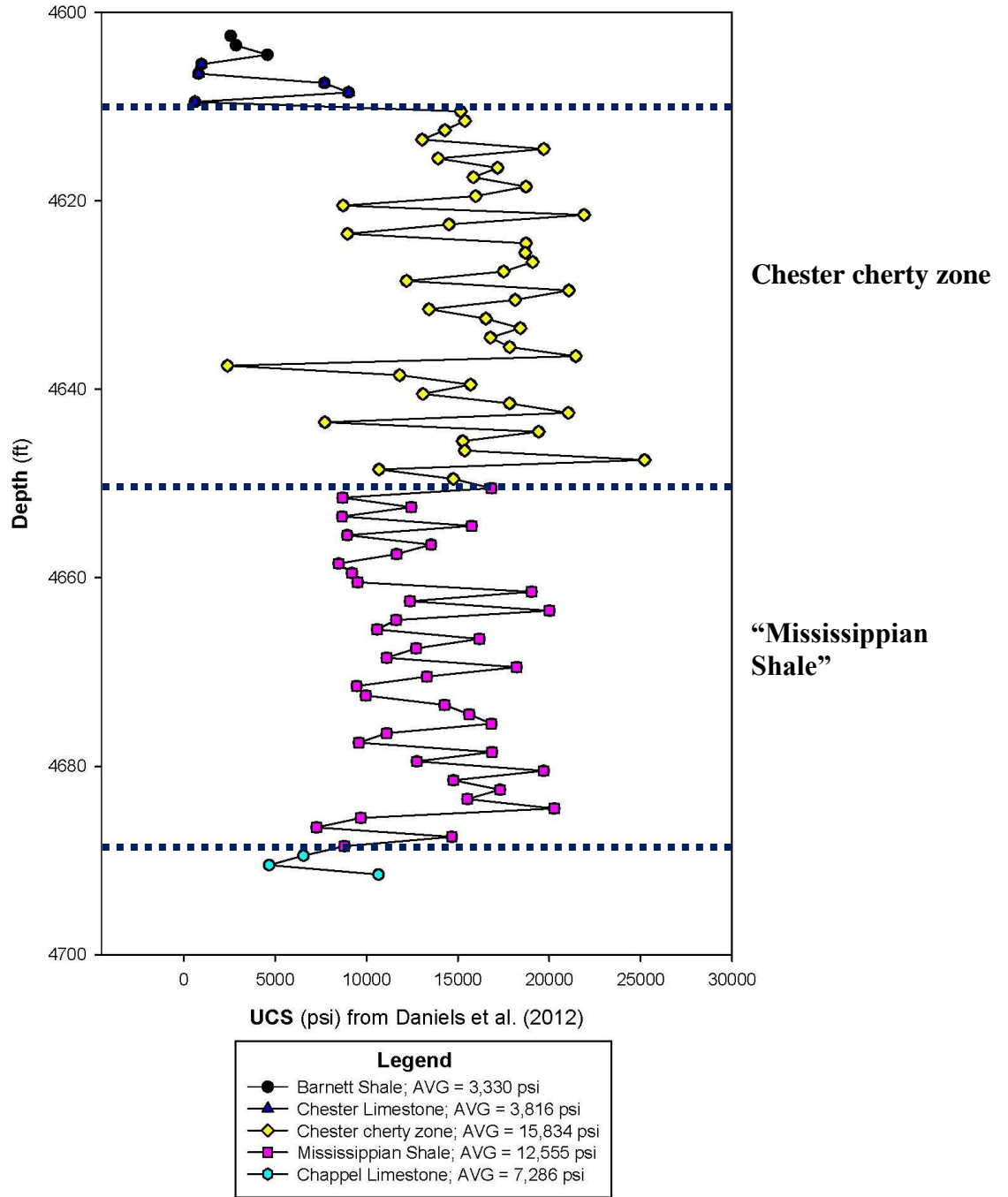


**Fig. 11:** Depth vs UCS calculated from the equation by Daniels et al. (2012) for the EOG W.B. Ranch #3 core. Each facies is separated out by color and shape of its symbol. Average UCS values for each facies are shown in the legend. Changes in rock mechanics can be inferred by combining this information with the lithology of each unit from the core description.

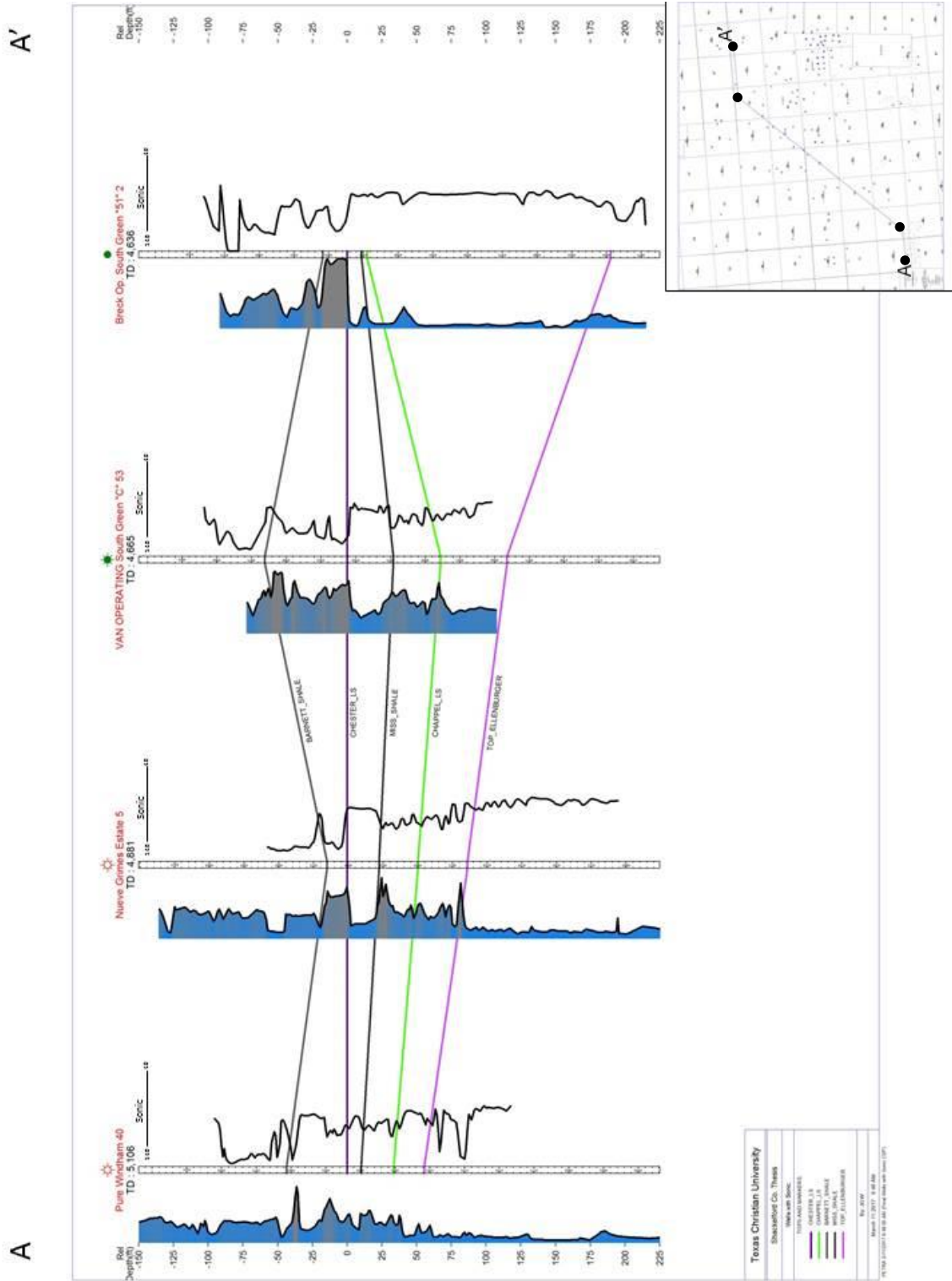


**Fig. 12:** Cross section A-A' shows the wells with sonic logs available for this study. The sonic data was compared to the results of the Bambino tests to determine rock strength and rock mechanics. Slower average sonic values were observed within the “Mississippian Shale” when compared to the Chester Limestone.

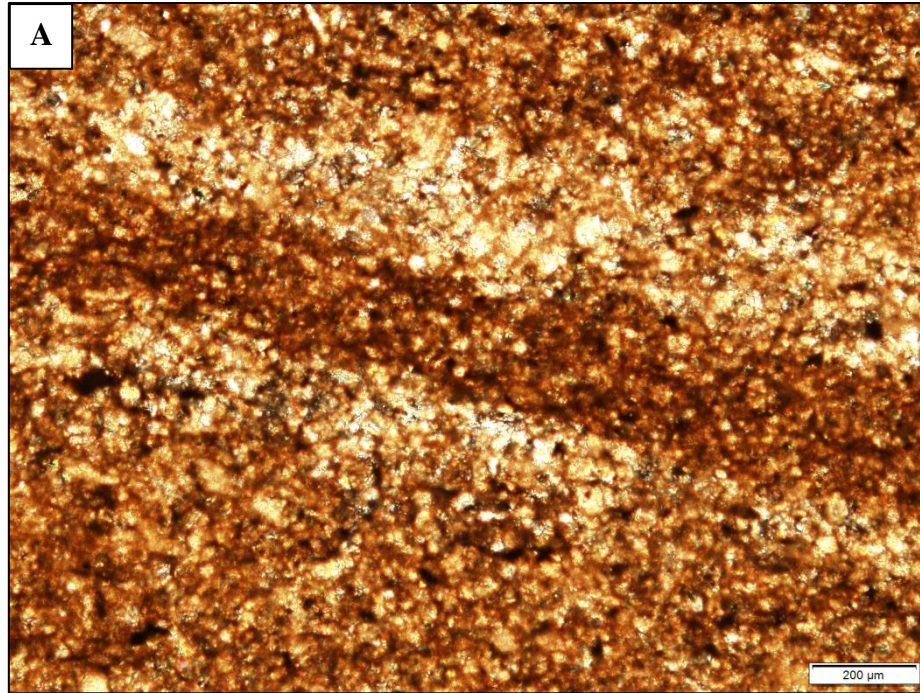


**Fig. 13A:** Thin section photomicrograph of facies E from 4,568.2 ft in the Green 812 core with 10x magnification, showing silt-sized quartz grains and planar horizontal laminations. **Fig. 13B:** Thin section photomicrograph of facies E from 4,568.2 ft in the Green 812 core with 20x magnification, showing silt-sized quartz grains.

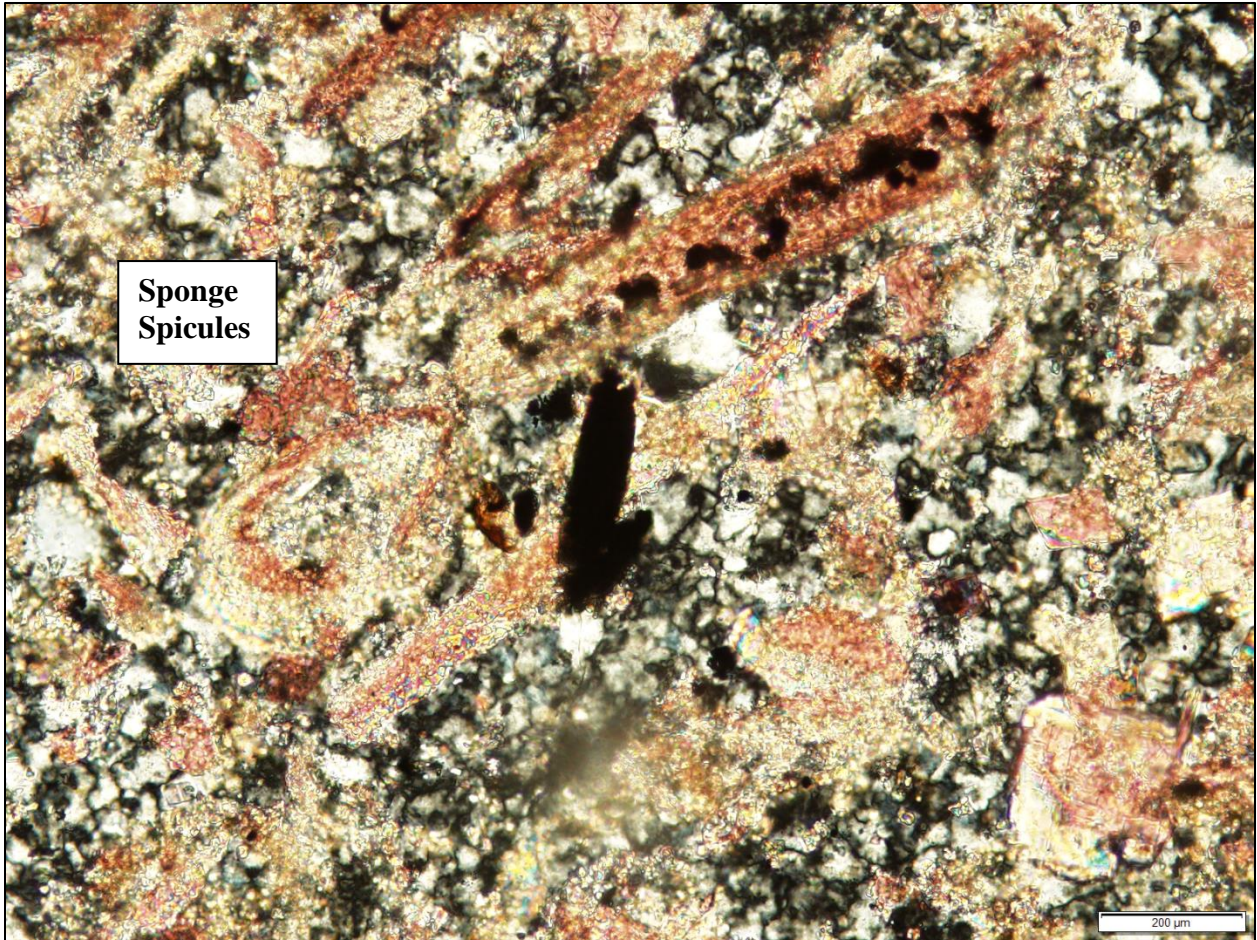


**Fig. 14:** Thin section photomicrograph of facies E from 4,548.1 ft in the Green 812 core with 20x magnification, siliceous sponge spicules found within the siltstone matrix of facies E. These sponge spicules are ~500 microns in length and are interpreted to be the silica source for the chert nodules found in the Chester Limestone.

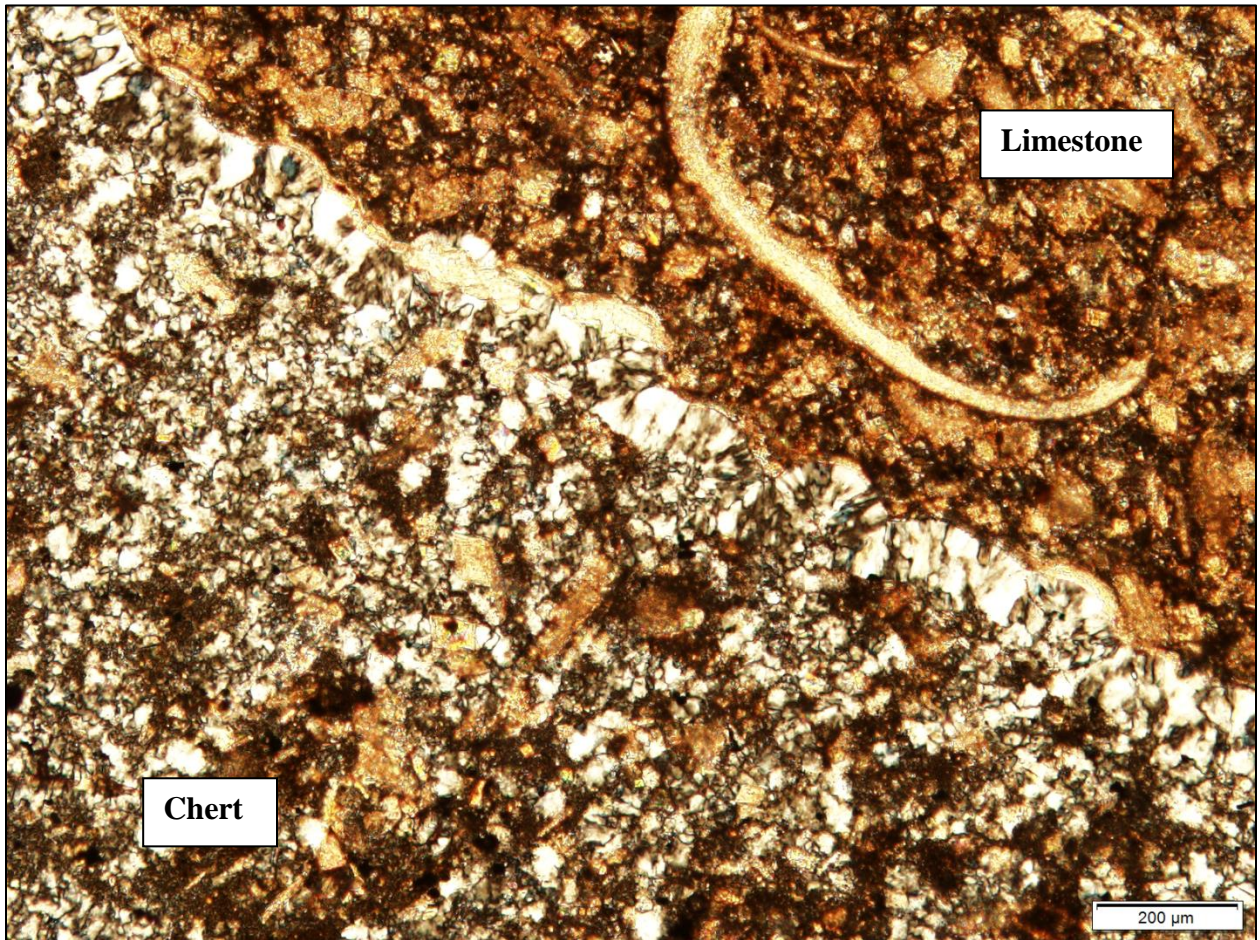


**Fig. 15:** Thin section photomicrograph of facies F from 4,563.5 ft in the Green 812 core that is 20x magnification and cross-polarized to show the quartz grains. This sample shows an ostracodal wackestone with a silty quartz matrix (stained pink) and part of a microcrystalline quartz chert nodule within the limestone.

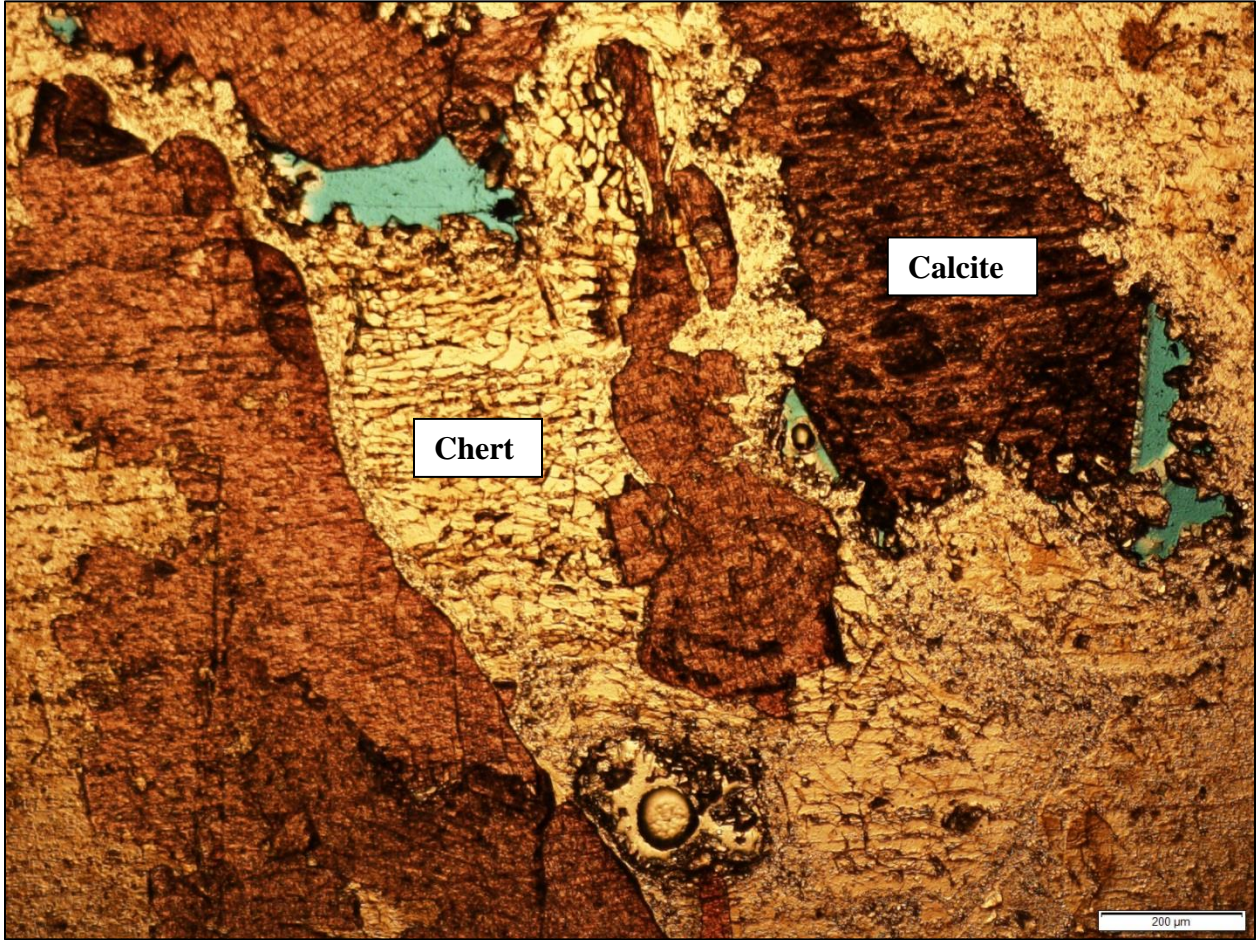
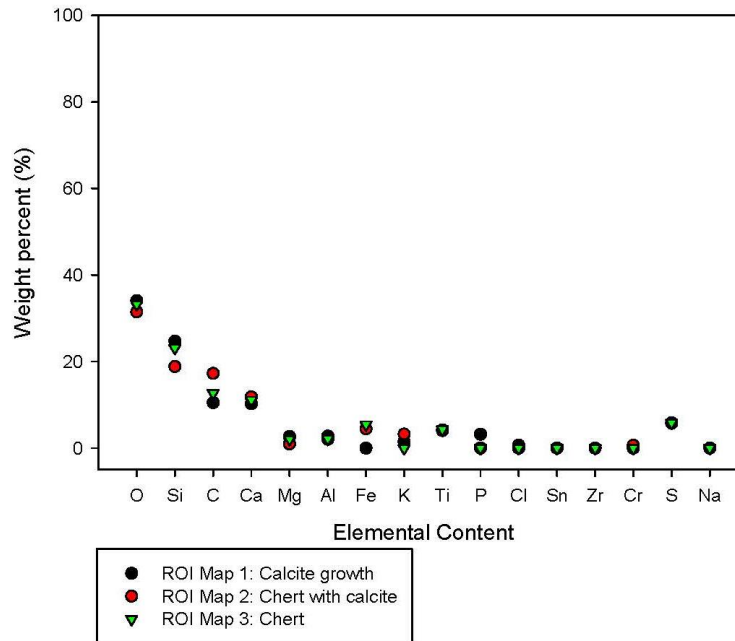


**Fig. 16:** Thin section photomicrograph of facies F from 4,563.1 ft in the Green 812 core that is 20x magnified. This photo shows pore space present in the chert nodules potentially created by the dissolution of calcite that formed in the interior of the chert. The pore spaces are close to 200 microns in length and are indicated by the blue epoxy. This type of secondary porosity may explain why the cherty facies of the Chester Limestone has quality reservoir attributes in some areas.

### Elemental Analysis of Facies F: Sample 1,390.95 m



### Elemental Analysis of Facies E: Sample 1,392.39 m

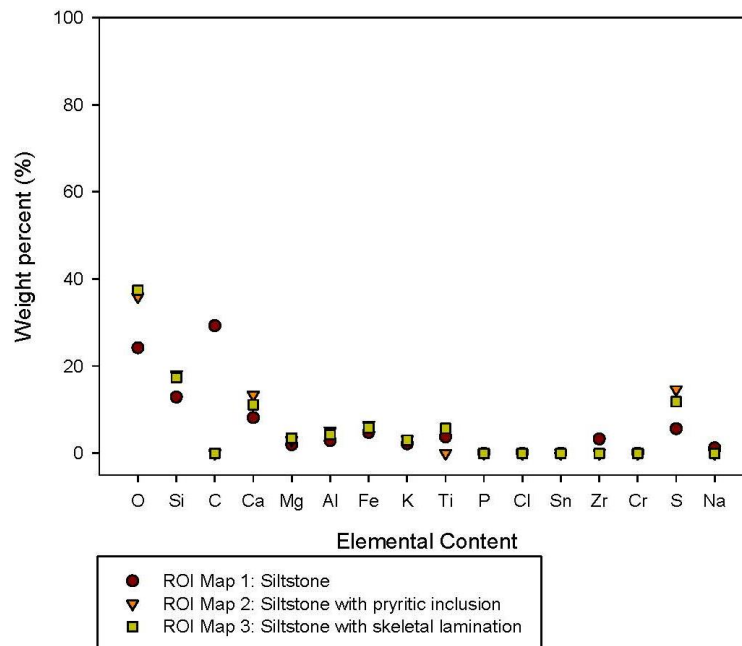


**Fig. 17:** The breakdown of elements present by weight percentage found in samples from facies E (sample 1,392.39 m) and facies F (sample 1,390.95 m) gathered from a BSE image and EDS software by Precimat Labs. Each ROI Map is composed of average values from individual points sampled.

## %Si vs %Al



**Fig. 18:** A chart of %Si vs %Al with values from both samples shown. This chart is used to make interpretations of the source of the silica as outlined in Rowe et al. (2012). The %Al is used as a proxy for clay minerals and is compared to %Si to determine a possible source of the silica found in the sample. Facies E falls closely in line with the clay line and is interpreted to be sourced by detrital silica (Rowe et al., 2012). Facies F shows some silica excess by values plotting above the clay line and is interpreted to be a biogenic silica source (Rowe et al., 2012).

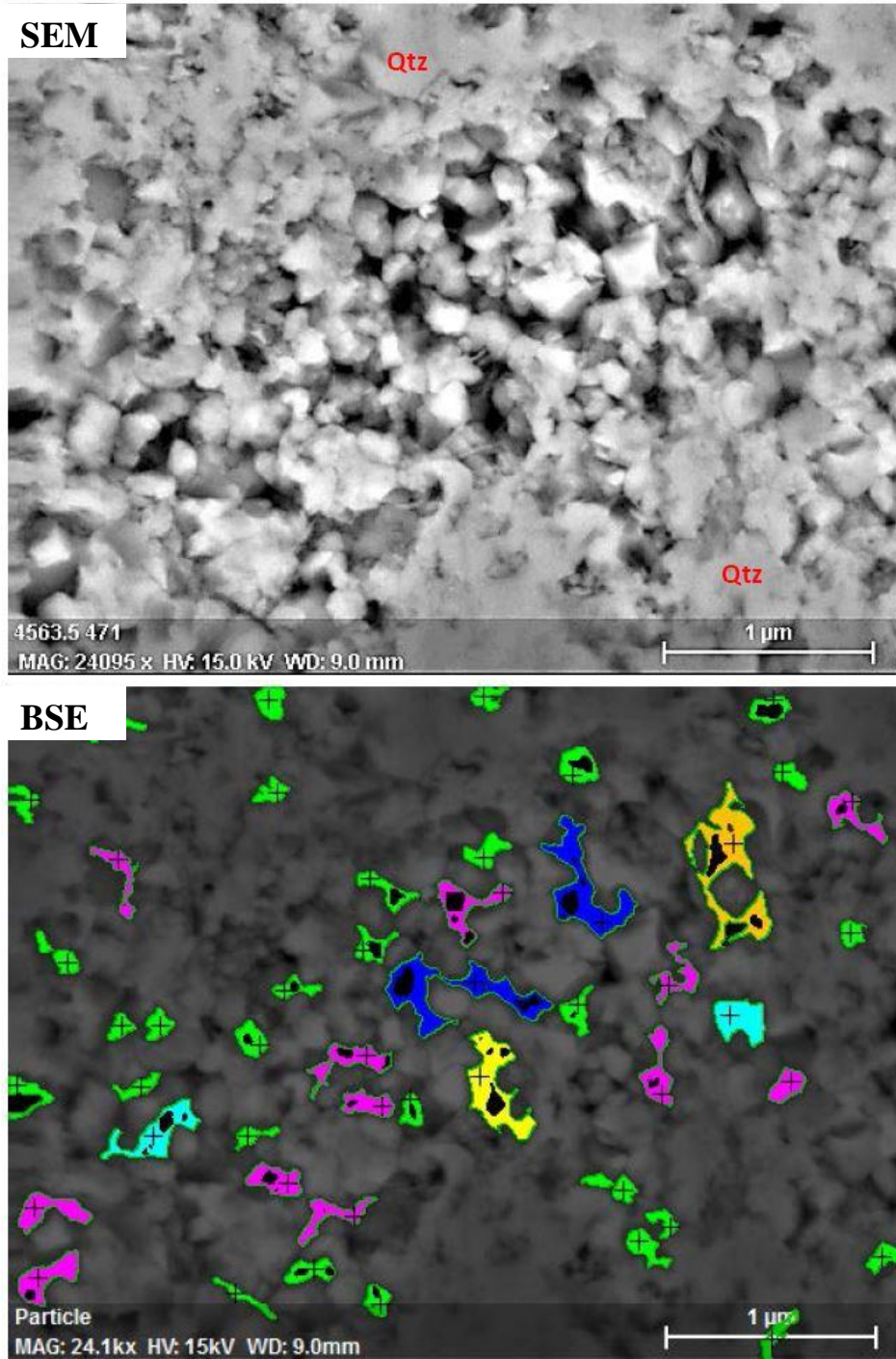


**Fig. 19:** A SEM and BSE photomicrograph that is magnified ~24,100x from a sample of facies F from the Green 812 core that identifies the dissolution porosity present within chert nodules. The microcrystalline quartz has voids between the grains that occurred due to diagenesis of calcite that was once present in the nodules. This represents the portion with the highest porosity in the Chester Limestone and is currently a target for conventional production. The colors ranging from light green to blue represent categories of the area of the pore features in the study. Green is the smallest and blue is the largest.

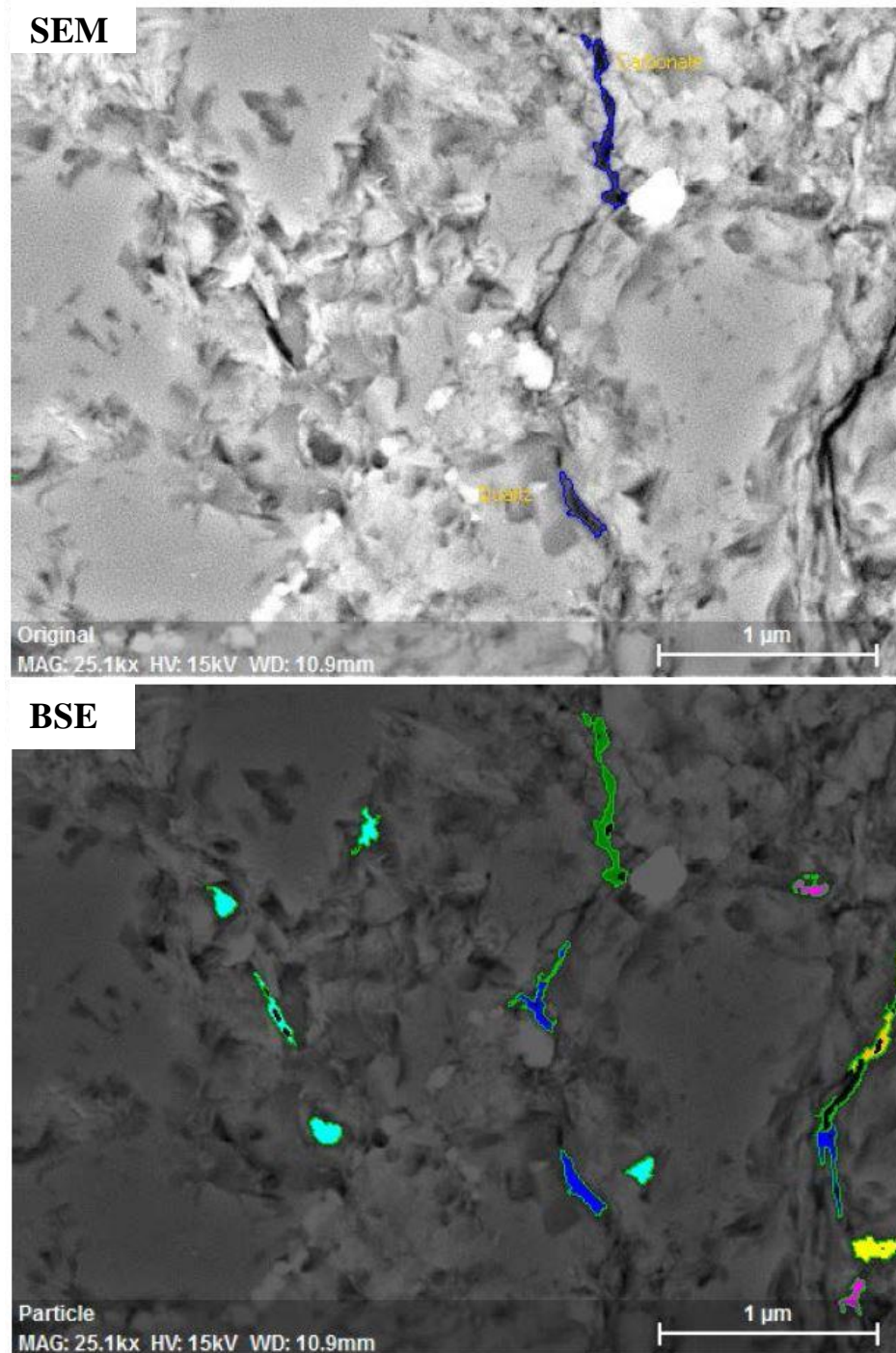


**Fig. 20:** A SEM and BSE photomicrograph that is magnified ~25,100x of facies E from the Green 812 core that identifies the matrix porosity present. The porosity present appears to be intergranular from the silt sized quartz grains present in this facies. The same colors are used for the area of the pore features in this figure as were in fig. 19.

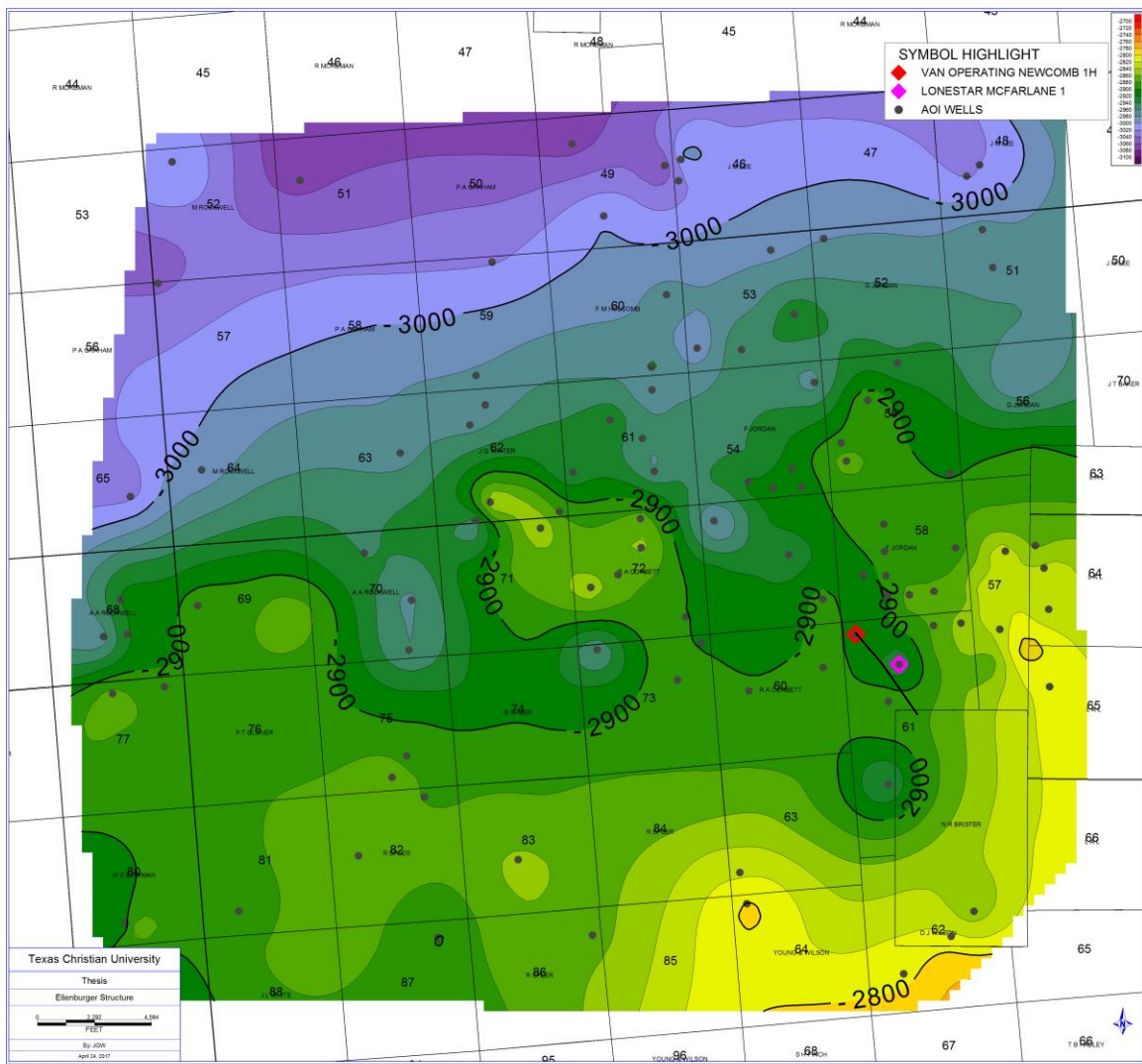


**Fig. 21:** A structural map made from the top of the Ellenburger Group. Depths are shown in subsea values. Elevation ranges from -3,100 ft up to -2,750 ft subsea. Purple is the deepest elevation and red is the highest elevation. Points used in mapping are posted in red. C.I. (contour interval) = 20 ft.

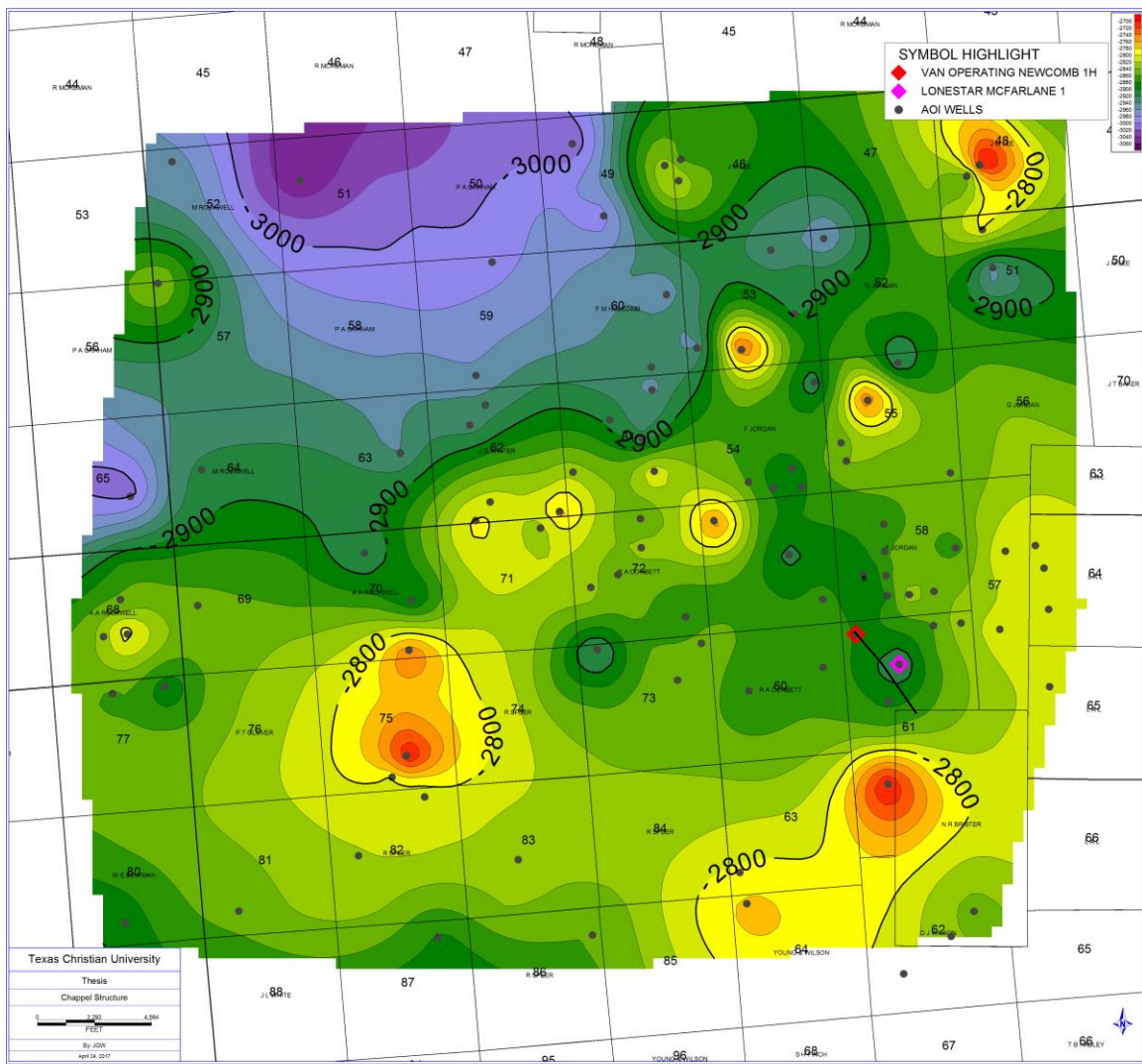


**Fig. 22:** A structural map made from the top of the Chappel Limestone. Depths are shown in subsea values. The elevation ranges from -3,000 ft up to -2,650 ft subsea. Purple is the deepest elevation and red is the highest elevation. Points used in mapping are posted in red. C.I. = 20 ft.

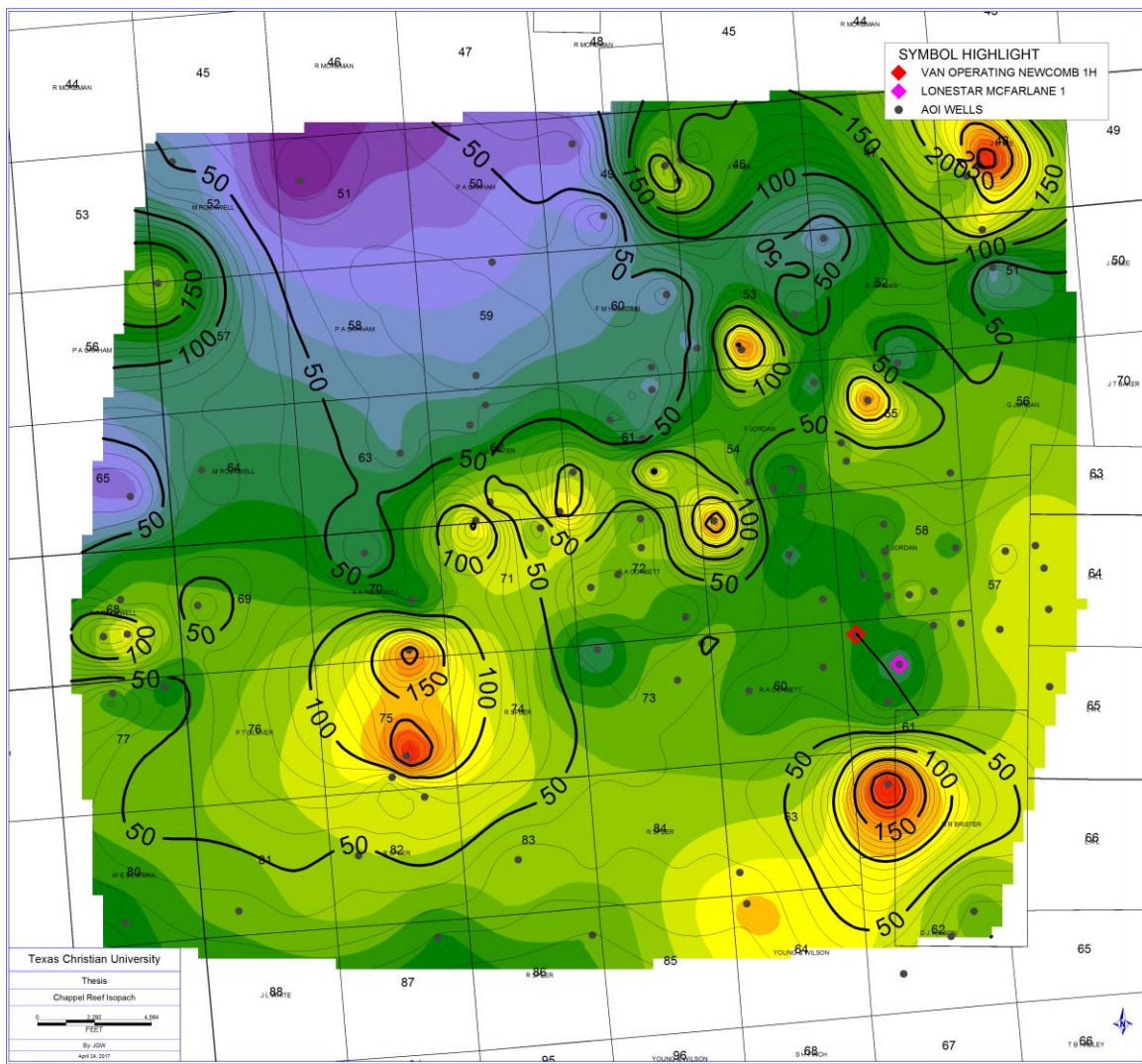


**Fig. 23:** This map shows the contours thickness of the Chappel Limestone overlaid with the structure of the Chappel Limestone (colors). Overlaying these two features helps to identify the location of the Chappel reefs in the AOI. Reefs were identified in areas with a thickness greater than 50 ft.

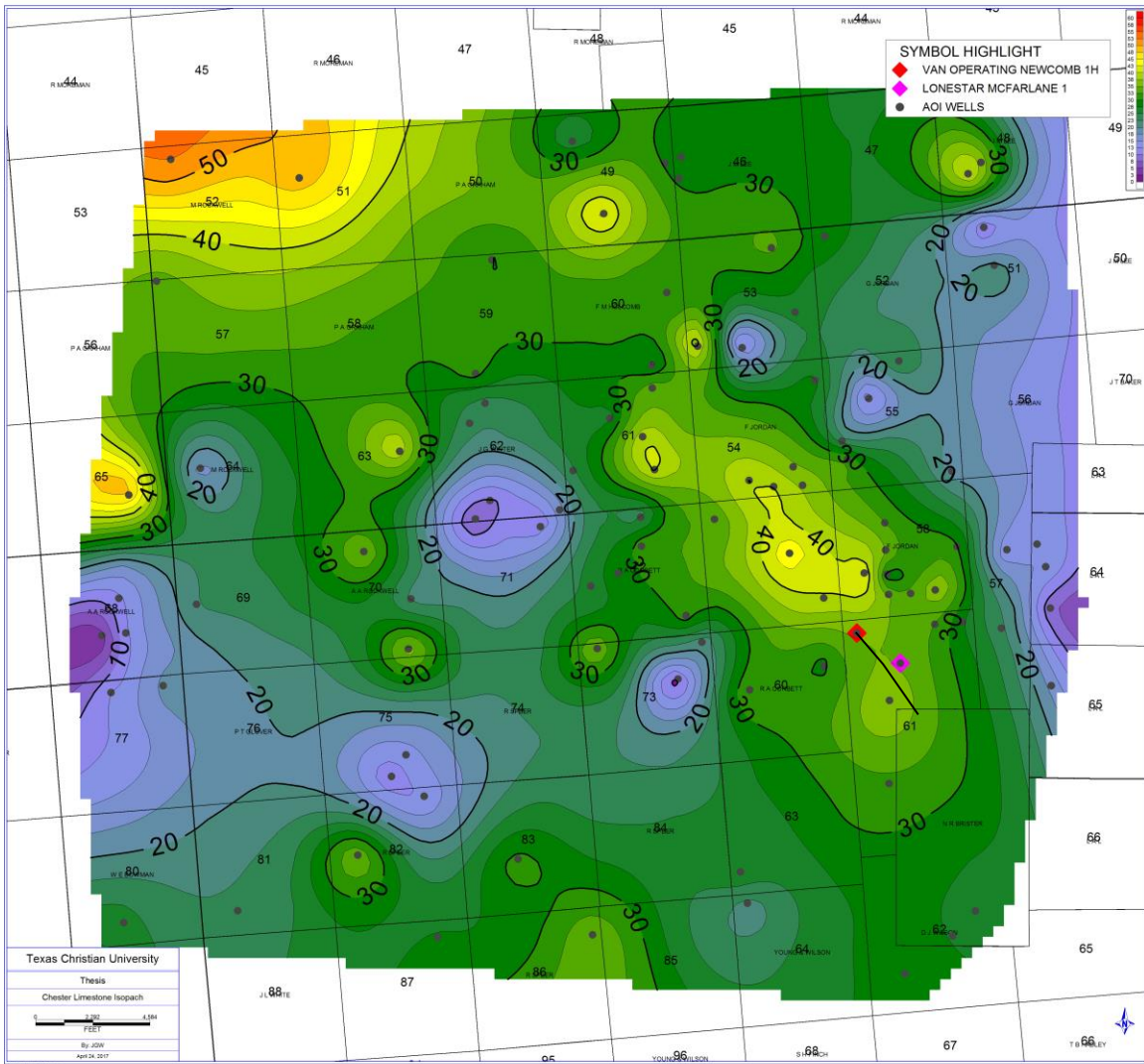


**Fig. 24:** An isopach (thickness) map of the Chester Limestone. Thickness ranges from 5' up to 55' in the Chester Limestone. Red is the thickest and purple is the thinnest. Abrupt thinning is observed on the crests of Chappel reefs. C.I. = 2.5 ft.

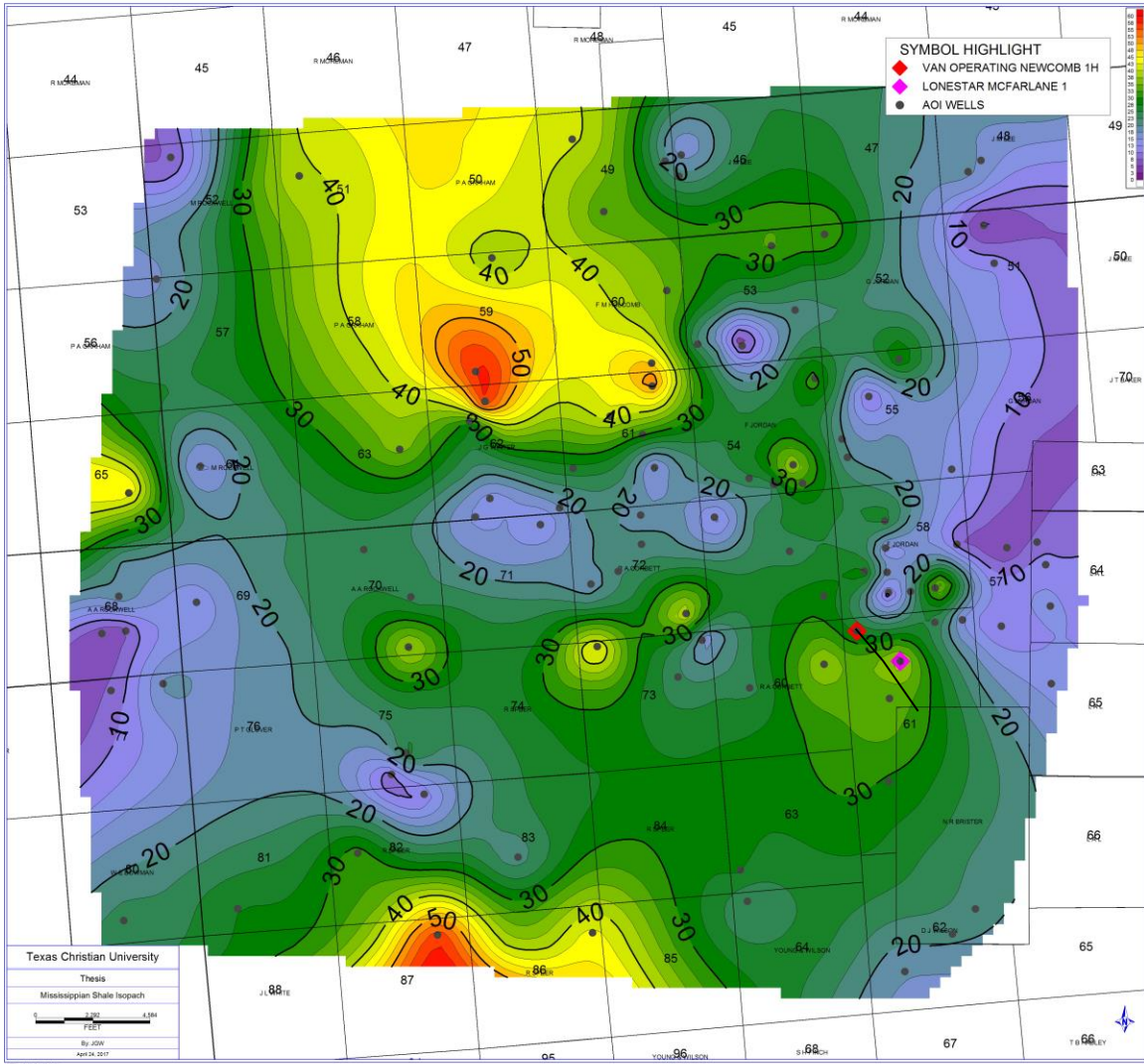


**Fig. 25:** An isopach (thickness) map of the “Mississippian Shale”. Thickness ranges from 3’ up to 60’ thick. Red is the thickest and purple is the thinnest. C.I. = 2.5 ft.

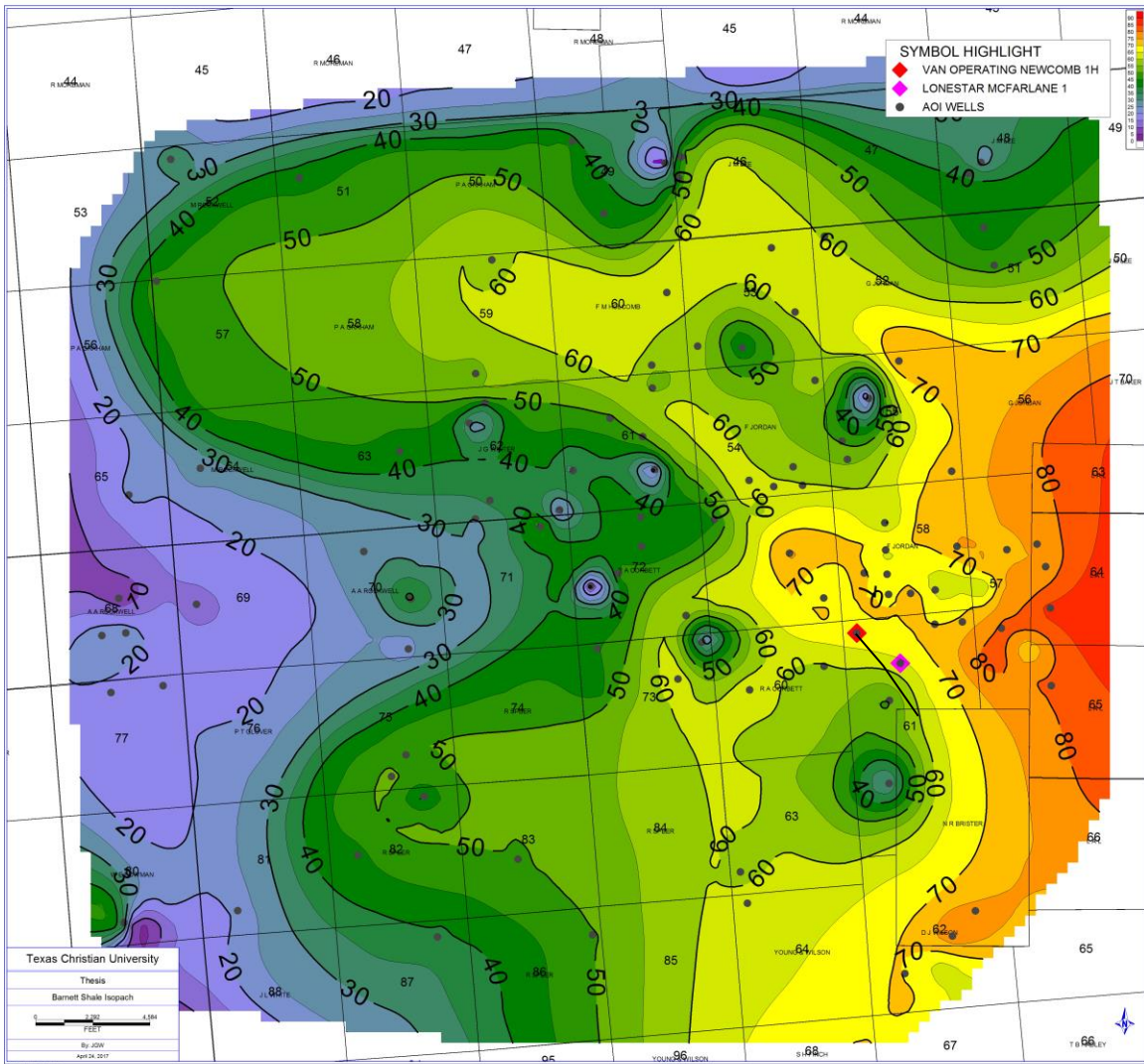


**Fig. 26:** An isopach (thickness) map of the Barnett Shale. Thickness ranges from 5’ up to 80’ thick. Red is the thickest and purple is the thinnest. Abrupt thinning can be noted over the crests of the pinnacle reefs. C.I. = 5 ft.

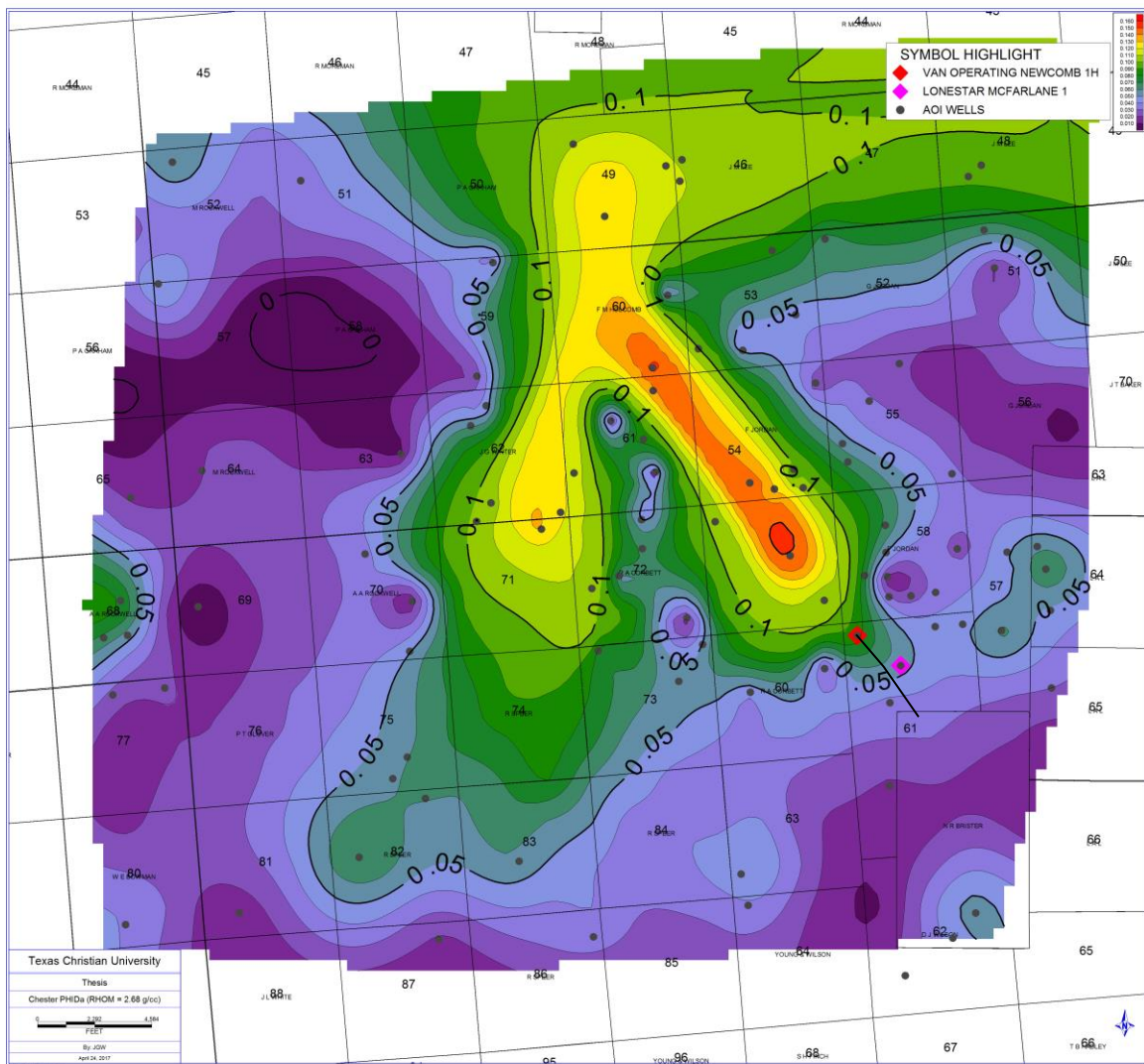


**Fig. 27:** The average calculated density porosity of the Chester Limestone. The matrix density used was 2.68 g/cc. The porosity values range from 0.02 up to 0.16. Purple represents the lowest porosity values and red represents the highest porosity values. C.I. = 0.01 (porosity).

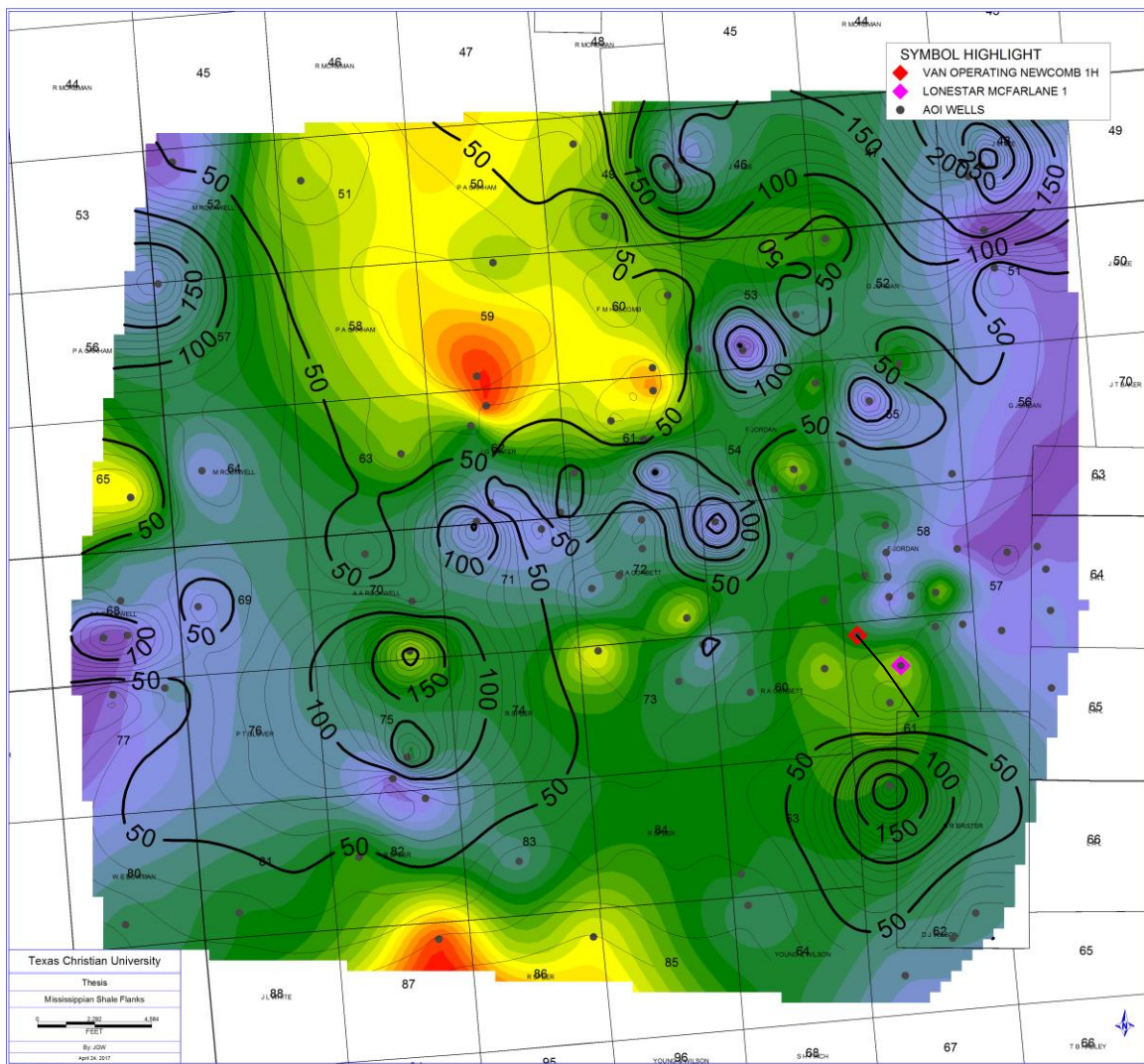


**Fig. 28:** The Chappel reef isopach contours overlaid on the “Mississippian Shale” isopach map (colors) to illustrate the flanking relationship between the two units. This map shows how the shale may be sourced by Chappel reef debris by how the thickest accumulations of shale are present in the reef structural lows. The “Mississippian Shale” isopach C.I. = 2.5 ft.

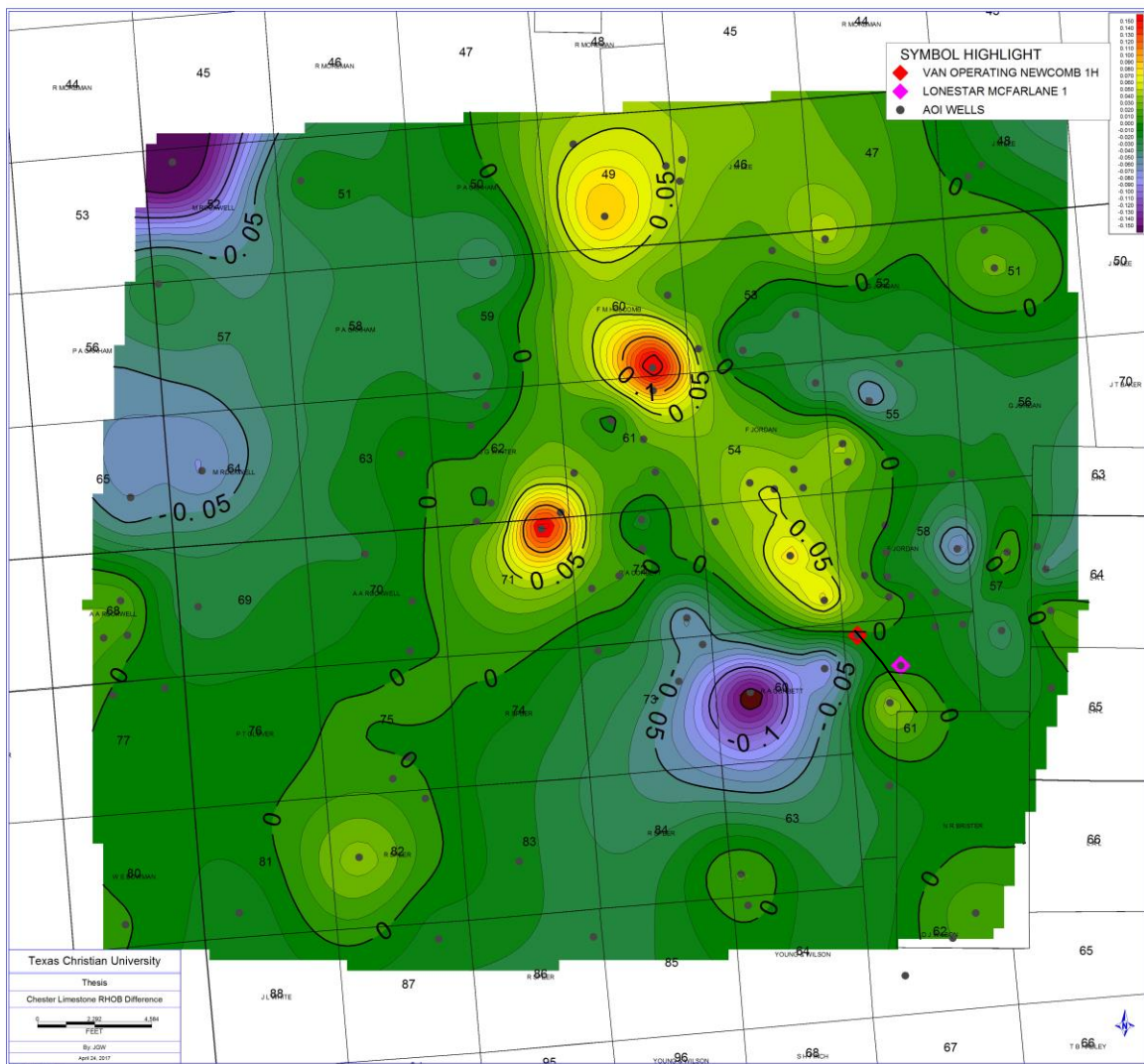


**Fig. 29:** This map illustrates the difference in average RHOB values of the “Mississippian Shale” and the Chester Limestone. The values posted in blue represent the Chester Limestone and the values in black represent the “Mississippian Shale”. This data highlights areas with the greatest change between the Chester Limestone and the “Mississippian Shale” in rock strength and rock mechanics. Elevated porosity in the Chester will drive positive values in this data, so it matches the average porosity map very closely. Values range from -0.06 (Chester average RHOB > “Mississippian Shale” average RHOB) up to 0.08 (“Mississippian Shale” average RHOB > Chester average RHOB). Red is the greatest difference between the values and purple is the smallest difference. C.I. = 0.01.

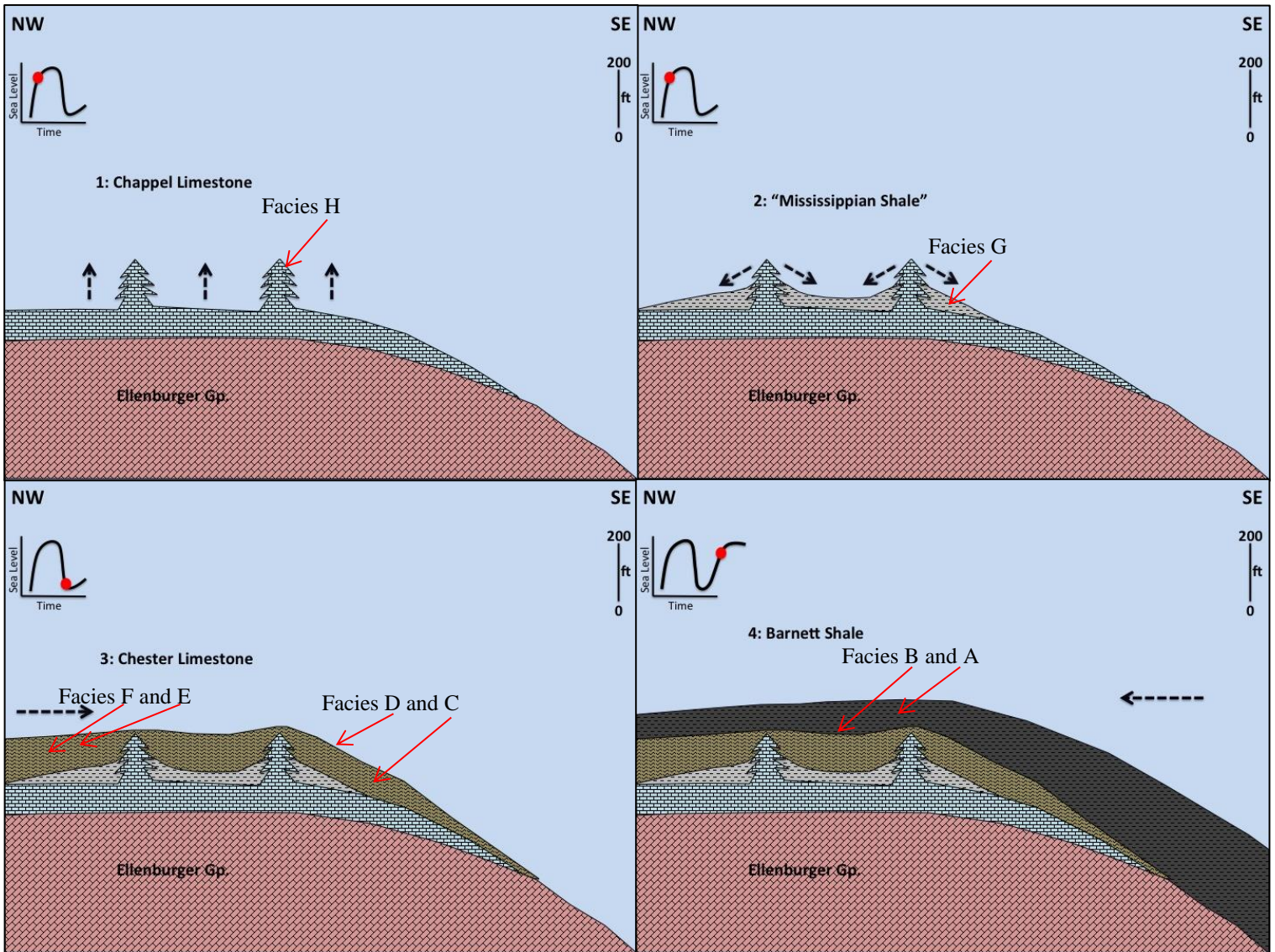


**Fig. 30:** A depositional model of the Chappel Limestone, "Mississippian Shale", Chester Limestone, and Barnett Shale. A relative sea-level vs time curve is put with each unit to give insight towards the water depth during deposition. The red arrows indicate the relative location of the facies and the black arrows indicate the direction of stacking patterns.

### Lonestar McFarlane 1 GR v RHOB

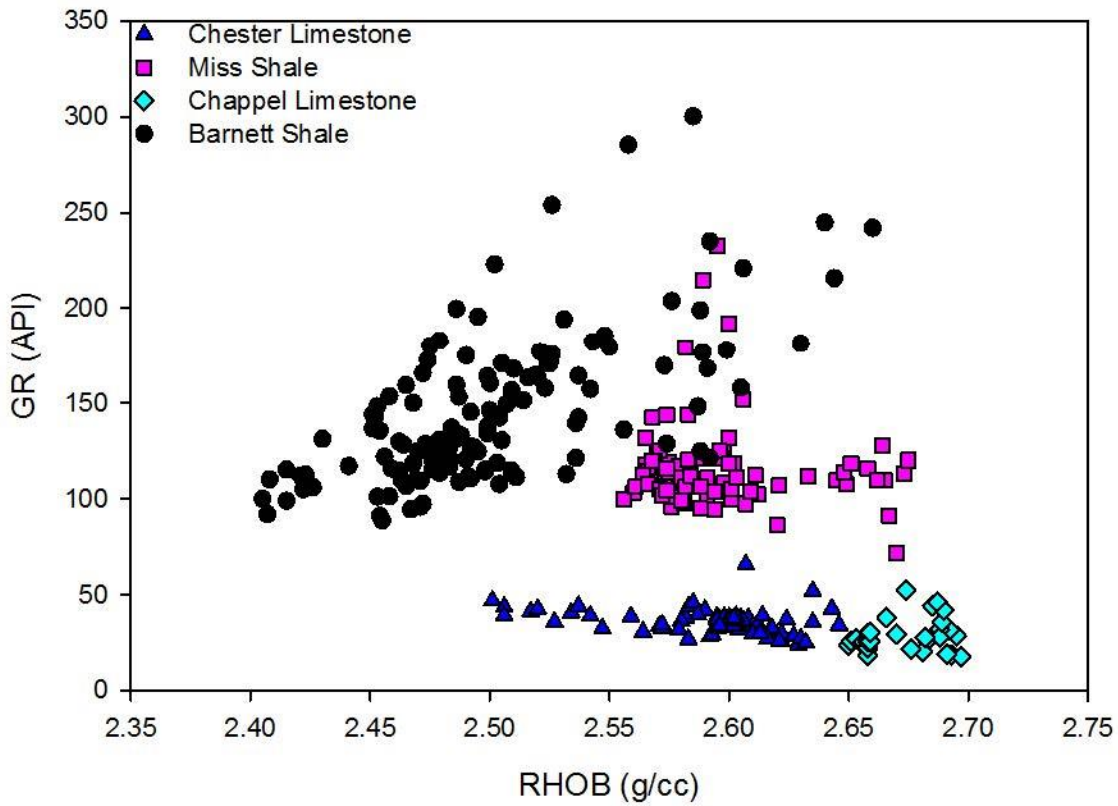


**Fig. 31:** This cross plot of gamma ray vs RHOB values comes from the type log from the Lonestar McFarlane 1 well. It breaks out the specific units of the play to identify their range of values found in the log signature.

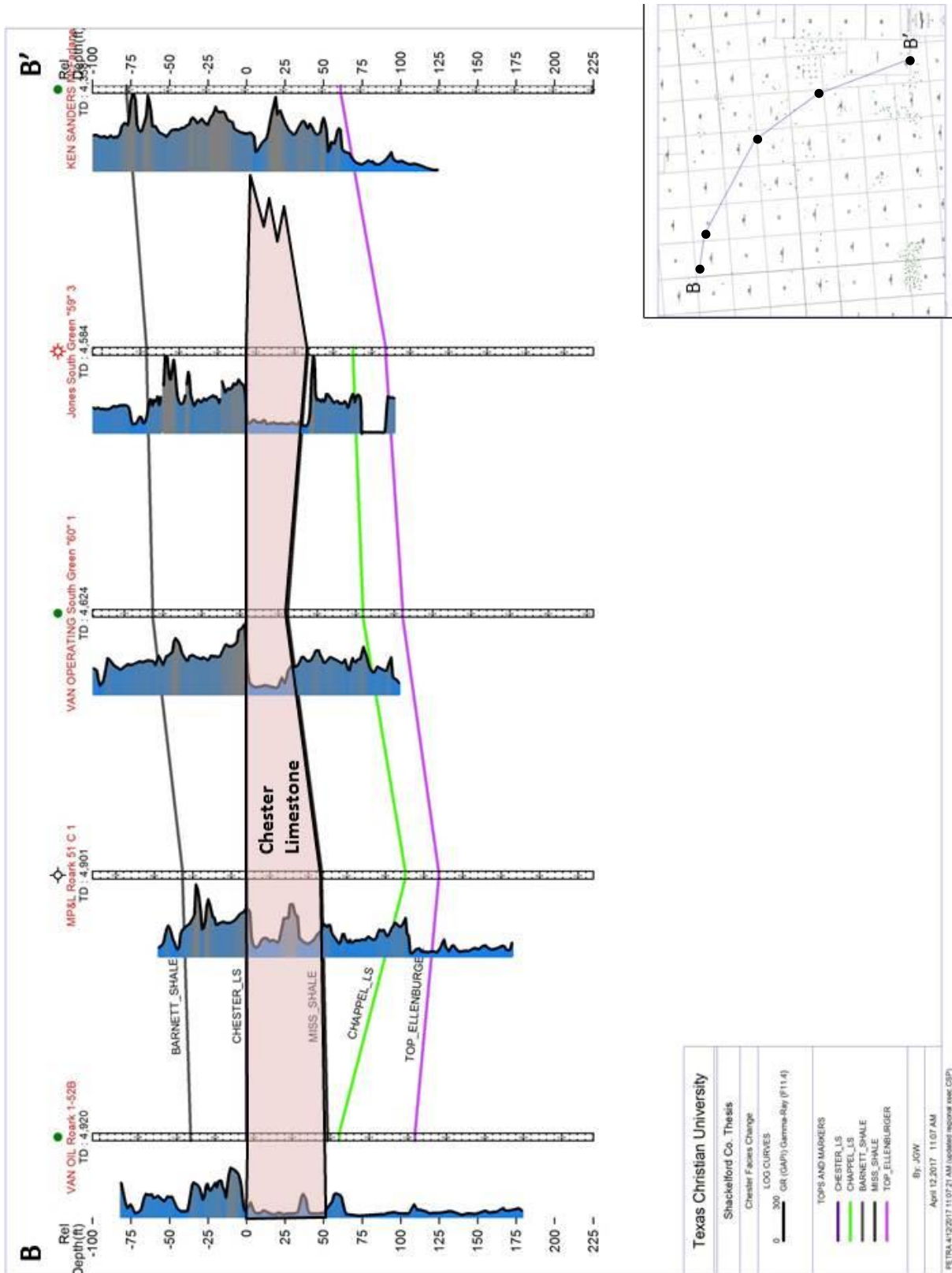


**Fig. 32:** Cross section B-B' shows the regional distribution of the limestone and siltstone facies in the Chester Limestone. Within the AOI towards the Chappel reef trend, the facies pinch out into a muddier facies that may represent the Barnett Shale to the SW.

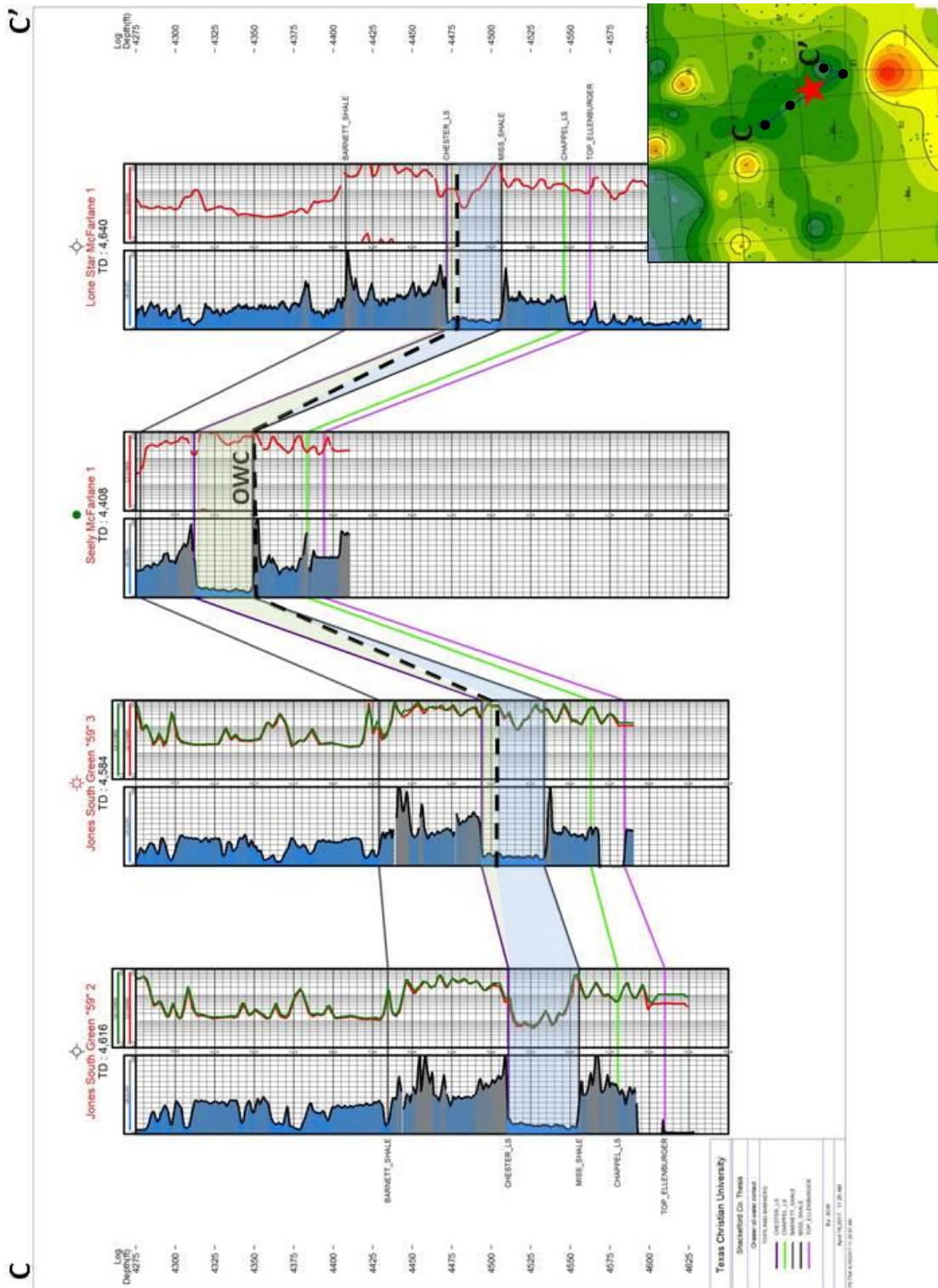


**Fig. 33:** Cross section C-C' showing an interpreted OWC occurring at the LoneStar McFarlane 1 and Jones South Green 59-3 wells, where the Chester is located within a local structural low feature in the Chappel canyon. The OWC is interpreted 1 due to the lower  $R_t$  response ( $<.8 \text{ ohm} \cdot \text{m}$  compared to the  $R_t$  in the up dip Seely McFarlane 1 well ( $\sim 35 \text{ ohm} \cdot \text{m}$ ). The Red star is the approximate location of the Newcomb 1H well.

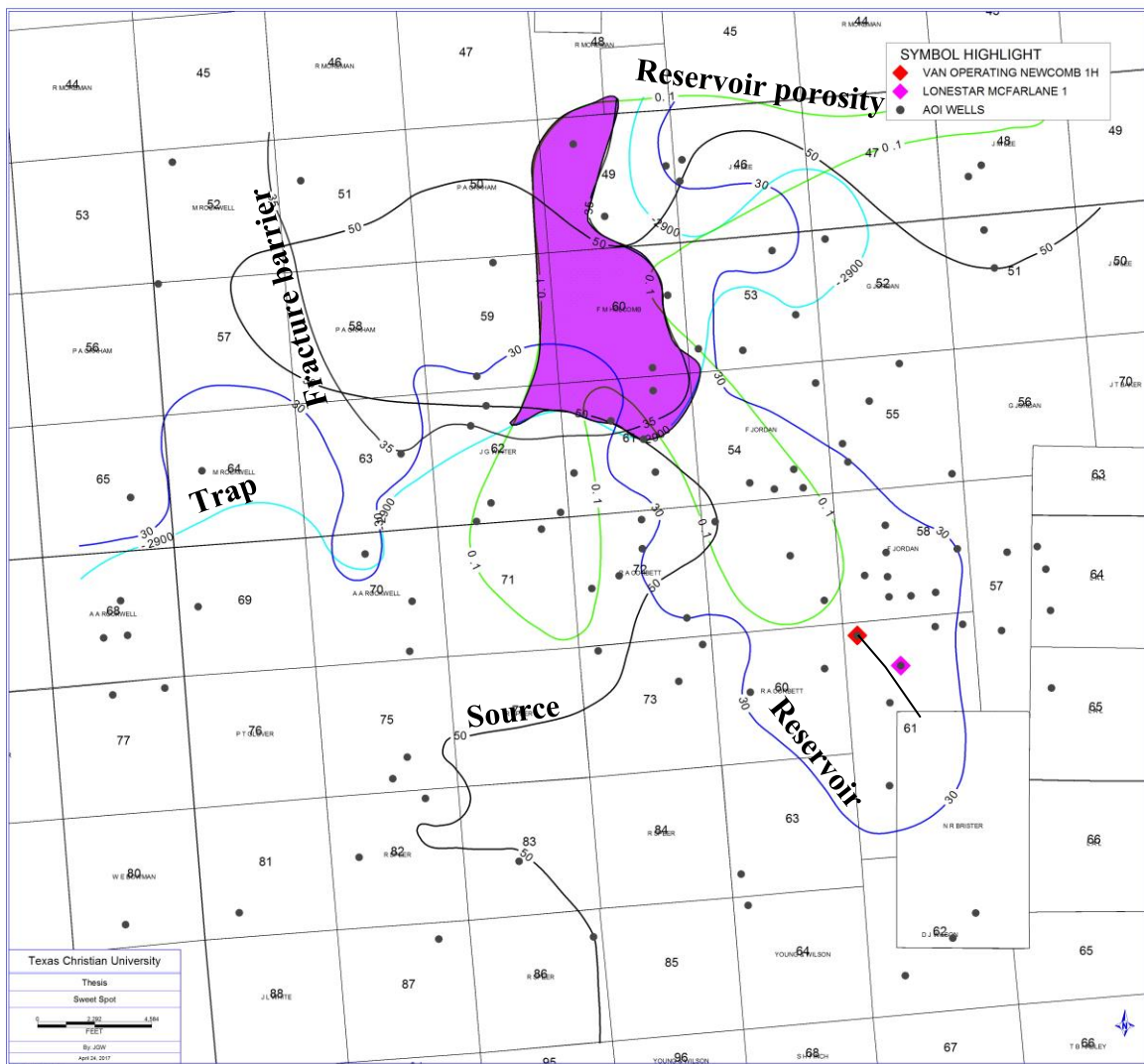


**Fig. 34:** A sweet spot map of the play generated by overlaying contours from each play component. This map has identified an area of ~1,200 ac that contains attributes from all of the play components that exceed values that were identified in the dry hole analysis. Source (black) = Barnett Shale thickness > 50 ft, Reservoir (blue) = Chester thickness > 30 ft, Reservoir porosity (green) = Chester PHIDa > 10%, Fracture barrier (gray) = “Mississippian Shale” thickness > 35 ft, and Trap (light blue) = structurally below the up-dip Chappel reef trend at -2,900 ft subsea.

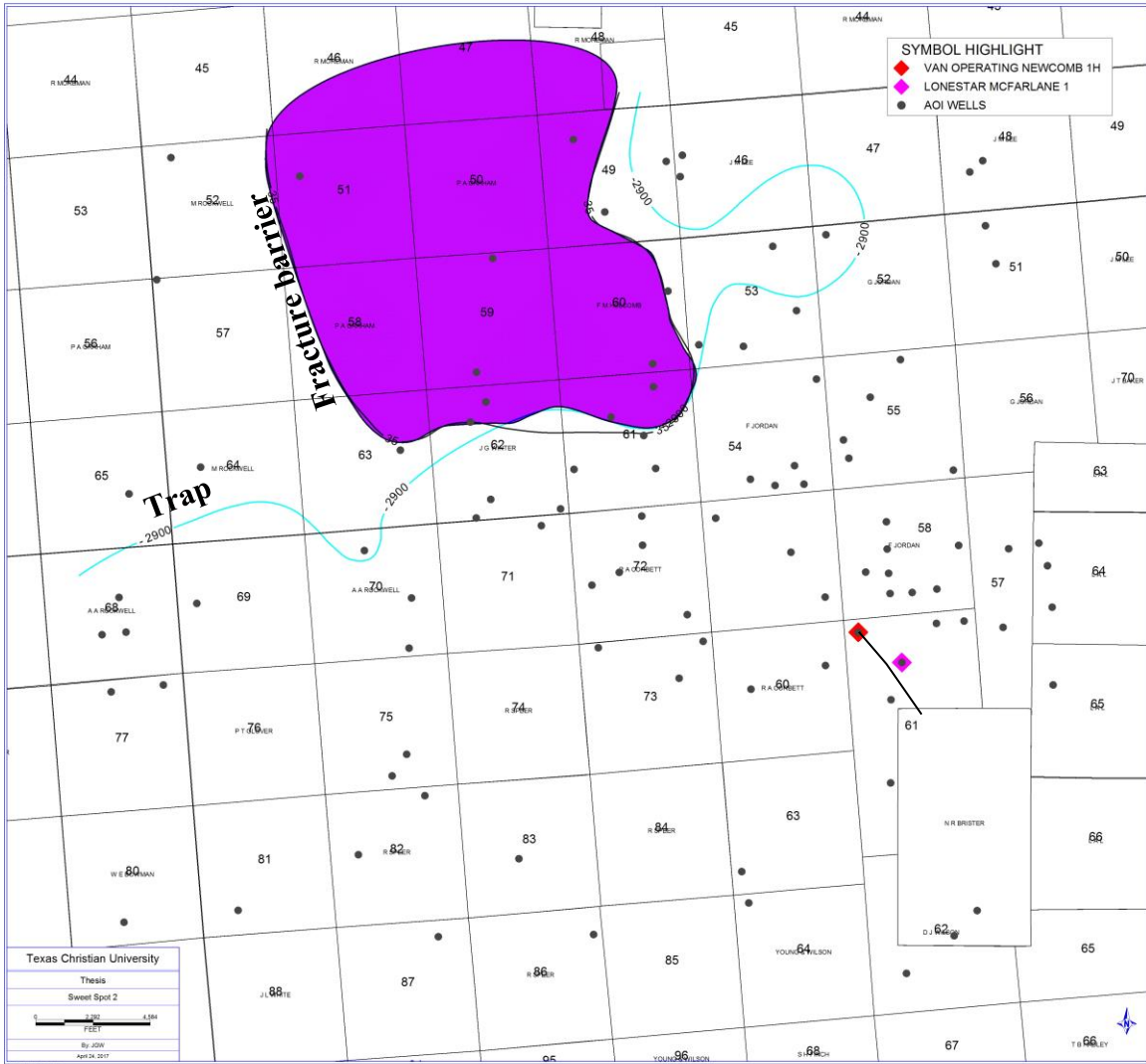
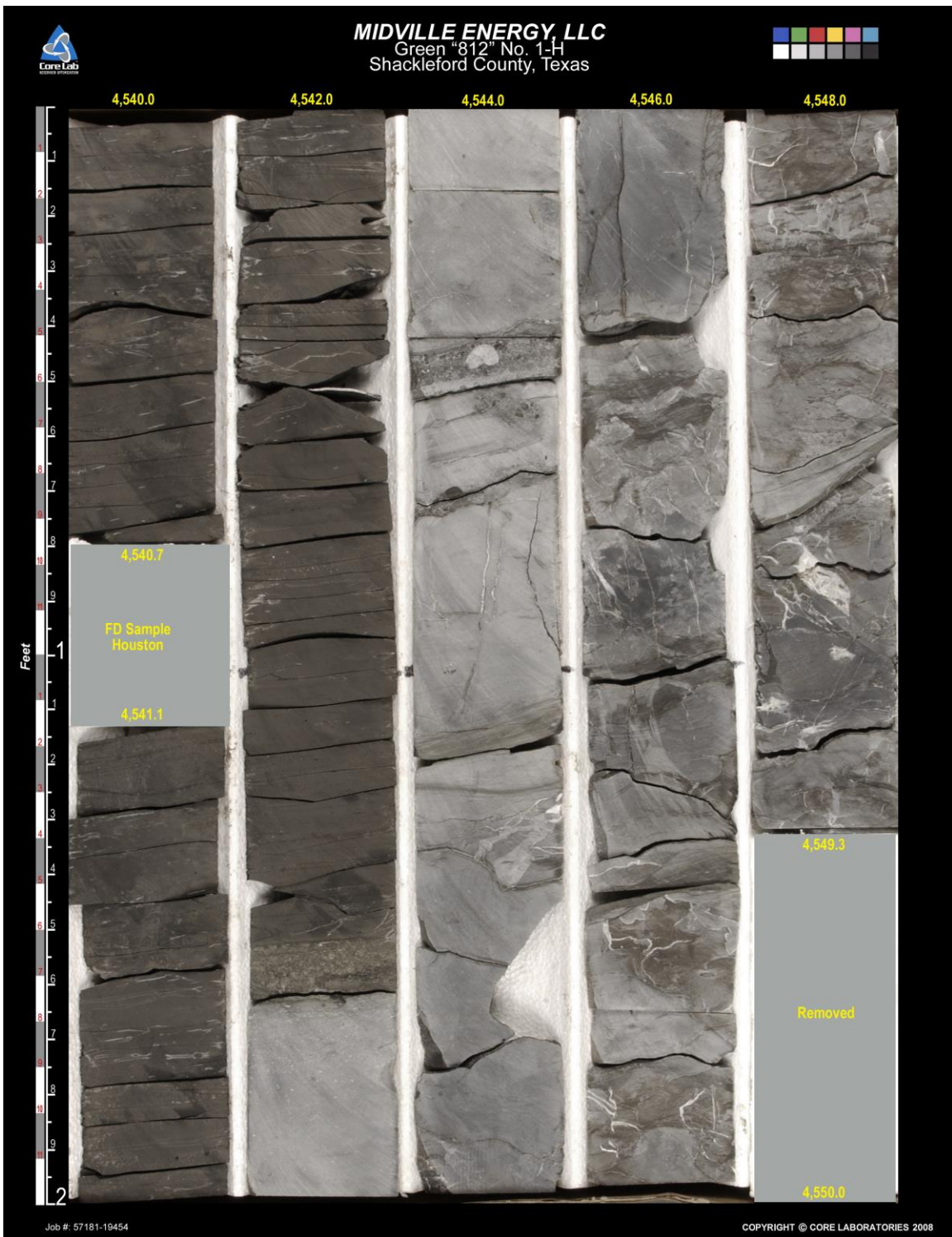


**Fig. 35:** A second sweet spot map that was created to alleviate problems arising from lack of porosity (bulk density logs) well control. This second map has identified an area of ~4,500 ac and may be more useful for identifying areas that contain potential for repeatable completions in this Chester-Barnett play. Trap (light blue) = structurally below the up-dip Chappel reef trend at -2,900 ft subsea and Fracture barrier (grey) = “Mississippian Shale” thickness > 35 ft.

**CORE PHOTOS**

# Midville Green 812 Core:





**MIDVILLE ENERGY, LLC**  
Green "812" No. 1-H  
Shackleford County, Texas



4,550.0

4,552.0

4,554.0

4,556.0

4,558.0



Job #: 57181-19454

COPYRIGHT © CORE LABORATORIES 2008



**MIDVILLE ENERGY, LLC**  
Green "812" No. 1-H  
Shackleford County, Texas



Job #: 57181-19454

COPYRIGHT © CORE LABORATORIES 2008



**MIDVILLE ENERGY, LLC**  
Green "812" No. 1-H  
Shackleford County, Texas



4,570.0

4,572.0

4,574.0

4,576.0

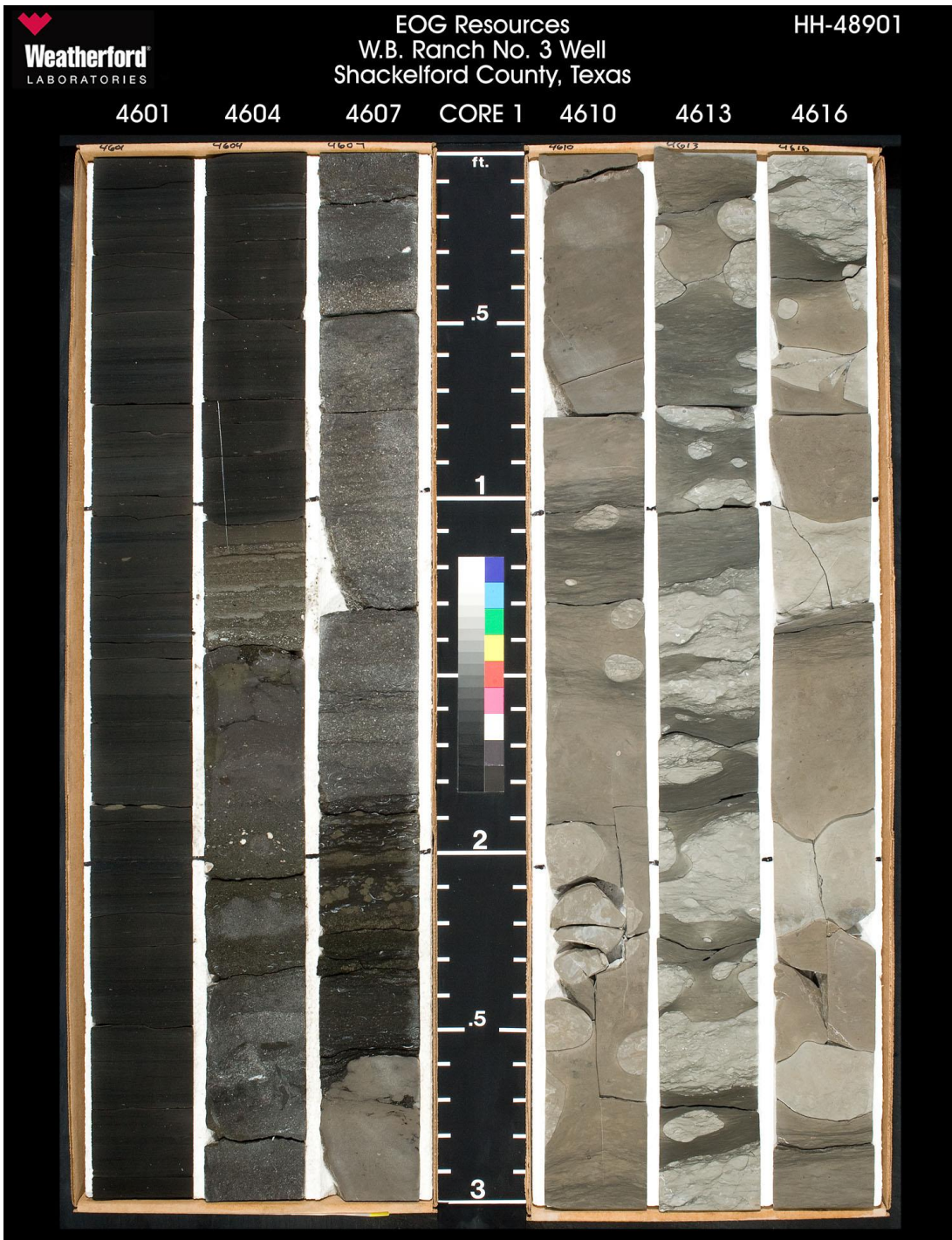
4,578.0



Job #: 57181-19454

COPYRIGHT © CORE LABORATORIES 2008

EOG W.B. Ranch #3 Core:



CORE 1

CORE 2

4619

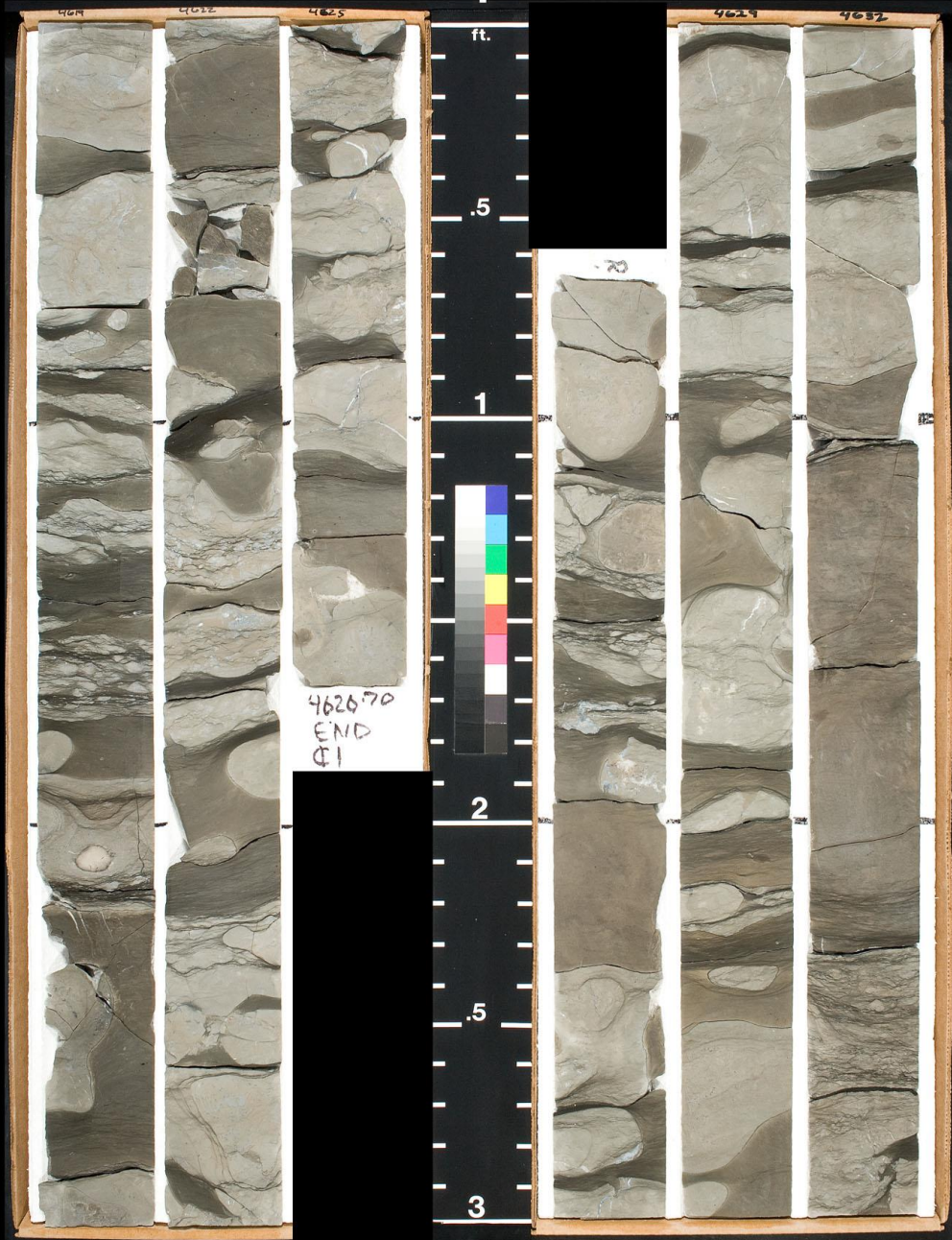
4622

4625

4626

4629

4632



4635

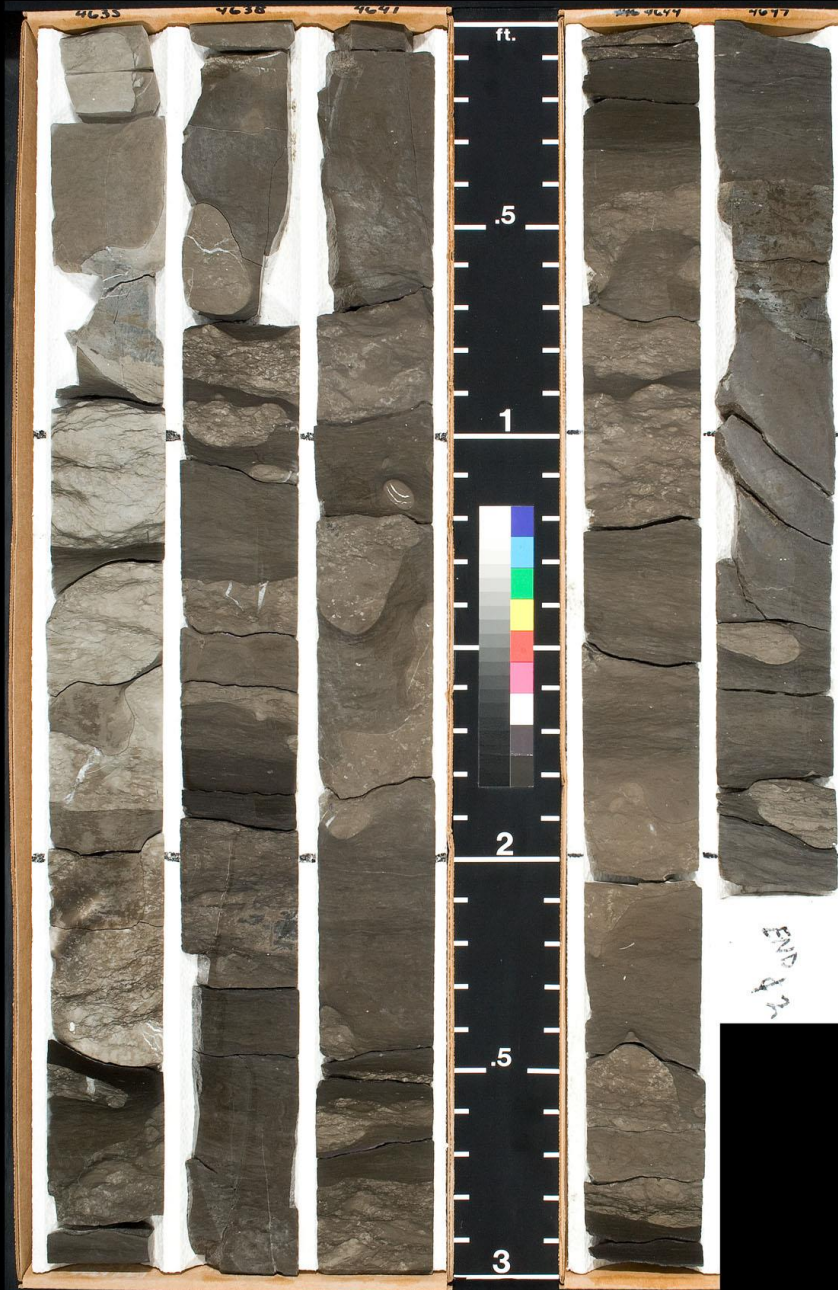
4638

4641

CORE 2

4644

4647



4649

4652

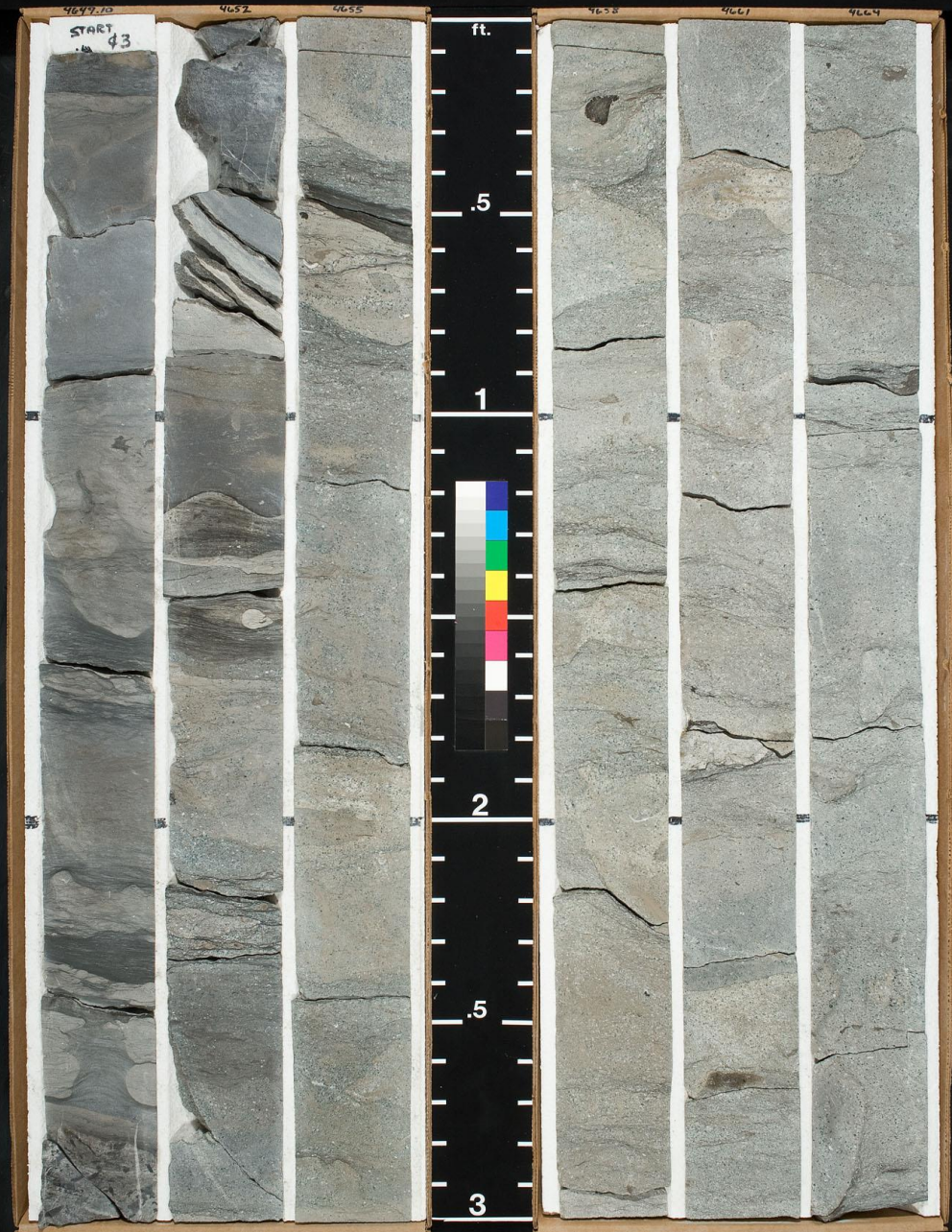
4655

CORE 3

4658

4661

4664



4667

4670

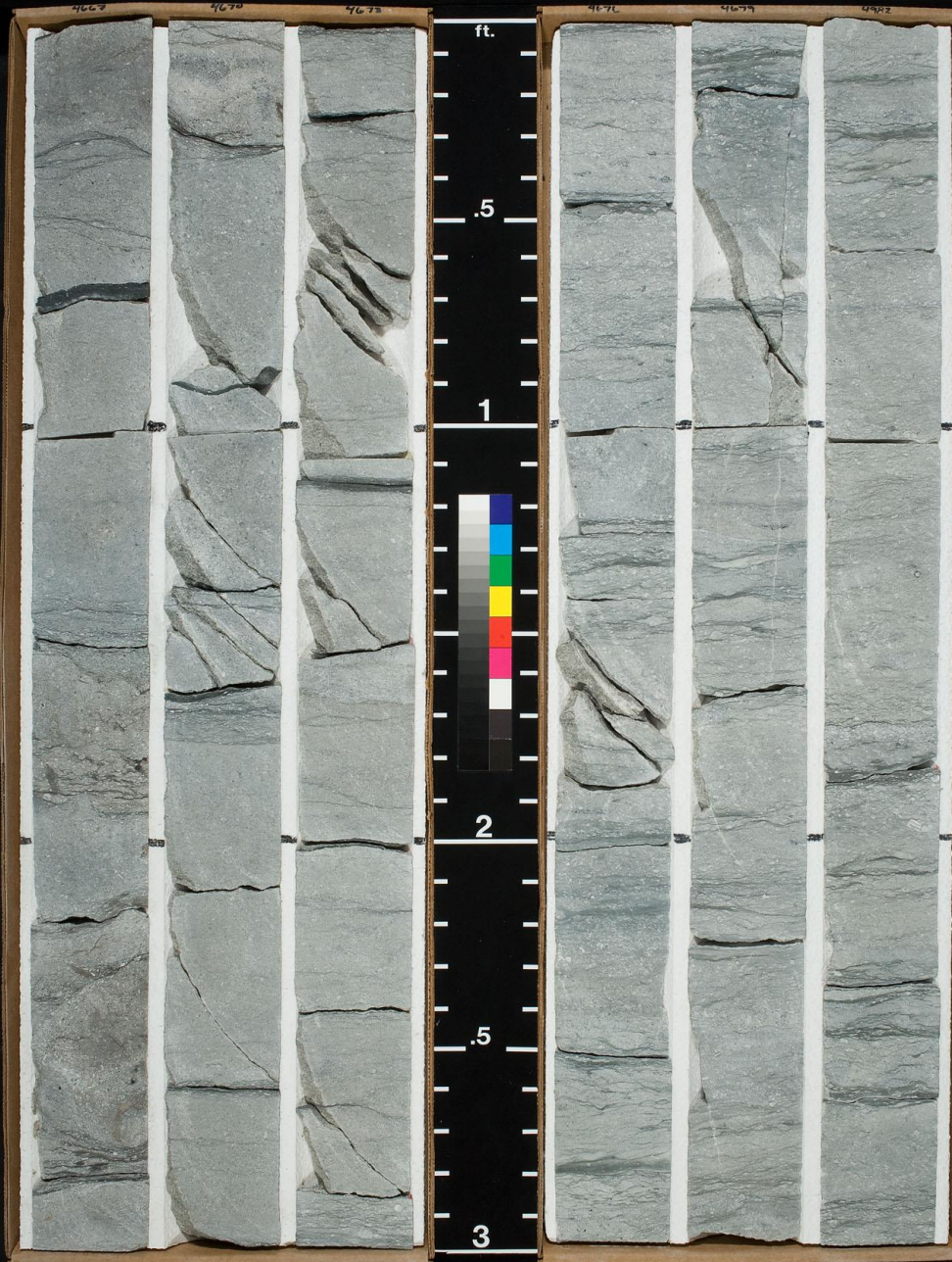
4673

CORE 3

4676

4679

4682

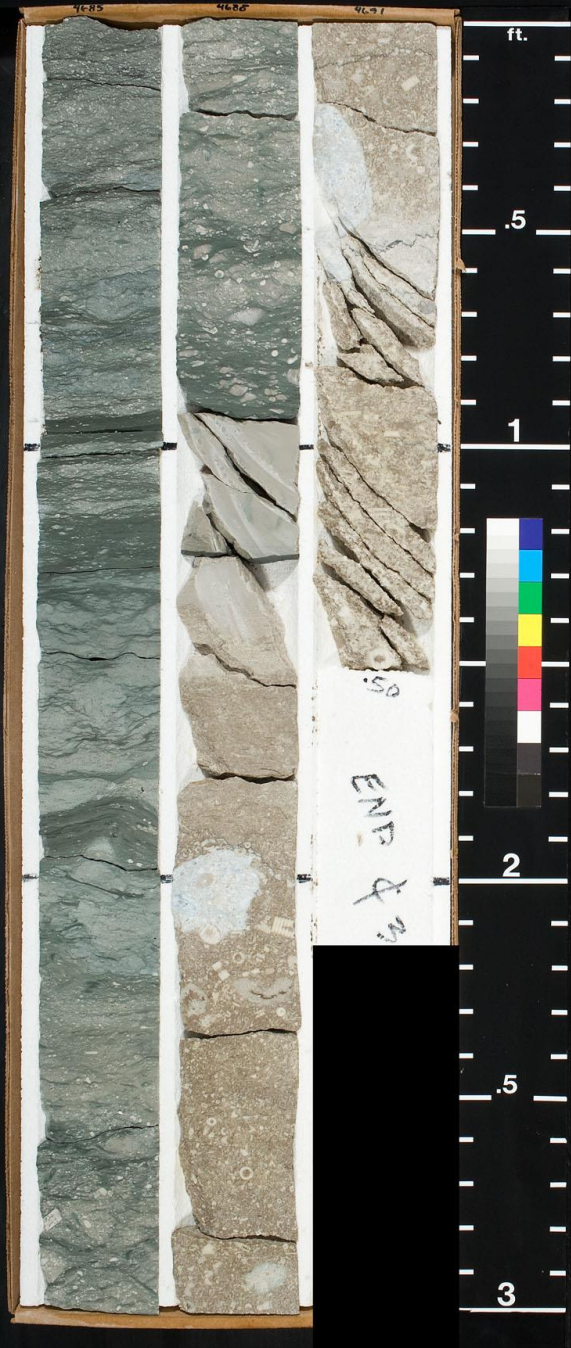


4685

4688

4691

CORE 3



## **TABLES**

**Table 1: Facies summary**

<b>Facies Name</b>	<b>Description</b>	<b>Reaction with HCl</b>
A	Black laminated siliceous mudrock that contains pyrite and vertical calcite-healed fractures	None
B	Brown mudstone that contains pyrite and phosphate nodules	None
C	Light grey pelecypod packstone that is weakly laminated and contains bryozoan remains	Strong
D	Grey mudstone-wackestone that contains pyrite	Strong
E	Dark grey calcareous siltstone that contains ripples and amorphous light grey chert nodules, commonly scoured at the base	Weak
F	Grey ostracodal wackestone-packstone that contains ripples and amorphous light grey chert nodules with an abrupt contact	Strong
G	Grey pelecypod packstone-grainstone that contains crinoid fragments, glauconite pellets, and pyrite; composed of whole shells and fragments interbedded with thin dark grey rippled mudrock beds (< 2" thick)	Strong
H	White crinoidal packstone-grainstone, contains pelecypods and bryozoan remains	Strong

**Table 2: Bambino Data from the EOG W.B. Ranch #3**

<b>Depth</b>	<b>HLD (L')</b>			<b>avg</b>	<b>Lithology</b>	<b>Fm</b>	<b>Daniels UCS (psi)</b>
	<b>1</b>	<b>2</b>	<b>3</b>				
4602.5	310	284	441	345.00	Mudrock	Barnett	2565.19
4603.5	375	338	367	360.00	Mudrock		2853.17
4604.5	442	426	436	434.67	Mudrock		4570.48
4605.5	256	179	264	233.00	Mudrock	Chester	961.53
4606.5	255	188	207	216.67	Ls		801.77
4607.5	488	535	583	535.33	Gs		7693.64
4608.5	581	572	558	570.33	Gs		9013.49
4609.5	201	185	197	194.33	Mudrock		610.86
4610.5	703	708	695	702.00	Silt	Chester pay	15150.04
4611.5	688	694	737	706.33	Silt		15384.92
4612.5	678	673	706	685.67	Silt		14284.12

4613.5	654	665	665	661.33	Silt		13050.35
4614.5	786	781	772	779.67	Chert		19694.43
4615.5	687	681	668	678.67	Silt		13922.34
4616.5	742	720	752	738.00	Ls		17167.69
4617.5	715	700	729	714.67	Ls		15842.72
4618.5	771	775	746	764.00	Ls		18719.94
4619.5	689	732	730	717.00	Chert		15972.35
4620.5	535	617	536	562.67	Silt		8713.63
4621.5	836	798	807	813.67	Chert		21912.27
4622.5	725	664	682	690.33	Silt		14528.41
4623.5	555	599	553	569.00	Silt		8960.90
4624.5	761	764	767	764.00	Chert		18719.94
4625.5	754	790	746	763.33	Chert		18679.13
4626.5	701	802	807	770.00	Chert		19089.64
4627.5	735	769	727	743.67	Chert		17499.14
4628.5	702	647	581	643.33	Silt		12180.39
4629.5	790	820	793	801.00	Chert		21069.41
4630.5	785	762	716	754.33	Chert		18133.40
4631.5	683	675	648	668.67	Ls		13415.14
4632.5	726	732	723	727.00	Chert		16535.11
4633.5	791	727	759	759.00	Ls		18415.16
4634.5	783	682	729	731.33	Ls		16782.61
4635.5	723	767	758	749.33	Ls		17834.41
4636.5	760	839	821	806.67	Chert		21444.02
4637.5	311	321	374	335.33	Mudrock		2389.26
4638.5	603	638	665	635.33	Ls		11805.25
4639.5	687	711	738	712.00	Ls		15695.35
4640.5	683	647	656	662.00	Ls Frac		13083.26
4641.5	716	734	798	749.33	Ls		17834.41
4642.5	795	799	808	800.67	Chert		21047.49
4643.5	584	502	522	536.00	Silt		7717.61
4644.5	753	774	799	775.33	Chert		19421.92
4645.5	713	697	702	704.00	Ls		15258.18
4646.5	714	700	704	706.00	Ls		15366.78
4647.5	838	880	864	860.67	Chert		25214.97
4648.5	562	597	672	610.33	Silt		10677.97
4649.5	718	707	658	694.33	Ls		14739.78
4650.5	746	716	735	732.33	Chert	End pay	16840.04
4651.5	540	564	582	562.00	Silt		8687.84
4652.5	621	654	671	648.67	Ls		12434.40
4653.5	535	585	564	561.33	Silt		8662.10
4654.5	682	735	722	713.00	Silt		15750.52
4655.5	551	536	618	568.33	Silt		8934.68

4656.5	653	648	712	671.00	Ls		13532.48
4657.5	624	610	661	631.67	Ls		11635.66
4658.5	584	561	524	556.33	Ls Silt		8470.49
4659.5	560	551	614	575.00	Ls Silt		9199.00
4660.5	596	581	571	582.67	Ls Silt		9508.71
4661.5	728	826	753	769.00	Chert		19027.72
4662.5	629	641	672	647.33	Ls Silt		12370.60
4663.5	764	811	779	784.67	Cherty Ls		20011.70
4664.5	653	607	634	631.33	Ls Silt		11620.31
4665.5	604	605	615	608.00	Ls Silt		10576.21
4666.5	711	724	727	720.67	Ls Silt		16177.34
						"Mississippian Shale"	
4667.5	631	646	686	654.33	Ls		12707.75
4668.5	590	676	594	620.00	Silt		11105.81
4669.5	713	770	784	755.67	Ls		18213.64
4670.5	701	661	637	666.33	Ls		13298.41
4671.5	589	572	583	581.33	Ls fracture		9454.40
4672.5	591	582	607	593.33	Ls		9949.88
4673.5	648	673	735	685.33	Ls		14266.77
4674.5	692	718	722	710.67	Ls		15621.97
4675.5	723	752	722	732.33	Ls		16840.04
4676.5	644	617	599	620.00	Silt Ls		11105.81
4677.5	560	599	594	584.33	Silt		9576.85
4678.5	762	727	709	732.67	Silt Ls		16859.20
4679.5	654	654	658	655.33	Ls		12756.36
4680.5	766	793	780	779.67	Ls		19694.43
4681.5	689	691	704	694.67	Ls		14757.48
4682.5	734	743	744	740.33	Ls		17303.71
4683.5	700	702	725	709.00	Ls		15530.54
4684.5	789	797	780	788.67	Ls		20267.71
4685.5	596	577	588	587.00	Silt		9686.49
4686.5	543	494	532	523.00	Silt		7258.14
4687.5	711	695	673	693.00	Ls		14669.12
4688.5	562	587	545	564.67	Silt		8791.27
4689.5	465	513	527	501.67	Ls	Chappel	6540.47
4690.5	403	448	464	438.33	Ls		4667.48
4691.5	627	583	619	609.67	Ls		10648.84

**Table 3: BSE Elemental data from facies E (sample 2) and facies F (sample 1)**

<b>Elements</b>	<b>Sample 1: ROI 1 (wt%)</b>	<b>Sample 1: ROI 2 (wt%)</b>	<b>Sample 1: ROI 3 (wt%)</b>	<b>Sample 2: ROI 1 (wt%)</b>	<b>Sample 2: ROI 2 (wt%)</b>	<b>Sample 2: ROI 3 (wt%)</b>
O	34.05	31.46	33.23	24.20	35.94	37.44
Si	24.69	18.85	23.16	12.88	18.10	17.37
C	10.50	17.23	12.73	29.25	0.00	0.00
Ca	10.25	11.80	11.1	8.15	13.40	11.14
Mg	2.66	0.95	2.07	1.95	3.04	3.46
Al	2.76	2.01	2.14	2.86	5.12	4.23
Fe	0.00	4.44	5.43	4.75	6.53	5.82
K	1.50	3.24	0.00	2.14	3.22	3.01
Ti	4.02	4.19	4.31	3.73	0.00	5.69
P	3.18	0.00	0.00	0.00	0.00	0.00
Cl	0.66	0.00	0.00	0.00	0.00	0.00
Sn	0.00	0.00	0.00	0.00	0.00	0.00
Zr	0.00	0.00	0.00	3.28	0.00	0.00
Cr	0.00	0.62	0.00	0.00	0.00	0.00
S	5.74	5.84	5.83	5.62	14.65	11.83
Sn	0.00	0.00	0.00	0.00	0.00	0.00
Na	0.00	0.00	0.00	1.20	0.00	0.00

## VITA

Personal Background	Jonathon Glover Weiss, Jr. Born August 22, 1992, Fort Worth, Texas
Education	Bachelor of Science in Geology, 2015 Baylor University, Waco, TX  Master of Science in Geology, 2017 Texas Christian University, Fort Worth, TX
Experience	Geoscience Intern, 2016-17 Range Resources, Fort Worth, TX  Geoscience Intern, Summer 2016 QEP Resources, Denver, CO  Geoscience Intern, Summer 2015 Crimson Energy Partners, IV, Fort Worth, TX  Geoscience Intern, Summer 2015 Mid-Continent Geological, Fort Worth, TX  Geoscience Intern, Summer 2014 Rust Oil Corporation, Fort Worth, TX
Professional Societies	American Association of Petroleum Geologists

## ABSTRACT

### A POTENTIAL EXTENSION OF THE BARNETT SHALE OIL PLAY: A SUBSURFACE PLAY ANALYSIS OF THE MISSISSIPPIAN (OSAGEAN- MERAMECIAN) STRATA IN SHACKELFORD COUNTY, TEXAS

JONATHON GLOVER WEISS, JR., M.S., 2017  
School of Geology, Energy, and the Environment  
Texas Christian University

Thesis Advisor: Dr. Xiangyang Xie, Assistant Professor of Geology  
Committee Members: Dr. Richard Denne and David Wells

Repeatable, unconventional Barnett Shale completions have been constrained to the gas-rich, eastern portion of the play in Fort Worth Basin due to the presence of fracture barriers protecting the play from unwanted water production from the underlying Ellenburger Group. This project conducts a subsurface study on the Mississippian-aged strata (Chappel Limestone through the Barnett Shale) within the oil-rich, western extent of the Barnett Shale play in Shackelford County, Texas. The subsurface study results identify two distinct depositional mechanisms of facies formation within the Chester Limestone that overlap to give play potential for oil-rich Barnett Shale completions west of the Viola pinchout in the Bend Arch-Fort Worth Basin area. The upper portion of the Chester Limestone contains a higher porosity cherty zone that shows reservoir potential. The basal portion of the Chester Limestone is referred to as the “Mississippian Shale”, and it shows potential to act as a fracture barrier that could prevent downward fracture growth into the Ellenburger in areas with widespread deposition and significance difference in rock mechanics (ductile) from the upper cherty zone (brittle). Subsurface correlations were done utilizing over 100 wells that contained gamma-ray (GR) and bulk density (RHOB) within the 64 mi<sup>2</sup> AOI (area of interest). Rock mechanics were tested utilizing the Equotip Bambino micro-rebound hammer and by observing the difference in RHOB of the play units. The main conclusions of this study include: (1) the identification of the “Mississippian Shale” as a potential fracture barrier for the Barnett Shale play to potentially extend the play in to the oil window; (2) sweet spot maps that identify areas with the most geologic potential to prevent downward growth of stimulation fractures into the Ellenburger in areas related to the growth of the Chappel reefs; (3) the identification of differences in depositional controls in the Chester Limestone and the “Mississippian Shale” that leads to identifying areas of overlap that enhance the play potential.